UNIVERSITY OF TROMSØ UIT

FACULTY OF SCIENCE AND TECHNOLOGY
DEPARTMENT OF CHEMISTRY

Biotech applications of protein kinase affinity interactions

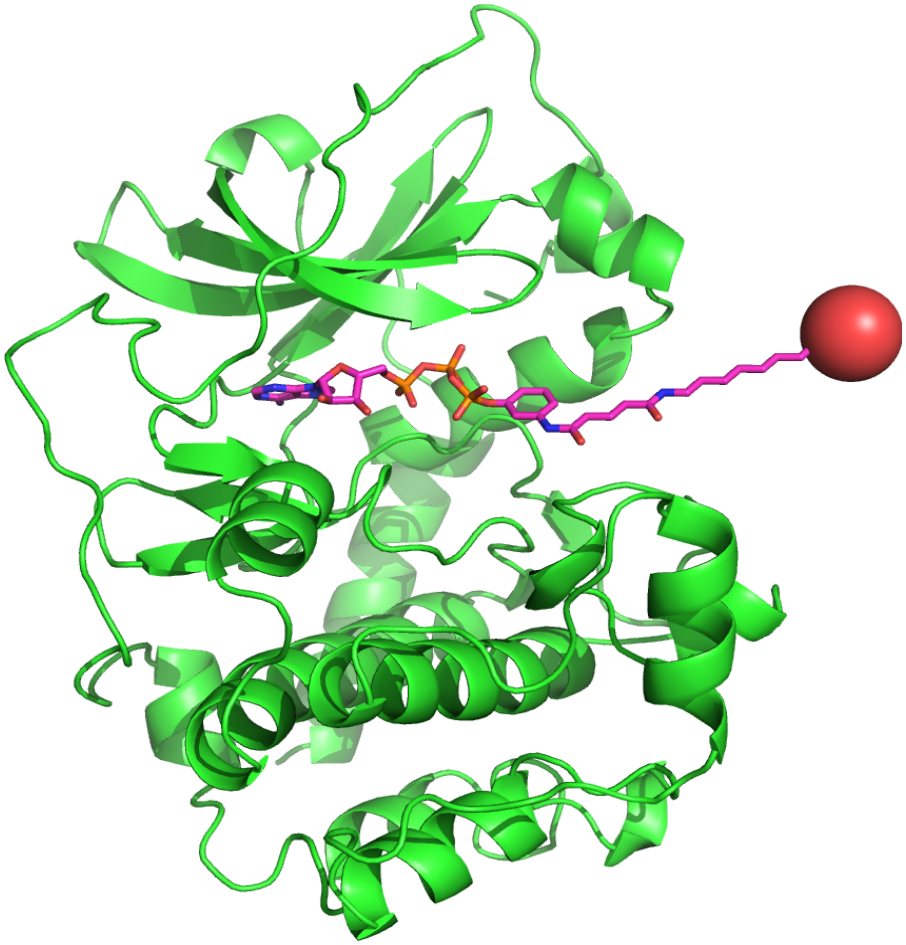

Bjarte Aarmo Lund

KJE-3900 Master's Thesis in Chemistry

May 2013

Abstract

Protein kinases provide one of the cell's most important methods for signaling and control. 2% of the encoding genome consists of protein kinase genes, and from 10-50% of the proteins in the cell are phosphorylated at some point in the cell cycle. Malfunction of protein kinases is connected to several disease-conditions, most prominently cancer, Alzheimer's and diabetes. Understanding the interactions of protein kinases gives deeper insight into the function of protein kinases, and builds a foundation for new treatments and diagnostics. A common feature of the protein kinases is their ability to bind to adenosine triphosphate (ATP). In this study a set of resin-linked ATP-analogs with distinct binding-strategies was used to probe the ATP-binding site to investigate the use as an affinity-chromatography-step in the purification of protein kinases and together with other studies of protein kinase/ligand interactions detect differences between protein kinases to give information on how to create new specific inhibitors for protein kinases.

For the model-protein kinase cAMP-dependent protein kinase/protein kinase A (PKA) a specific affinity-chromatography-resin with immobilized protein kinase inhibitor (PKI) was studied using different eluants and mutants.

Binding to ATP-analog-resins was observed for 70 kDa heat shock proteins (HSP70), Abelson tyrosine-protein kinase 1 (ABL1), dual specificity tyrosine-phosphorylation-regulated kinase 1A (DYRK1A) and PKA, and there were differences in which of the resins each protein bound to.

Several different mutants were tested on immobilized PKI, including one new mutant which did not show any binding to PKI. It was also shown that by using bisubstrate inhibitors as eluants, it is possible to only elute specific isoforms of PKA.

The observation of distinct binding-behavior to the differently linked ATP-analogs gives indications on how new inhibitors may be designed with higher selectivity, as well as showing potential as components of a protein purification strategy.

The work on immobilized PKI with bisubstrate inhibitors as eluants revealed that it is possible to elute only the active form of PKA from the PKI-resin, simplifying the later chromatographic steps. The non-PKI-binding protein kinase A sevenfold mutant model of Aurora B (PKA Aur7)-mutant has potential use in co-expression with kinase-dead mutants to yield more stable autophosphorylated PKA it it can be shown to be active, while being easy to purify away since it does not bind to the PKI-resin as the other PKA-variants would.

Keywords: Protein Kinase, Affinity, Interactions, PKA, ABL, HSP70, Crystallization, Thermofluor, Bisubstrate, Inhibitors, PKI, DYRK, Aurora B, mutagenesis, phosphorylation, ATP

Acknowledgements

I want to thank my supervisor Richard A. Engh for introducing me for the world of protein kinases, and giving me the opportunity to do this stimulating project. While I had no formal co-supervisor I had great help and support in the kinase-group, I especially want to thank Alexander Pflug and Peter Kyomuhendo who mentored me in my first attempts with protein kinases. I had many discussions with Dilip Narayanan about protein kinases, heat shock proteins and chemoinformatics, and they were important to me. The work on PKA would have been much harder without Kazi Asraful Alam, and I could not have done anything on DYRKs without the help of Ulli Rothweiler and Marina Alexeeva.

I also had the pleasure of collaborating with Taavi Ivan, from the group of Dr. Asko Uri at the University of Tartu, on the topic of the adenosine–oligoarginine conjugate (ARC)-bisubstrate inhibitors and PKA.

The inhibitors 34a and 47a were provided by Leo Hardegger in Prof. F. Diederich's group at ETH Zürich. The structural characterisation of these compounds would not be possible without the beamtime and support provided by Helmholtz-Zentrum Berlin für Materialien und Energie (HZB).

NanoTemper, with their representative Emilia Danilowicz-Luebert provided access to the Monolith NT.115 and NT.LabelFree-machines, and I am grateful for the demonstration of the possibilities of this technology.

I want to thank the Institute of Chemistry, and especially the people of NorStruct, both for an amazing infrastructure and a really solid community. I have really appreciated the good work and social atmosphere. During the structure determination I had many useful discussions with Hanna-Kirsti Schrøder Leiros and Ingar Leiros, and Gro Bjerga helped me a lot during the site-directed mutagenesis.

Big thanks to Dilip Narayanan and Shanley Swanson for proofreading the thesis.

I am very grateful for my family, especially my beloved wife Ida and my fantastic son Matteus, having you around me with your attention and love means everything to me.

Thanks to God for all his blessings over my life.

Contents

List of Figures

List of Tables

Acronyms

6AH-ATP-Agarose N^6-(6-Amino)hexyl-ATP-Agarose. 16, 47, 58, 69, 70, 75, 85

8AH-ATP-Agarose 8 – [(6-Amino)hexyl]-amino-ATP-Agarose. 16, 69, 75, 85

ABL1 Abelson tyrosine-protein kinase 1. 2, 9, 25, 34, 35, 48, 49, 70, 71, 75, 81, 85

ADP adenosine diphosphate. 20, 69

AMP ampicillin. 33, 36, 39, 40, 43, 45, 56

ANP adenyl-5'-yl imidodiphosphate. 5, 7

AP-ATP-Agarose aminophenyl-ATP-Agarose. 16, 49, 58, 66, 70, 71, 75, 85

aPK atypical protein kinase. 1, 2

ARC adenosine–oligoarginine conjugate. 11, 37, 40, 52, 53, 60, 73, 74

ATP adenosine triphosphate. 1, 2, 5, 7, 10, 11, 15, 16, 20, 24, 26, 27, 31, 37, 41, 42, 60, 63, 69–71, 75, 78, 79, 81, 85

AURKA Aurora A kinase. 24

AURKB Aurora B kinase. 26, 33, 45, 69

BSA bovine serum albumin. 34

cAMP cyclic adenosine monophosphate. 24

CCP4 Collaborative Computational Project No. 4. 42

cDNA complementary DNA. 13

CHL chloramphenicol. 31–33, 36, 45

CML chronic myelogenous leukaemia. 9, 10

CV column volume. 33, 34, 37

DTT dithiothreitol. 29, 31, 33, 35

DYRK dual specificity tyrosine-phosphorylation-regulated kinase. 26, 75

DYRK1A dual specificity tyrosine-phosphorylation-regulated kinase 1A. 26, 34, 48, 70, 75, 85

DYRK1B dual specificity tyrosine-phosphorylation-regulated kinase 1B. 26, 33, 34, 45, 47, 70

E.coli *Escherichia coli*. 13, 14, 25, 49, 75, 85

EDA-ATP-Agarose 2'/3'-EDA-ATP-Agarose. 16, 48, 70, 71, 75, 85

EDC 1-ethyl-3-(3-dimethylaminopropyl)carbodiimide. 41

EDTA ethylenediaminetetraacetic acid. 32, 34

ePK eukaryotic protein kinase. 1, 2

ESI electrospray ionisation. 19

FFT Fast Fourier Transformation. 71

FT flow-through. 29, 47, 49

H-89 N-[2-[[3-(4-Bromophenyl)-2-propenyl]amino]ethyl]-5-isoquinolinesulfonamide . 37, 40, 53, 60

HEPES 2-[4-(2-hydroxyethyl)piperazin-1-yl]ethanesulfonic acid. 37

HSP70 70 kDa heat shock proteins. 26, 27, 31, 33, 45, 69, 71, 85

HSPB1 27 kDa heat shock proteins. 12

IEX ion-exchange chromatography. 16, 74

IMAC immobilized metal ion-affinity chromatography. 15, 49, 71

IPTG isopropyl β-D-1-thiogalactopyranoside. 32, 36

KAN kanamycin. 31, 32, 36, 45

LB lysogeny broth. 29, 31–33, 36, 39, 43, 45, 56

LIC ligation-independent cloning. 13

MAD multiple-wavelength anomalous dispersion. 80

MOPS 3-(N-morpholino)propanesulfonic acid. 41, 42

MPD 2-Methyl-2,4-pentanediol. 42

mRNA messenger RNA. 13

MS/MS Tandem mass spectrometry. 18, 19, 21, 33, 35, 48, 49, 73, 75

MST microscale thermophoresis. 21, 42, 63, 79, 86

NAD+ nicotinamide adenine dinucleotide. 20

NADH reduced nicotinamide adenine dinucleotide. 20, 31

NBD nucliotide binding domain. 26, 27

NHS N-Hydroxysuccinimide. 41, 42, 79

OD600 optical density at 600 nm. 32, 36, 45, 47

PBS phosphate buffered saline. 29, 32–35, 41

PCR polymerase chain reaction. 38, 39, 42, 56

PDB Protein Data Bank. 7, 10

PEP phosphoenolpyruvic acid. 20, 31

PHENIX Python-based Hierarchical ENvironment for Integrated Xtallography. 43

PKA cAMP-dependent protein kinase/protein kinase A. 1, 2, 5, 7, 9–11, 18, 24, 25, 31, 37, 47, 52, 70, 73, 75, 78–80, 85

PKA Aur6 protein kinase A sixfold mutant model of Aurora B. 24, 36–38, 52, 53, 56, 62, 73, 74, 79, 81

PKA Aur7 protein kinase A sevenfold mutant model of Aurora B. 24, 38, 40, 56, 58, 66, 74, 75, 85

PKAB3 protein kinase A threefold mutant model of AKT. 22, 24, 40, 42, 58, 60, 62, 63, 66, 75, 78–81, 86

PKAR4 protein kinase A fourfold mutant model of Rho. 24, 43, 66

PKAR5 protein kinase A fivefold mutant model of Rho. 24, 43, 66, 81

PKA-Rho protein kinase A mutant model of Rho. 43, 66, 81

PKB AKT/protein kinase B. 1, 2, 12, 24, 79, 86

PKC protein Kinase C. 10

PKI protein kinase inhibitor. 10, 24, 37, 40–42, 52, 53, 56, 62, 63, 73–75, 78, 79, 85

qPCR real-time polymerase chain reaction. 19, 20

RMSD root mean square deviation. 81

SAD single-wavelength anomalous dispersion. 80

SDS-PAGE Sodium dodecyl sulphate polyacrylamide gel electrophoresis. 14, 18, 21, 29, 33–35, 45, 47–49, 52, 56, 58, 62, 66, 71, 73, 78, 81

SOC super Optimal broth with Catabolite repression. 31, 33, 35

SPR surface plasmon resonance. 20, 79

Src proto-oncogene tyrosine-protein kinase Src. 9, 10

TB terrific broth. 29, 36

TF trigger factor. 14, 25, 35, 49, 71, 85

TOF Time-of-Flight. 19

TRIS 2-Amino-2-hydroxymethyl-propane-1,3-diol. 35, 37

UV280 absorbance at 280 nm. 35, 36, 74

YOPH Yersinia protein-tyrosine phosphatase. 34, 48

YT yeast extract and tryptone. 36

Chapter 1

Introduction

Protein kinases belong to the groups of transferases in the sub-group of the phosphorus-transferring groups. Protein kinases can be divided into several sub-sub-groups based on the acceptor-group of the phosphate which they transfer. The most common groups are protein-serine/threonine kinases (EC 2.7.11) and protein-tyrosine kinases (EC 2.7.10) which catalyze the transfer of a phosphate group from ATP to a serine/threonine or a tyrosine on a substrate peptide as shown in Equation 1.1.[115].

$$\mathrm{ATP} + [\mathrm{Protein}]{-}\mathrm{OH} \longrightarrow \mathrm{ADP} + [\mathrm{Protein}]{-}\mathrm{O}{-}\mathrm{Phosphate} \tag{1.1}$$

Protein kinases was first described to regulate protein function by phosphorylation 60 years ago, and the after the first mapping of the human genome it was clear that over 500 protein kinases are encoded in the human genome, accounting to almost 2% of the total protein encoding genes according to estimates[89].

Protein kinases are known to mediate signal transduction between eukaryotic cells by the modification of substrate activity as well as controlling cellular processes from cell division and metabolism to the nervous and immune systems.

As protein kinases control processes by phosphorylation, their activity is to a large extent controlled by phosphorylation. Some protein kinases will autophosphorylate, either by an inter- or an intramolecular event[15, and references therein].

The importance of understanding protein kinases can hardly be overstated considering the impact function and malfunction has on the organism. Major diseases such as cancer, Alzheimers disease, autoimmune disease, diabetes, drug addiction and neurological disorders have been shown to have a protein kinase connection[39, 69, 35]. Several human pathogens also use protein kinases, which are targeted as drug targets, such as tuberculosis-causing *Mycobacterium tuberculosis* and one of the parasites responsible for Malaria *Plasmodium falciparum*[95]. AKT/protein kinase B (PKB) was recently implicated in the viral entry of Herpes virus into cells, and inhibitors of PKB were shown to prevent viral infection[27]. PKA has been linked to aging; mutants of PKA with lower activity makes yeast live longer and mice with a dysfunctional regulatory subunit of PKA had longer and healthier lives[24].

1.1 Sequence

Protein kinases are one of the major families of genes in eukaryotes, and most contain a eukaryotic protein kinase (ePK) catalytic domain[89]. However, there exist at least 13 families of atypical protein kinase (aPK) which have protein kinase activity, but which lack sequence similarity to the ePKs.

The sequence of the catalytical domain of PKA and ABL1 is shown in Figure 1.1.

The current grouping of protein kinases involves 9 major groups with over 100 families and over 200 subfamilies[89].

It appears that the ePK is a very well conserved superfamily, and even with much duplication and broad distribution only small modifications are found. The aPK appear to be ancient as well, and the phylogenetics indicate that they evolved independently of the ePK[34].

However, outside of the catalytical domain there is no sequence similarity except for closely related kinases, because of the huge diversity of substrates and interaction partners[34].

Over 60% of protein kinases are multi-domain proteins, often the catalytical domain is tethered to another domain responsible for regulation, substrate specificity, etc. For large protein kinases it is not uncommon that only the catalytical domain is classified, and that the other domains are unassigned. For human protein kinases there is an average coverage of 58%[67].

Because of high sequence-identity differences in selectivity between protein kinases can often be attributed to a handful of point-mutations, allowing the use of "surrogate" kinases which have favorable properties regarding solubility or crystallizability, but which carries mutations giving selectivity of the kinase in interest. This has been done for PKB[53], Rho-Kinase[18] and Aurora kinases[101] with PKA as surrogate for example[1].

1.2 Structure

The protein kinases share eleven conserved subdomains forming a catalytic domain[20]. This catalytical core has been shown to be flexible with rotational movements of the two lobes. The active site is located in the cleft formed by the two lobes, the cavity has space for the entire ATP molecule, but with the γ-phosphate oriented outwards. Right next to the cleft is the substrate binding site, so that the γ-phosphate is close to the substrate-peptide.

The N-lobe is the smaller of the two lobes, and is named for its location in the amino terminal of the protein. It is dominated by a five-stranded antiparallel β-sheet ($\beta 1 - \beta 5$) and also has a α-helix designated C($\alpha 3$). The C-helix interacts with different parts of the protein, and its conformation is an indicator of the overall state of the kinase. In the active form of the kinase the conserved Glutamic acid is oriented towards the conserved lysine in β-strand 3. For several protein kinases including PKA this lobe is used for protein-protein interactions. The first two strands contain a loop with a glycine-rich sequence GXGXXGXV known as the glycine-rich loop, which is known to be

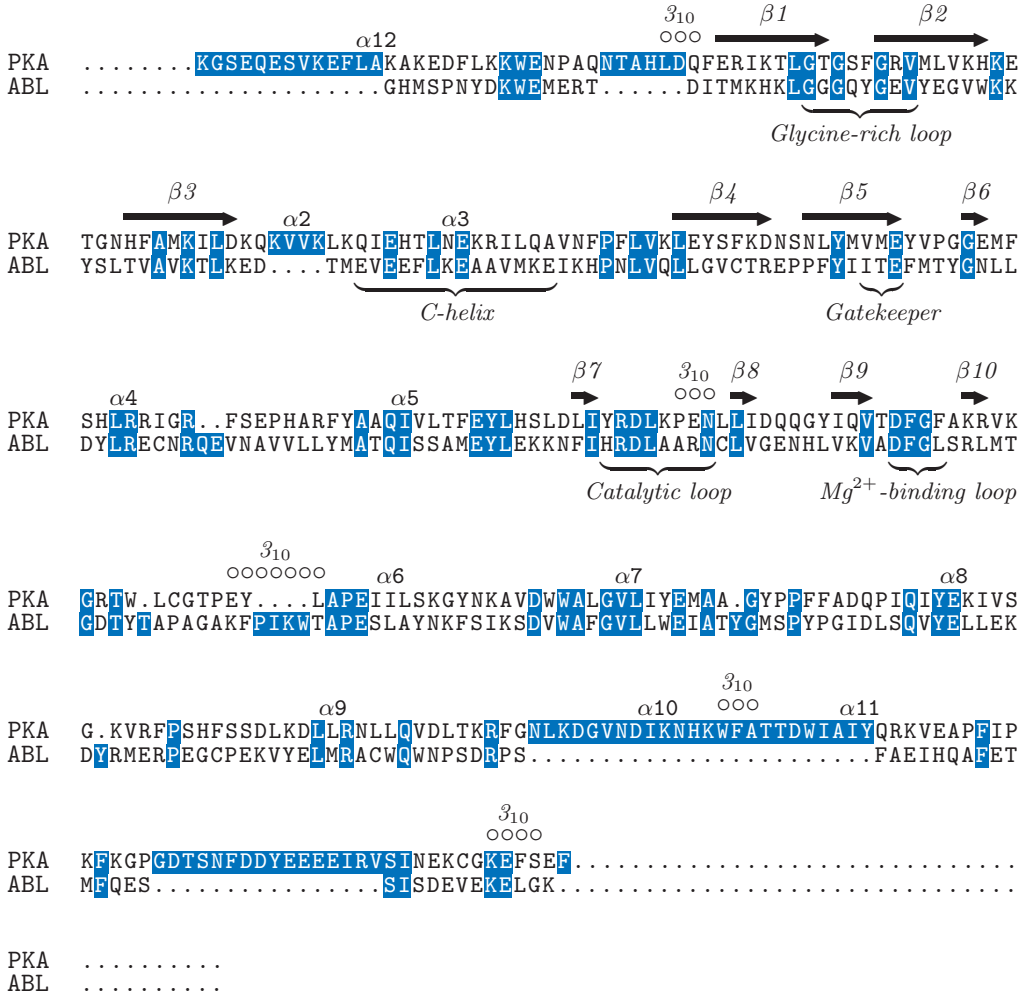

Figure 1.1: Sequence alignment of PKA and ABL1. Secondary structure elements are shown for PKA based on predictions from the STRIDE web-service[50]

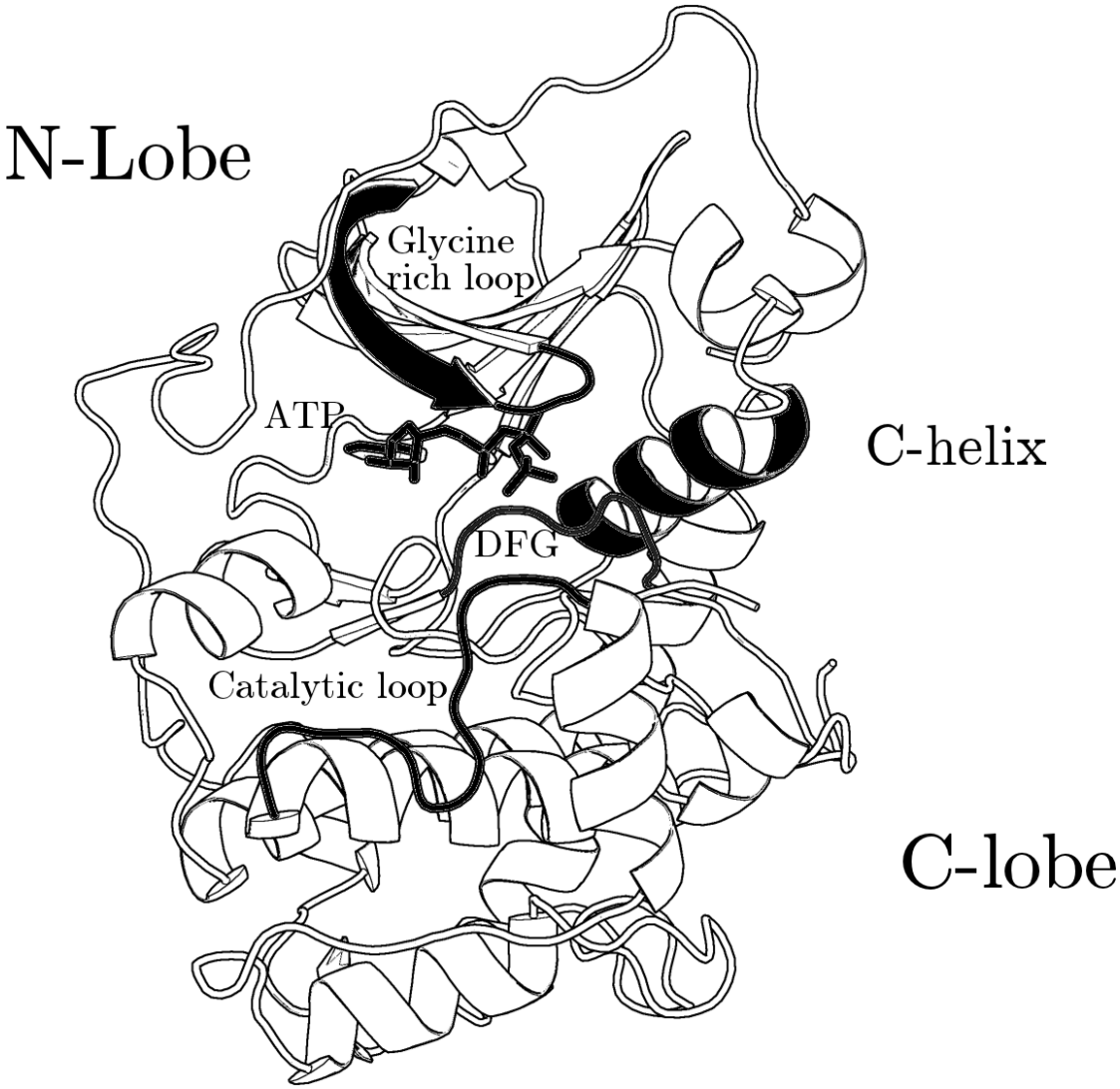

Figure 1.2: Cartoon-representation of PKA illustrating some of the main structural features of protein kinases

very flexible[125]. The absence of side-chains for the Glycines allows close contact between the nucleotide of ATP and the peptide backbone. Lys-72 in the third strand has contacts with the α and β-phosphates of ATP. A salt-bridge to Glu-91 in the C-helix ensures the positioning of Lys-72[20]. Methionine 120 in PKA, is known as the "gatekeeper", closes off a hydrophobic pocket beyond the adenine-binding site. Smaller "gatekeepers" allow inhibitors to bind in this hydrophobic pocket. ABL1 has a Threonine in this position as is shown from Figure 1.1, which allows for entrance to the hydrophobic pocket.

The C-lobe is larger and interacts with the phosphates of ATP to facilitate the phosphoryl transfer while also providing a docking surface for the substrate peptide[125]. The core of the C-lobe consist of seven α-helices and four β-strands. The catalytic loop is also situated in the C-lobe together with the Mg^{2+}-positioning loop with the DFG-motif which is not moved by substrate binding.

The DFG-motif has in many cases been shown to indicate the activity of a kinase, if the DFG-motif is oriented outwards, phosphate-transfer does not occur, and the kinase is inactive[8, and references therein]. Some of the structural features are shown in Figure 1.2.

1.3 Cofactors, ligands and substrates

1.3.1 Cofactors

Metals are often important for enzyme activity and function, and protein kinases are also sensitive to metals. A transition state mimic of PKA was crystallized with AlF_3 in trigonal bipyramidal geometry giving structural evidence for the in-line mechanism of phosphoryl transfer in PKA[87].

1.3.1.1 Magnesium

Magnesium is known to be a important cofactor for protein kinases. Protein kinases have binding sites for two divalent cations, and while other cations can take the place of Magnesium, the activity of the protein kinases is usually highest with Magnesium[114]. The primary Magnesium ion is coordinated by the oxygens of the α and β phosphates of ATP together with Asp184 in the DFG-motif (see Figure 1.1), while the second is coordinated by the oxygens of the α and γ phosphates of ATP together with Asn171[139]. This is illustrated in Figure 1.3.

1.3.1.2 Manganese

The transition metal Manganese can take the place of Magnesium in several enzymatic systems, including PKA. [19] PKA binds up to two Manganese-atoms in the active site, one (M^2)[1] coordinates the β and γ phosphates of ATP while the second (M^1) coordinates the α and γ. M^2 is coordinated in a octahedral geometry distorted by the neighboring Asp184 and is a high-affinity binding site essential to kinase function, while the M^1 is

[1] the numbering-scheme is according to the research paper of the structure of PKA with MnAMP-PNP

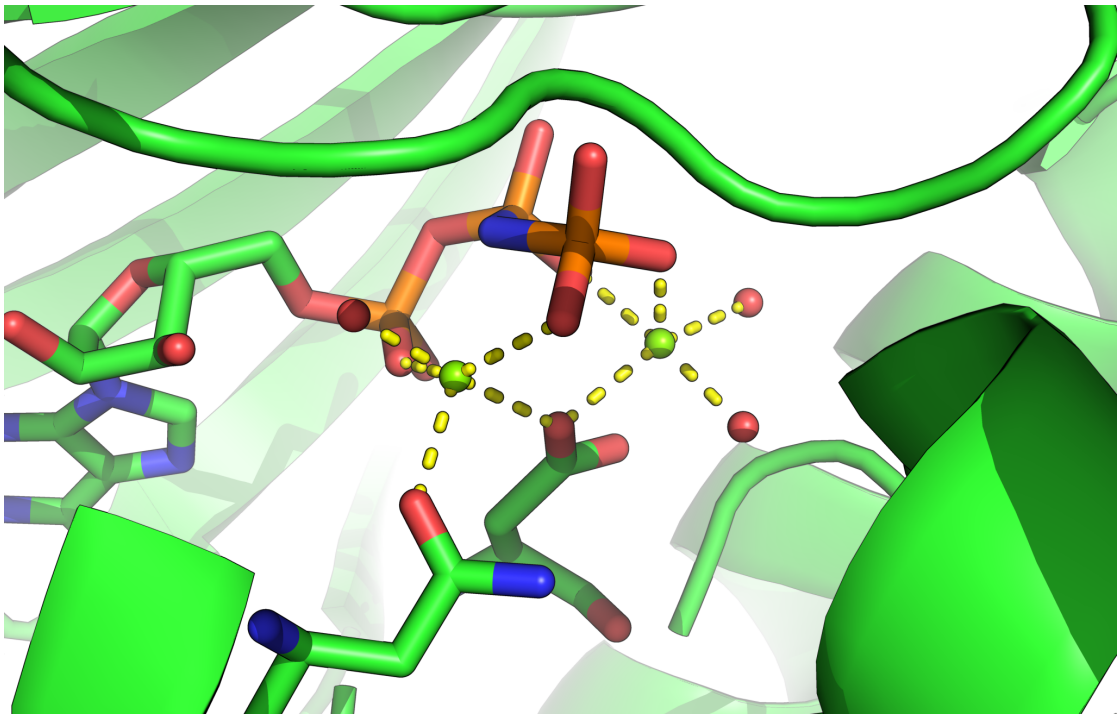

Figure 1.3: Two Magnesium-ions (green spheres) coordinated by the oxygens of Asn 171 and Asp184 in PKA, waters (red spheres) and ANP[74]

in an unusual trigonal bipyrimidal geometry which when bound reduces the activity of PKA[19].

1.3.1.3 Vanadate

The transition metal Vanadate is used by researchers to study transition state analogs of enzymes which in nature react by phosphoryl transfer, as in the case of kinases. Vanadate forms pentacoordinate, trigonal bipyramidal geometry with oxygen giving VO_4^{3-}, as phosphate is expected to do in the enzymes transition state. Not very many structures with vanadate are deposited with the Protein Data Bank (PDB), but these structures span four of the six enzyme-classification categories of enzymes. At neutral and acidic conditions Vanadate forms oligomers, predominately a orange-yellow $V_{10}O_{28}^{6-}$, which is obviously not suited for binding in the active site. Vanadate can be "activated" in alkaline solution by heating up to 100 ℃[36].

1.3.2 Ligands

1.3.2.1 Adenosine triphosphate

ATP bind to the "hinge" connecting the to lobes of the catalytical domain[46]. The ribose and triphosphate bind in a hydrophilic channel leading to the substrate binding site.

The adenine ring is bound in a hydrophobic pocket. In PKA this pocket consists of Leu49, Val57, Ala70, Met120, Tyr122, Val123 (all from the N-lobe) and Leu173 from the C-lobe. The hydrophobic character of this pocket is conserved between protein kinases. There are also two hydrogen bonds responsible for keeping the adenine in the pocket, the main-chain carbonyl of Glu121 interacts with the N6 amino group of the adenine ring, and in PKA the side-chain hydroxyl of Thr183 forms hydrogen bonds with the N7 nitrogen[139] The ribose-ring has its primary interactions with the 2'-OH and 3'-OH which forms hydrogen bonds with the side-chain of Glu127 and the main-chain carbonyl of Glu170 in PKA[139].

The side-chains of Lys72 and Glu91 are coordinating the α-phosphate, while the backbones of Gly55 and Phe54 positions the β-phosphate. The phosphates which are not transferred, the α and β, are kept in place by interactions with the N-lobe, while the transferable γ-phosphate is positioned by the catalytic loop of the C-lobe to facilitate catalysis.

1.3.3 Substrates

While protein kinases share a common catalytic domain their target substrates are diverse, and phosphorylation occurs at discrete sites. SH2-domains and other binding motifs mediate some kinase-substrate selectivity, but there are also specificity determinants in the catalytical domain of the protein kinase[17, 129, and references therein].

A Serine/Threonine kinase has a more shallow catalytical cleft than the Tyrosine-kinases, because the Tyrosine residue is longer than the Serine and Threonine residues.

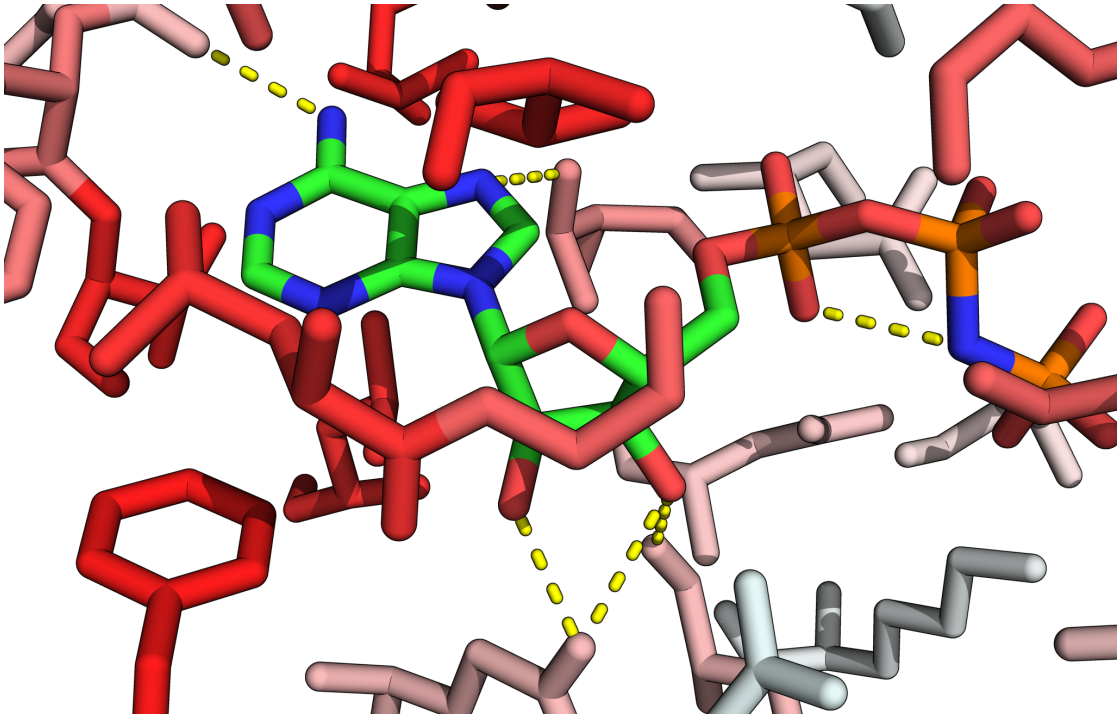

Figure 1.4: Binding of ANP to PKA showing the interactions between the adenine and ribose ring and the protein kinase. Residues of the protein kinase is colored according to the Eisenberg hydrophobicity scale, with the most hydrophobic being most red[40, 74]

Table 1.1: Substrate specificity for selected protein kinases, with X marking any amino acid,B hydrophobic amino acids (except proline) and * marking the phosphorylated residue

Protein	Sequence	Reference
PKA	XRRXS*X	[68]
ABL1	(L,I,V)Y*XXP	[29]
Aurora-A	(R,K,N)-R-X-(S,T)*-B	[48]
EGF receptor	TAENAEY*LRVAP	[68]
Insulin receptor kinase	Y*MxM	[121]

Serine/Threonine kinases has been shown to phosphorylate Tyrosines, while the converse is not described[129, and references therein]. However, free amino acids make poor substrates for protein kinases; additional amino acids in both N-terminal and C-terminal contributes significantly to the binding.

The phosphorylation-site itself contributes to the binding affinity of the substrate, for PKA the pseudosubstrate LRRAALG has a K_i of 490 µM while the substrate LRRASLG (Kemptide) has a K_m value of 16 µM. Generally protein kinases interact with four amino acids on either side of the phosphorylation-site[129, and references therein]. In general the recognition of the substrate-sequence is dependent on five categories of amino acids in the sequence[105]:

1. Basic residues such as Arginine and/or Lysine
2. Proline with its rigid geometry
3. Carboxylic residues, Aspartic acid and Glutamic acid
4. Hydrophobic residues such as Leucine or Valine
5. Phosphorylated amino-acids

Yet the substrate site needs to be accessible for the protein kinase to bind and phosphorylate[68]. The substrate sequence specificity for selected protein kinases is shown in Table 1.1.

The phosphorylation state of both the substrate and the protein kinase may affect the binding affinity of the substrate. This is proposed to be a "kinetic proofreading"-mechanism where random off-target phosphorylations might be corrected by phosphatases as other phosphorylations are also necessary for the signal to be transducted[129, and references therein].

1.4 Drugs and inhibitors

Plasma-membrane associated protein tyrosine kinases have been studied extensively as they are often mutated or over-expressed in an active form in different types of cancer.

For example, proto-oncogene tyrosine-protein kinase Src (Src) is involved in nearly all breast cancers, and ABL1 is fused to the gene Bcr by chromosomal translocation, giving rise to a constitutively active Bcr-Abl which is involved in nearly all chronic myelogenous leukaemias (CMLs)[28].

As the catalytic domain is highly conserved between protein kinases, it was long believed that it would not be possible to develop a selective inhibitor for protein kinases, especially as the natural-product staurosporine was shown to be very broadly active against kinases[69, 51].

It turned out that it was in fact possible to design selective inhibitors, with Fasudil approved in 1995[52], and Imatinib/Gleevec some time later[25]. Imatinib was later to be known as the first "rationally" designed drug, as the researchers started from a known protein Kinase C (PKC) inhibitor, gradually modifying the lead compound from a strong PKC-inhibitor, to a potent inhibitor for both tyrosine kinases and PKC, and then abolishing the inhibition of PKC as well as adding a polar side-chain to increase solubility[25]. The design of Imatinib is typical of the fragment-based drug design strategy, which is commonly used for designing protein kinase inhibitors together with structure-guided design[6, and references therein]. Imatinib has also achieved up to 80% response-rates for CML-patients[46], and the structure revealed that the specificity involves binding to an allosteric site[23, and references therein].

Many inhibitors thought to be selective have later been shown to hit multiple protein kinases, this may be due to the fact that to establish selectivity you have to test all the protein kinases[38], using biochemical or cellular assays[46].

Even with the improvements made in selectivity for protein kinase inhibitors, off-target effects are still an issue for therapeutic use[103], as off-target effects can cause serious side-effects making the therapeutic unusable for patients[11, and references therein].

Protein kinases are also attractive drug-targets since normal cells can function with inhibited protein kinases[46]. Dasatinib which is used against imatinib-resistant CML potentially inhibits all nine members of the Src-family and most likely other tyrosine kinases as well, but the side-effects are preferable to the traditional cytotoxic chemotherapies.

Most protein kinase inhibitors are ATP-competitive, for example the PDB contains approximately 50 unique hinge-binding ligands for PKA[83]. This is unexpected as it is known that the residues of the ATP-site are highly conserved, however only a portion of the drug-molecules interact with the ATP-binding pocket, the rest are interacting with other less conserved parts of the protein kinase[28].

An important exception for PKA is the PKI pseudo-substrate peptide which bind in the place of the substrate peptide[19], inhibiting PKA. PKI was discovered in skeletal muscle extract in the 60's, but it was first isolated in 1971[35]. However, both PKA and PKI are found throughout the body, and PKI exists in several isoforms which has different inhibitory potency.

The inhibitors of protein kinases can be divided into four categories as shown below[46].

Type I The classical protein kinase inhibitors, bind competitively to the ATP-binding site

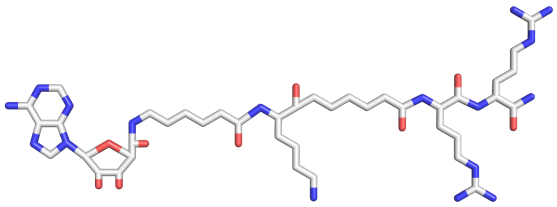

Figure 1.5: ARC-1012 is a bisubstrate inhibitor for PKA with its adenosine-moiety to bind to the ATP-binding site and the two arginines to bind to the substrate binding site.

Type II Inhibitors which lock the protein kinase in an inactive form by targeting a hydrophobic pocket adjacent to the ATP-binding site.

Type III Allosteric inhibitors which bind at a site outside of the ATP-binding site at the kinase

Type IV Covalent inhibitors which form a irreversible bond to the active site of the kinase, most often to a Cysteine.

As reviewed earlier[83], some inhibitors are made to interact with several sites, so that they no longer fit into one of the four categories above. Using fragment-based design, in which fragments which bind to distinct sites of the protein kinase are linked together in a manner that retains their binding[78], even more selective inhibitors can be created.

Bisubstrate inhibitors interact with two substrate-sites, such as the ATP-binding site and the peptide-substrate site[98]. Targeting two or more substrate-sites in the enzyme may increase the potency and specificity of the inhibitor[98]. It has been shown that the binding energy of a bisubstrate inhibitor is equal to the sum of the binding energies of the fragments[78] with a contribution from the linker up to $11\,\mathrm{kcal\,mol^{-1}}$[98] (Equation 1.2).

$$\Delta G_{\texttt{binding}} = \Delta G_1 + \Delta G_2 + \Delta G_{\texttt{linker}} \tag{1.2}$$

Several groups have introduced bisubstrate inhibitors for kinases[99, 80, 78].

Of special interest is the work done by an Estonian group that has constructed ARCs, where adenosine is conjugated with a polypeptide-chain with many arginines[78, 131, 103]. One of these ARCs is shown in Figure 1.5[103]. The same group demonstrated the use of bisubstrate inhibitors for affinity chromatography with these compounds, yielding homogeneous protein after a single purification step[81].

1.5 Heat shock proteins

Heat shock proteins are released in response to stressful conditions in a wide range of organisms. Some heat shock proteins are always present in the cell for quality control purposes, but the production is increased dramatically during stress-conditions. The nature of this protection lays in the chaperone activity of the heat shock proteins[94].

Heat shock proteins often form oligomers, ranging from dimers to multimers of more than 20 members[94].

Common for the heat shock proteins are the α-crystalline domain of approximately 90 residues. The domain has six to eight β-strands organized in two β-sheets. The amino terminal of this domain is often phosphorylated by protein kinases[94].

The phosphorylation of the α-crystalline domain has been shown to influence the oligomerisation state of the complex, for example, the large oligomers of 27 kDa heat shock proteins (HSPB1) will disassociate upon phosphorylation to smaller dimers and tetramers[94].

However, heat shock proteins can also modulate protein kinase activity, and there is data that HSPB1 binds and activates PKB which protects cells from apoptosis and deactivates the pro-death JNK-pathway[107, 94].

1.6 Affinity interactions

Affinity is the binding strength between a molecule and its ligand. The interactions which creates these bonds are non-covalent intermolecular forces. These forces are much weaker than covalent bonds individually, but when several intermolecular interactions occur in the same direction, the combined force may be sufficient to overcome the thermal motion of the system and make an ordered interaction[122].

Several forms of intermolecular interactions exist, most important are the:

1. Ionic interactions
2. Hydrogen bonds
3. Hydrophobic interactions

Ionic bonds can be very strong; in salts they can approach covalent bonds in strength ($500\,\mathrm{kJ\,mol^{-1}}$), hydrogen bonds are more frequent in protein structures, but weaker ($10\text{-}40\,\mathrm{kJ\,mol^{-1}}$). The hydrophobic interactions, or more correctly, the van der Waals bonds are rich in number, but much weaker individually than the other interactions ($1\,\mathrm{kJ\,mol^{-1}}$)[61].

In proteins, charged amino acids (e.g. Aspartic acid or Histidine) are able to form ionic bonds, polar side-chains (e.g. Serine or Threonine) and the amino and carboxyl-group of the main-chain can form hydrogen bonds, and hydrophobic side-chains (e.g. Leucine or Valine) can form van der Waals[106].

The total energy of interaction can be summarized as in Equation 1.3. Electrostatic interactions are the ionic interactions, induction happens when charged molecules interact with permanent dipoles, while dispersion is the instantaneous interaction between polarized molecules. Repulsion occurs when the orbitals of non-bonded atoms starts to overlap, and is very much distance-dependent[61, 113].

$$E_{\texttt{total}} = E_{\texttt{electrostatic}} + E_{\texttt{induction}} + E_{\texttt{dispersion}} + E_{\texttt{repulsion}} \tag{1.3}$$

$\pi - \pi$ interactions are a special case, and the contributing factors are not fully understood. Yet, it is clear that the π-orbitals of aromatic amino acids are able to interact. Aromatic rings with $\pi - \pi$ interactions are most often found to align themselves off-centered parallel displaced or in a T-shaped structure[92].

1.7 Protein production

To obtain amounts of protein sufficient for investigation it is often required to express the protein of interest in another host than its natural host because most proteins are only expressed in heavily regulated amounts whereas in overexpression of recombinant proteins with strong promoters can result in expression levels up to 40% of the total cell protein content[93].

Earlier this was a huge challenge, but today this is overcome for a wide range of proteins from different hosts and organisms. Today it is possible to express in bacteria, yeast, plant cells, insect cells and even human cells. Modern biotechnology allows the researcher to decide whether the full-length protein should be expressed or only a fragment. The protein can also be fused together with functional domains and motifs from other sources to "tag" the protein, giving the protein new features useful for the research work[57].

Proteins are encoded by genes, stored in the DNA of the cells. When expressing a eukaryotic gene in a prokaryote the DNA of the eukaryotic cells cannot be used directly since it contains introns which prokaryote lack systems to handle. Instead the gene has to be processed by the RNA polymerase, into messenger RNA (mRNA). Then the mRNA is extracted from the cell, and processed by a reverse transcriptase into a single-stranded DNA which can then be complemented to double-stranded DNA, this complementary DNA (cDNA) is stable and reliable. However, genes can also be synthesized in cases where cDNA is hard to obtain[57].

Choosing a suitable construct of the gene is of great significance; having multiple constructs doubles the chance that the resulting protein would be soluble[57]. This normally involves truncating at either the amino- or the carboxyl-terminal of the protein-sequence. By truncating regions associated with membrane binding and disordered regions (which would not be water-soluble) and leaving structure elements intact chances for soluble proteins are increased.

Cloning is most commonly performed using recombinant enzymes or ligation-independent cloning (LIC)[57].

Escherichia coli (*E.coli*) is very often used as the host for recombinant protein production, and compared to other hosts it is simple and inexpensive[93, 100]. It also works for a wide range of proteins, from simple prokaryotic proteins to full-length human proteins (even integral membrane proteins). Large-scale experiments show that 50% of eukaryotic and prokaryotic proteins express in soluble form in *E.coli*. However *E.coli* lacks the sophisticated machinery of eukaryotic cells, and does not have the same range of post-translational modifications and folding assistants as the eukaryotic cells have.

Choosing the correct strain of *E.coli* is also important, as different strains carry different genes. Some are deficient in certain genes, the BL21 (DE3) strain lacks the Ion and ompT proteases which protects the protein of interest from being digested. Many strains also carry antibiotic-resistance genes. The strain should also be compatible with the vector in use.

The choice of vector is made depending on the features needed. It is often beneficial to have a vector with fusion-tags, such as the hexahistidine-tag (commercially known as HisTrap) for simplified protein purification which will be discussed in section 1.8 or a TF-fusion for stabilization of unstable proteins.

Expression in *E.coli* often leads to the production of insoluble aggregates of misfolded protein, and depending on the ratio of soluble to insoluble protein expressed refolding might be necessary to obtain the amounts of protein needed. Some steps can be taken to reduce the amount of inclusion bodies: the growth temperature can be lowered, lowering the concentration of the inducing agent as well as increasing the aeration. Coexpression with chaperones such as TF might also improve folding [93].

After producing the protein in the bacteria, it must be recovered from the bacteria. Often the whole cell is disrupted mechanically using methods such as sonication and French press, with or without the help of enzymes such as Lysozyme which breaks down the cell-wall and DNase which breaks down nucleic acids[57]. Some proteins are secreted from the cell, thereby bypassing the entire problem[93].

1.8 Protein purification

After breaking the cells, the resulting cell-lysate is a mixture of cell-components including proteases which when uninhibited presents a threat to expressed proteins[63]. Protease activity can manifest itself after several purification-steps, and might manifest itself with lowered enzyme activity or loss of the protein sample as visualized on SDS-PAGE. It is important to add protease inhibitors to the samples to prevent unspecific cleavage of the expressed protein[16].

The cell-lysate contains debris from the broken cells; membranes, ribosomes and other organelles which should be removed since they would interfere with later steps. This can be done by centrifugation. Larger particles, such as the nuclei, will move quickly with the centrifugal force and form a pellet. Tuning the speed and time of the centrifugation allows proteins to be separated from the cell debris[5].

After clearing the cell lysate by centrifugation, it is possible to start to purify the target protein from the host proteins. Protein purification is often done in two or three

steps[63] as it is very uncommon for proteins to be purified in only one step:

1. Capture
2. Intermediate purification
3. Polish

In the capture step, the target protein is isolated from the bulk of the host proteins, while the polish step is aimed to ensure that the target protein is the only protein present and that it exists in only one form. The polishing step should remove aggregates and degradation products [63]. Three main techniques are in use today: Affinity-, Ion exchange- and size-exclusion-chromatography[5].

1.8.1 Affinity interaction chromatography

Affinity chromatography uses the attractive forces described in section 1.6 to adsorb a protein to a solid phase. Many different forms of affinity chromatography exists, most forms of ligands can be used in some manner. Antibodies, inhibitors, nucleic acids, hormones and sugars to mention a few examples[63]. The method is very powerful, because the specificity of ligand-binding can be very high for some ligands, while other ligands can be more group-selective. Some considerations for the ligands include

1. The binding should be reversible
2. The specificity should be suitable for the current application
3. The binding should be strong enough for stable complexes to form
4. But the bonds should also easily be broken by a change in buffers
5. The ligand needs to bind to a matrix somehow

1.8.1.1 Immobilized metal ion-affinity chromatography

Immobilized metal ion-affinity chromatography (IMAC) is also often included as a form of affinity chromatography, and is currently one of the most used methods for protein purification, especially using immobilized Nickel. Together with a metal-binding motif, such as the hexahistidine-tag which is easily engineered into the sequence. Longer histidine-stretches could also be beneficial for even tighter binding[63].

Proteins may be eluted from these columns by Imidazole or Histidine, or by modifying pH and ionic strength.

The interactions between the Histidines and the nickel-ion is illustrated in Figure 1.6.

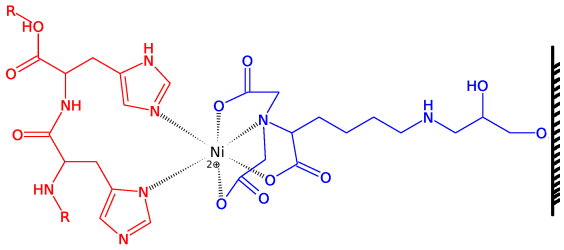

Figure 1.6: Binding of histidine-residues to a Ni-NTA-matrix, adapted from "The QIAexpressionist"[33]

1.8.1.2 ATP-analog resins

A huge variety of proteins bind to ATP, from protein kinases to motor proteins. A major issue is the binding of the ligand to the matrix, chemically modifying ATP to bind to a matrix may interfere with the protein-ATP-interaction. For this reason, it is beneficial to use a set of ATP-analog with different linkage strategies[13].

N^6-(6-Amino)hexyl-ATP-Agarose (6AH-ATP-Agarose) (Figure 1.7a) and $8-$[(6-Amino)hexyl]-amino-ATP-Agarose (8AH-ATP-Agarose) (Figure 1.7b) are two analogs, which have modifications on the adenine-moiety.

2'/3'-EDA-ATP-Agarose (EDA-ATP-Agarose) (Figure 1.7c) is modified on either the 2' or the 3'-site on the ribose ring.

AP-ATP-Agarose (Figure 1.7d) is modified on the γ-phosphate[12], with a phenyl-ring as a part of the linker making compound. The phenyl-ring provides the same interactions as the tyrosine of the substrate of a tyrosine protein kinase would[130].

A search of the literature shows that linkage on the γ-phosphate is the most commonly used linkage-strategy for protein kinases[64, 37, 60] as other linkage groups would be susceptible to steric hindrance[60], yet at least one protein kinase has been purified by ribose-linked ATP[65].

1.8.2 Ion-exchange chromatography

Ion-exchange chromatography (IEX) has been in use for over 50 years for proteins (ion exchange was first demonstrated in 1850 by Thompson), and has been tremendously popular. The method has high resolving power, high capacity for protein binding and its many variants offer versatility[63].

The key to the function of the ion exchangers is the functional site, either a positively (anion exchanger) or a negatively (cation exchanger) charged group (in rare cases both) which gives rise to electrostatic interactions between the protein and the ion exchanger[63].

Ion exchange is often used as a capture step, as proteins of interest can be adsorbed from a large volume into the much smaller column volume. Most commonly proteins are adsorbed from a buffer of low ionic strength, and eluted/desorbed by a buffer of higher ionic strength[63].

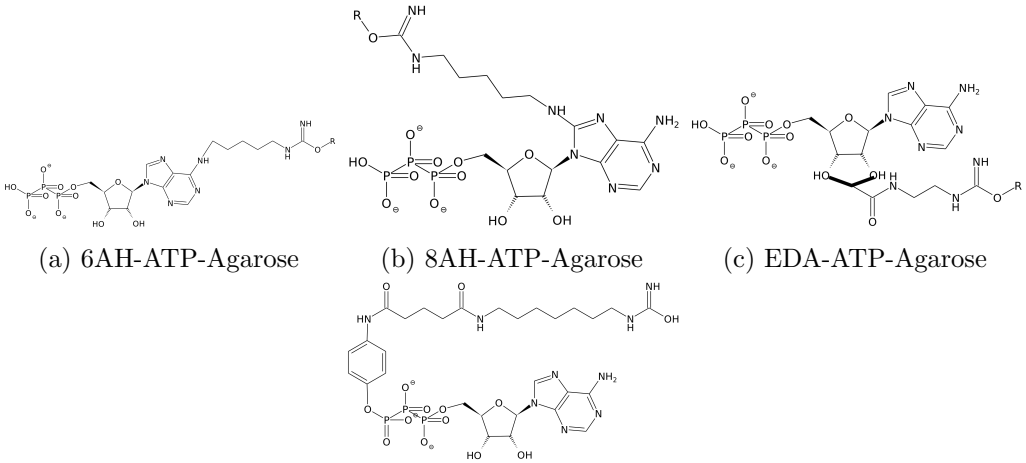

(a) 6AH-ATP-Agarose (b) 8AH-ATP-Agarose (c) EDA-ATP-Agarose

(d) AP-ATP-Agarose

Figure 1.7: The set of ATP-analogs used in this project

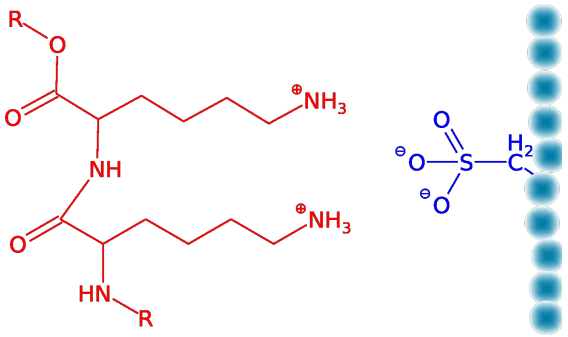

Figure 1.8: Binding of a positive peptide to a negatively charged strong cation-exchanger

Obviously the net charge of the protein is the main variable, but other factors also influence this, such as charge distribution, the choice of solvent-ions, non-electrostatic interactions with the matrix, temperature and additives[63].

The binding protein is in continuous competition with solvent ions for the charged groups on the ion exchanger, when the concentration of competing solvent-ions is increasing weakly interacting proteins will be displaced first[63].

The ion exchangers are often classified according to their pK_a value, weak exchangers have pK_a-values in the pH-ranges commonly used, and a change of pH in the sample can be used to change the nature of the ion exchanger from charged to uncharged. Strong exchangers have pK_a values outside of normal working pH-ranges, and will "always" be charged.

1.8.3 Size exclusion chromatography

Size exclusion chromatography, commonly referred to as gel-filtration, is perhaps the simplest chromatographic method to grasp. The first attempts were described in 1955 by Lindqvist et al., when they used swollen maize starch at very low flow rates, but the method only gained popularity after Porath and Flodin demonstrated size-exclusion chromatography with crosslinked Dextran in 1959. Applications range from desalting of protein solutions, purification of protein mixtures to determination of molecular mass of organic polymers [63].

The principle of separation is the non-specific interaction between the pores of the matrix and the solute, and the time the solute needs to pass through the liquid phase of the column [63]. Larger molecules will not fit into the smaller pores of the matrix, and will follow the flow through the column, and elute early. Smaller molecules will interact with many pores, and elute later.

1.9 Protein characterization

1.9.1 Sodium dodecyl sulphate polyacrylamide gel electrophoresis

SDS-PAGE separates polypeptides such as proteins according to their molecular weights. The detergent molecules of SDS form complexes with the protein molecules covering the surface of the protein with a fairly uniform distribution of 1.4 g SDS/g protein. As an anionic detergent SDS ensures that the charge of the protein is masked, which makes all proteins regardless of their pI migrate towards the anode in the electrophoresis-apparatus[133].

SDS-PAGE only provides an estimation of molecular weight when the migration of the sample is compared to a co-migrated set of molecular weight standards[133].

There is evidence that phosphorylation can give rise to mobility shifts in SDS-PAGE-experiments[73]. Phosphorylation of Thr-197 in PKA has been shown to shift the migration of PKA on SDS-PAGE[123, 138].

1.9.2 Tandem mass spectrometry

The principle of mass spectrometers is the measurement of motion of charged particles in an electric or magnetic field. Sample molecules are ionized in a gas phase, and separated according to their mass : charge ratio (m/z)[133].

In the field of proteomics the main criteria for a mass spectrometer is their sensitivity, mass accuracy and whether they can be used for tandem experiments[133].

There are many different techniques for ionizing the sample molecules; one of the methods is electrospray ionisation (ESI). The sample is led through an narrow capillary tube, under the influence of an electric field. The potential difference generates a force which drives the sample to form a cone from the tip of the capillary of fine mist. The solvent evaporates from the tiny droplets while the charge remains, ESI produces multiply charged ions[133].

After the ionization the ions need to be separated. The simplest form is the Time-of-Flight (TOF) analyser where larger molecules use longer times to reach the detector according to Equation 1.4 where k is a proportionality constant depending on instrument-factors[133].

$$\texttt{time of flight} = k\sqrt{m/z} \tag{1.4}$$

A quadropole analyzer consists of four parallel hyperbolic rods which have an alternating electric field, which only allows ions of certain m/z-values to reach the detector. By varying the voltage, a wide mass range may be observed. The quadropole can be combined with a non-scanning reflectron TOF analyzer which gives high mass accuracy, resolution and sensitivity[133].

In Tandem mass spectrometry (MS/MS) a instrument capable of selecting ions with a particular m/z-ratio is used to subject the selected ions to a second fragmentation within the mass spectrometer[133].

MS/MS is interesting in the field of proteomics because it can be used to identify a protein sample, by the use of peptide mass fingerprints. The pure protein sample is subjected to treatment with either proteases or chemical cleavage agents to generate shorter peptide fragments. Software such as MASCOT (`http://www.matrix-science.com`) searches databases of "theoretical" digests of protein sequences to match the experimentally determined masses. The protein identified is the one that gives the best match between theoretical and experimentally determined masses. Post-translational modifications such as methylation, oxidation and *phosphorylation* has to be taken into special consideration[133].

1.9.3 Biochemical assays

Due to the high importance of protein kinases as drug targets many assays have been developed to assist in developing new kinase inhibitors. These assays include both biochemical based functional assays and competitive binding assays. Fluorescence-based detection assays are easy to automate, but are susceptible to interference from the sample[86].

The KinomeScan offered by Ambit uses a competitive approach, where DNA-tagged protein kinases are interacting with biotinylated inhibitors bound to Streptavidin-covered beads. Test compounds with high affinity for the protein kinase will break the interaction with the biotinylated inhibitors, and elute the protein kinase. The hit is then quantified by subjecting the DNA to real-time polymerase chain reaction (qPCR)[86].

Radiometric based assays are very reliable and sensitive, and since they normally depend only on the labeling of ATP they can be quite universal[86].

1.9.3.1 Cook-assay

The Cook-assay couples the protein kinase activity (production of ADP from ATP) with pyruvate kinase and lactic dehydrogenase- activity. The pyruvate kinase phosphorylates ADP, transferring the phosphate-group from phosphoenolpyruvic acid (PEP) producing pyruvate and ATP. The lactate dehydrogenase converts the pyruvate into lactate, oxidising reduced nicotinamide adenine dinucleotide (NADH) yielding nicotinamide adenine dinucleotide (NAD+) in the process. The interconversion of NADH to NAD+ can be observed by a spectrophotometer set to monitor at 340 nm.

Compared to the previous radioisotopic assays, this assay is safer (no radioactive compounds) and cheaper, at cost of sensitivity[30].

It has been shown that protein kinases behave according to Michaelis Menten model of enzyme kinetics[110], which relates the rate of enzymatic reaction to the substrate concentration (Equation 1.5), for both ATP and substrate.

$$v = \frac{V_{\max}[S]}{K_m + [S]} \tag{1.5}$$

Inhibitors may also be characterized by the Cook-assay. The relationship between the rate of the reaction and the logarithm of the concentration of the inhibitor is known to be described best by a four-parameter logistic fit[118] shown in Equation 1.6 where the IC50-value is parameter C. IC50 is the concentration where 50% of the enzymes activity is inhibited.

$$y = D + \frac{A - D}{1 + (\frac{x}{C})^B} \tag{1.6}$$

1.9.4 Surface plasmon resonance

Biacore®is the trademark used by GE Healthcare for their surface plasmon resonance (SPR)-system. The principle behind SPR is the tethering of a "ligand" to a sensor surface, with an "analyte" flowing over the surface. The accumulation of analytes close to the surface (in association to the ligand-molecules) causes a change in the refractive index of the buffer near the surface measured by the optical detection system. The changes in refractive index over time are plotted as a sensorgram[112].

The detection-system allows real-time observation of the binding process, allowing both kinetic and thermodynamic characterisation of the interaction. The primary variable is the molecular weight of the interacting partners, and a major challenge has been interactions between small inhibitors and larger proteins[131, and references therein].

1.9.5 Thermofluor

Thermofluor®is a trademark used to describe the method of fluorescence-based microplate thermal shift assay. A hydrophobic fluoroprobe which fluorescence is quenched in aqueous environments is used to monitor the folding of the protein. The thermal unfolding of a protein exposes the hydrophobic core of the protein, decreasing the quenching of the hydrophobic fluoroprobe which allows for fluorescence emission to be measured. A qPCR-machine is used to gradually heat the protein beyond its melting point, while measuring the fluorescence-signal for the fluoroprobe[97].

The method was originally developed for development of new drug discovery, but has also found use as a tool to optimize buffer-conditions. The principle idea is that an inhibitor would bind to the protein in a stabilizing manner, increasing the melting point of the protein. Only 1-15 µg of protein is needed for each well, which together with the plate-format of the experiment makes it very suitable for high-throughput screening[43].

It has been shown that the change in T_m is proportional to the ligand concentration and the binding affinity[90].

1.9.6 Microscale thermophoresis

Thermophoresis is the movement of molecules in a heat-gradient, analogous to the electrophoresis of SDS-PAGE. This movement creates a local change in concentration (Equation 1.7) as molecules are moving. The movement of molecules in a heat gradient has been shown to depend on the Soret coefficient (S_T) and the temperature gradient. It has been suggested that the Soret coefficient may be described by Equation 1.8 where A is the surface area of the molecule, k is the Boltzmann constant, T is the temperature, ΔS_{hyd} is the hydration entropy, the Debye-Huckel screening length (λ_{DH}), the dielectric constant (ϵ) and its temperature derivate (β)[134].

$$\frac{c}{c_0} = \exp[-S_T * (T - T_0)] \tag{1.7}$$

$$S_T = \frac{A}{kT}\left(-\Delta s_{\text{hyd}}(T) + \frac{\beta\sigma_{\text{eff}}^2}{4\epsilon\epsilon_0 T} \times \lambda_{\text{DH}}\right) \tag{1.8}$$

This means that the movement of a molecule in a temperature-gradient primarily depend on its size, charge and hydration shell. Protein-protein interactions may change the surface-area of the protein, hydration shell and charge, while a protein-ion interaction may only change the charge. Small uncharged molecules may change the hydration shell, by rearranging or removing waters from the protein surface. Since any of these changes is enough to get a difference in thermophoresis, MST may quantify binding affinities ranging from protein-ion to protein-protein.

MST is a fast method, suitable for use with most buffer-systems and without immobilization. Proteins containing tryptophanes may be used directly, as tryptophan provides enough fluorescent signal, or with labelled samples. A K_d-measurement may be done within 10 min[66].

MST is the patented technology of NanoTemper Technologies GmbH.

1.9.7 Structure determination and X-ray crystallography

The primary structure of a protein is determined by the amino-acid sequence, either by MS/MS or by the translated nucleotide-sequence. The secondary structure of a protein can be estimated by tools such as circular dichroism. The most common method of obtaining a detailed image of the tertiary structure of protein molecules, allowing resolution of individual atoms, is X-ray crystallography[22]. Structures of quaternary complexes can be determined directly by the low-resolution method electron microscopy,

Diffraction data from a single crystal, gives information about the average position of the electron cloud of the molecule. This is only an indirect view, and the resulting model is only a model, not an image[111].

A crystal is defined as an ordered three-dimensional array of millions of identical units. The repeating unit is referred to as the *unit cell*, which may contain one or more molecules. While the packing of unit cells in crystals may be compared to stacking boxes in a warehouse, protein molecules are nothing like boxes. Protein molecules are more spheric in shape, and their packing introduces holes and channels which normally takes up half the volume of the unit cell (Figure 1.9), and for this reason their crystallization requires careful consideration of a large number of parameters combined[22] with a stroke of luck.

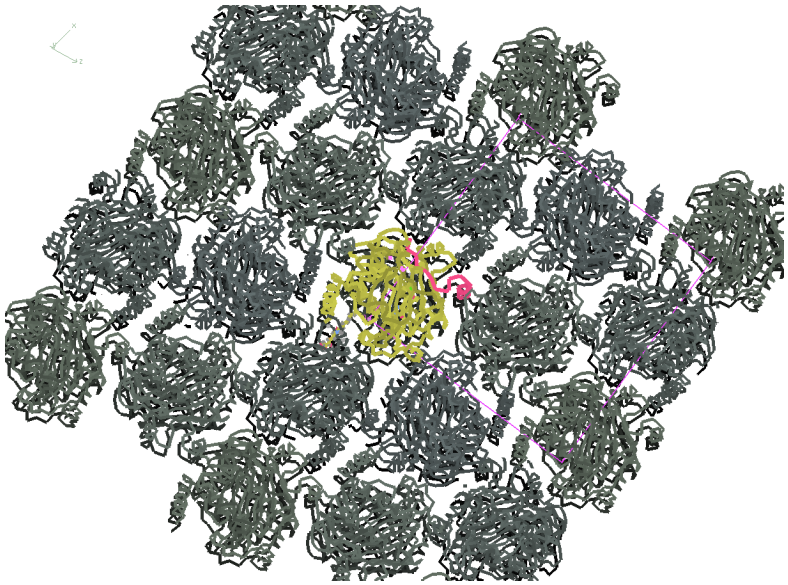

Figure 1.9: Crystal structure of PKAB3 showing the repeating protein unit cells. The purple box indicates one unit cell.

The protein sample generally needs to be pure and homogeneous, 97% purity or higher is recommended[22]. The protein sample needs to be gradually brought to a state of supersaturation where it is possible for crystal-seeds to form. Different crystallization methods are used to reach this goal, but the most successful method has been the hanging-

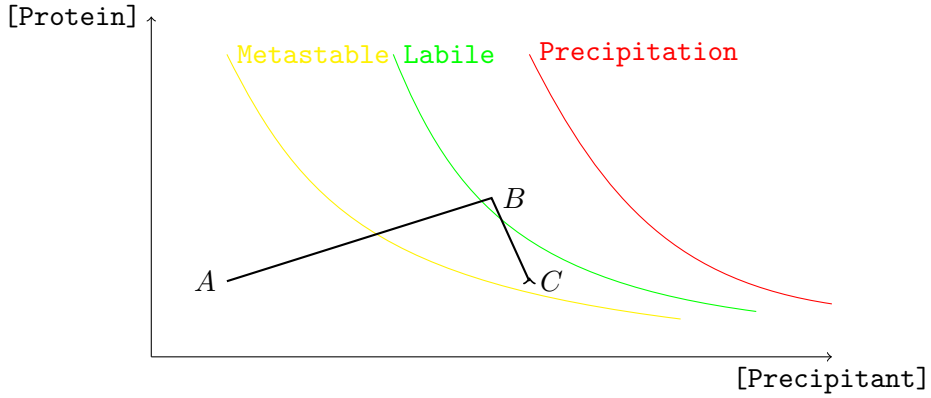

Figure 1.10: Phase-diagram for a hanging-drop experiment, with point a being the inital state (unsaturated) of the system. B is the supersaturated (labile) state where crystals are formed, the crystals will grow while the protein concentration drops until the phase-barrier to the metastable zone is reached again in point C.

drop method, where vapour diffusion gradually brings the solution to supersaturation as shown in Figure 1.10.

Proteins can pack in different crystal-forms depending on the crystallisation conditions, and in general the different forms will only differ in a few side-chains involved in crystal packing[22].

1.9.7.1 Hardware

X-rays are photons with very high energy. They are produced when electrons are accelerated into an anode (conventional "home" sources) or when electrons are accelerated close to the speed of light in synchrotrons. Synchrotron radiation is stronger than what is achievable by the anode-based x-ray generators, and is also tunable in terms of wavelength, whereas the anode-generated x-rays are inherently monochromatic.

Depending on the application, a monochromator might be used to give x-ray radiation of a narrow window of wavelengths.

A goniometer is used to rotate the crystal in one or more dimensions to explore all the possible diffraction spots of the crystal. Rotating the beam would be much more difficult.

The high energy of the x-rays pose a threat to the crystal, radiation damage which both disrupts and disorders protein molecules, which decreases the diffraction intensity and resolution, increases B-factors and unit cell dimensions as well as site-specific damages. Disulfide bonds may be broken, Aspartates and Glutamates are decarboxylated and tyrosine is dehydroxylated. Bromine and other "heavy" atoms are also at risk[108, 109]. For this reason it is important with cryo-cooling of the crystal, this is accomplished by a jet of nitrogen gas at $-150\,^{\circ}\mathrm{C}$[22].

1.9.7.2 Application

A crystal structure alone is of limited value, however together with other sources of information a structure can indicate binding sites and guide the drug design-process[23, and references therein]. Crystal structures are quite rigid and only small movements can be observed (and these complicate the structure determination significantly). This is a major contrast to the flexible protein in the cell. Comparing multiple crystal-structures in different crystal forms can reveal more about flexible regions,

In order to obtain crystals it is often necessary to modify the protein, as in the case for protein kinases where the catalytical domain is often studied alone. Other modifications include removing flexible peptide termini and flexible side-chains[23, and references therein], by alterations of the gene (mutation or change of construct) or by enzymatic action by proteases to remove the flexible termini or chemical modification with Gluteraldehyde to cross-link the protein[84].

A crystal structure should only be part of the overall picture together with results from other methods such as NMR[23, and references therein].

1.10 Aims of study

The overall aim of this project was to study the different interactions of protein kinase catalytical domains, and evaluate the possible applications of these.

Four main applications have been identified and discussed in this project:

1. Verification of binding
2. Folding diagnostics
3. Differentiation of phosphorylation states
4. Inhibitor design

The thesis has been sectioned to follow these four topics, although there is some degree of overlap between the topics. In the conclusion these topics has been recombined into two bigger categories.

1.10.1 cAMP-dependent protein kinase/protein kinase A

PKA is used as a model-protein-kinase, as it has many known structures with the first structure solved in 1993[19]. It is been used as a surrogate or "ersatz" kinase, to carry mutations making it more similar to other protein kinases[52, 18, 101, 53, 1]. PKA has also established procedures for recombinant expression, purification and crystallization[54, and references therein].

PKA is also interesting on its own, as it is involved in signaling pathways for metabolism, transcription, cell proliferation and differentiation, ion channel regulation and memory function[52, and references therein].

The catalytical domain of PKA is regulated by a regulatory domain, and in absence of cyclic adenosine monophosphate (cAMP) the two subunits form a inactive holoenzyme, but in when cAMP is present in high concentrations the catalytical domain is monomeric and active. In this project the affinity interactions in the ATP-binding site and the peptide

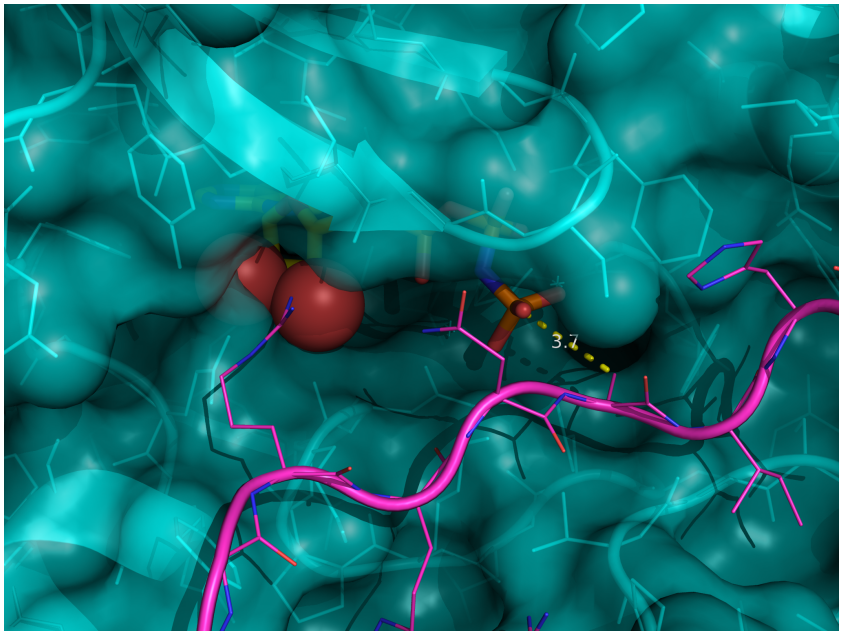

Figure 1.11: One aim of the study was to investigate what linkage modes were applicable for the ATP-binding site. The surface of PKA is shown in cyan, with PKI shown in pink, and ATP in yellow/orange with red spheres for the hydroxyls of the ribose-ring.

substrate binding site will be investigated. Five different constructs of the catalytical domain have been used: PKAB3 which is PKA with three mutations making it similar in the ATP-binding site towards PKB[54]; PKAR4 and protein kinase A fivefold mutant model of Rho (PKAR5) to make PKA more similar to Rho-kinase and to study the selectivity for the ATP-analogs; PKA Aur6 which is PKA with six mutations making the protein more similar to Aurora A kinase (AURKA) in the ATP-binding site[104] and finally PKA Aur7 which was engineered from PKA Aur6 to alter the binding of PKI by a single mutation.

1.10.2 Abelson tyrosine-protein kinase 1

ABL1 was early identified as a proto-oncogene, with its normal function being cytoskeletal reorganization, cell migration and response to conditions such as DNA damage and oxidative stress. In normal cells ABL1 is transiently activated by growth factors, but in the case of leukemia ABL1 is found to be constitutively active due to structural changes such as the fusion with Bcr[72, and references therein].

As with PKA, the catalytical domain subunit alone is much more active than the holoenzyme. Traditionally ABL1 was expressed in insect cells, however work is done to express in *E.coli*. There are issues with low yield due to cell toxicity caused by the active protein kinase. This can be countered by coexpression with YopH phosphatase which renders ABL1 inactive[100]. Work has also been done to coexpress a fusion protein with TF to promote stability and assist folding of ABL1[76]. This project will focus on studying the interactions of the catalytical domain with ATP-analog resins, and to investigate whether this could be a complimentary method for the expression in *E.coli* or to promote folding of partially unfolded protein.

1.10.3 Dual specificity tyrosine-phosphorylation-regulated kinases

Dual specificity tyrosine-phosphorylation-regulated kinases (DYRKs) belong to the CMGC-group of protein kinases, and they are of ancient origin with presence in four out of five of the kingdoms of life. They are named dual-specificity protein kinases because they are able to phosphorylate tyrosine, serine and threonine-residues, however tyrosine-activity is only observed for autophosphorylation. DYRKs are known as priming kinases, substrates phosphorylated by DYRKs is more efficiently phosphorylated by other protein kinases[10, and references therein]. DYRKs are important for differentiation in different tissues.

In humans DYRK1A is expressed in the brain, and mediates survival and differentiation of neural cells. Downs syndrome is caused by an extra copy of chromosome 21 where the gene for DYRK1A is located, and the resulting overexpression impairs differentiation of neural cells leading to mental retardation[49, and references therein]. DYRK1B which is also known as Mirk is normally expressed in skeletal muscle. DYRK1B is also active in several cancers, where it makes the cells unable to stay in quiescence[49, and references therein].

In this project the catalytical domains of DYRKs are tested against ATP-analog resins to evaluate their potential as purification-steps and to elucidate the details of the ATP-binding of the catalytical domains.

1.10.4 Aurora B kinase

AURKB together with the other Aurora kinases is active in aligning chromosomes during cytokinesis which is important for cells to divide in a proper manner[7, 96, and references therein]. Because of its central role in the mitosis, AURKB is a interesting anti-cancer drug. Inhibitors of AURKB prevent the alignment of the chromosomes, and disables the spindle checkpoint function and cytokinesis. Cells treated with inhibitors of AURKB exit mitosis without dividing, and are no longer viable[55, and references therein].

The development of selective inhibitors for AURKB could lead to anti-cancer drugs with fewer side-effects[55], and aid the development of selective inhibitors it is important to have good protocols for purification, which is why the catalytical domain of AURKB in this project is evaluated against a set of ATP-analog resins.

1.10.5 70 kDa heat shock proteins

HSP70 is a heat shock protein, a chaperone, involved in several cellular processes which is crucial for life. There is evidence linking HSP70 to cancer, and the development of potent inhibitors could be used as a treatment for cancer[135]. The N-terminal of HSP70 is the nucliotide binding domain (NBD), which has the ATPase fold for binding ATP. The C-terminal binds to a peptide substrate. The binding and release of peptide-substrates is linked to the ATPase activity of HSP70[136].

In this project only the NBD domain of HSP70 is studied to serve as an comparison to the ATP-binding mechanism of protein kinases. The high affinity HSP70 has for ATP, together with the well known protocols for expression and purification, make it an easy target to work with for this purpose.

Chapter 2

Methods

2.1 General protocols

2.1.1 Sodium dodecyl sulphate polyacrylamide gel electrophoresis

4–20% Mini-PROTEAN® TGX™ (Bio-Rad) were used where not otherwise specified. 5 µL of 4X NuPAGE® LDS Sample Buffer (Invitrogen) were mixed with either 5 µL (for cell lysates and flow-through (FT)-fractions) or 20 µL of protein sample. 6 µL of Mark12™ Unstained Standard (Invitrogen) were also applied for each gel for molecular weight approximations. The gels were run in a Mini-PROTEAN® Tetra Cell (Bio-Rad) at 200 V for approximately 35 min.

Following the run gels were washed with water, heated in a microwave-oven for 1 min and left to cool for 1 min before discarding the wash-water. The wash-procedure was repeated two more times. The washed gels were stained with SimplyBlue™ SafeStain (Invitrogen), and heated to boiling in a microwave-oven before being washed with water.

Gels were imaged using a Gel Doc™ system (Bio-Rad).

Table 2.1: 1000x Trace-elements for use in autoinduction media[124]

Salt	Concentration
$FeCl_3$	50 mM
$CaCl_2$	20 mM
$MnCl_2$	10 mM
$ZnSO_4$	10 mM
$CoCl_2$	2 mM
$CuSO_4$	2 mM
$NiCl_2$	2 mM
Na_2MoO_4	2 mM
H_3BO_3	2 mM

Table 2.2: 20× NPS-mix for use in autoinduction media[124]

Salt	Concentration
$(NH_4)_2SO_4$	0.5 M
KH_2PO_4	1 M
$NaHPO_4$	1 M

Table 2.3: 50×5052-mix for use in autoinduction media[124]

Component	Concentration (w/w)
Glycerol	25%
Glucose	2.5%
Lactose	10%

Table 2.4: Growth-media used in the production of recombinant proteins

	Contents
lysogeny broth (LB)	1% bacto-tryptone, 0.5% yeast-extract, 1% NaCl in MQ-water
LB-agar	1% bacto-tryptone, 0.5% yeast-extract, 1% NaCl, 1.5% agar-agar in MQ-water
terrific broth (TB)	1.2% peptone, 2.4% yeast extract, 72 mM K_2HPO_4, 17 mM KH_2PO_4, 0.4% glycerol in MQ-water
2xYT	1.6% bacto-tryptone, 1% yeast extract, 0.5% NaCl
ZY	1% bacto-tryptone, 0.5% yeast-extract
ZYP-5052	1 mM $MgSO_4$, 1× trace-elements mix (Table 2.1), 1× 5052-mix (Table 2.3), 1× NPS-mix (Table 2.2) in ZY-media.
NZY+	1% NZ amine, 0.5% yeast-extract, 0.5% NaCl, 12.5 mM $MgCl_2$, 12.5 mM $MgSO_4$, 20 mM Glucose

2.1.2 ATP-analog binding assay

Sample preparation Dialyze the sample against phosphate buffered saline (PBS)-buffer. Add 5x Binding-buffer (Jena Bioscience, AK-102B-S) and dithiothreitol (DTT) to a final concentration of 1 mM

Equilibration of resin Add 500 µL of 1X wash-buffer (prepared from 5X Wash-buffer, Jena-Bioscience, AK-102W-S) with 1 mM Sodium Orthovanadate and 1 mM DTT added to 50 µL of resin-material. Vortex to resuspend and spin down at 1000 g for 1 min. Remove supernantant carefully. Repeat two more times

Binding Add protein sample to the resins. Incubate at 4 ℃ for at least 2-3 h with agitation. Spin down at 1000 g for 1 min and remove supernantant carefully

Washing Resuspend resin in 1 mL ice-cold wash-buffer. Spin down at 1000 g for 1 min and remove supernantant carefully. Repeat two more times.

Elution Resuspend resin in 150 µL ice-cold 1x Elution buffer (prepared from 5X elution buffer, Jena Bioscience, AK-102E-S) with 1 mM Sodium Orthovanadate and 1 mM DTT. Incubate at 4 ℃ for at least 20 min with agitation. Spin down at 1000 g for 1 min and remove supernantant carefully. Repeat two more times.

2.1.3 Transformation

Approximately 100 ng of plasmid were mixed with 100 µL of BL21 cells (or otherwise specified) by gentle tapping against the table. The mix was incubated for 30 min in a ice-bath, and then heat-shocked at 42 ℃ for 45 s. After the heat-shock the sample was cooled down in a ice-bath for 2 min before approximately 500 µL of pre-heated super Optimal broth with Catabolite repression (SOC)-media was added. The transformation mix was kept at 37 ℃ for 1 h before being plated on LB-plates with appropriate antibiotics.

25 mL overnight pre-cultures of LB with appropriate antibiotics were made with single-colonies from the transformation-reaction in a shaking incubator at 37 ℃.

2.1.4 Cook-assay

To each well in a 96-well-plate 75 µL of reaction-mix (Table 2.5), 10 µL 200 nM PKA-sample and 5 µL of inhibitor is added before the reaction is started by the addition of 10 µL 10 µM ATP. The reaction is monitored as decreasing absorption at 340 nm using the SpectraMax M2e-plate-reader (Molecular Devices).

Table 2.5: Reaction-mix for Cook-assay[102]

Component	Final concentration	Volume
200 mM MOPS pH 6.8	100 mM	0.5 mL
1 M KCl	100 mM	0.1 mL
1 M $MgCl_2$	10 mM	10 µL
100 mM PEP	1 mM	10 µL
20 mM Kemptide	0.1 mM	5 µL
1 M $\beta-$Mercaptoethanol	1 mM	1 µL
Pyruvate kinase (900 U/mL) / lactic dehydrogenase (900 U/mL)	15 U/mL	15 µL
10.7 mM NADH	0.152 mg mL^{-1}	20 µL
H_2O		89 µL
		750 µL reaction mix

2.2 Verification of binding

2.2.1 70kDa **Heat shock protein**

2.2.1.1 Expression

1 µL of His-tagged nucleotide-binding domain construct of HSP70 in a pET28-vector was added to 100 µL of thawed BL21 DE3 RIL-cells, and the mix was incubated on ice for 20 min. The cells were then heat shocked for 45 s at 42 °C, and then cooled down again in the icebath. 200 µL of prewarmed SOC-media was added, and the mix was incubated for one hour at 37 °C in a shaker. 50 µL and 200 µL was plated on LB-plates with kanamycin (KAN) and chloramphenicol (CHL) added. The plates were then incubated overnight at 37 °C.

Three precultures of 25 mL LB-media with KAN/CHL was inoculated with single colonies from the plate with 50 µL transformation-mix. The precultures were incubated overnight at 37 °C in a shaker.

Four 2.5 L flasks with 750 mL of LB-media with KAN/CHL was inoculated with 20 mL of preculture and grown at 37 °C in a shaker set to 200 rpm until the optical density at 600 nm (OD600) reached high levels. The temperature was decreased to 20 °C, and the flasks were left to cool at the bench for awhile before adding 750 µL of 1 M isopropyl β-D-1-thiogalactopyranoside (IPTG) to each flask. The flasks were then returned to the shaker and left overnight.

The cells were harvested using centrifugation at 5000 rpm for 20 min, and the pellets were resuspended in 20 mL PBS-buffer with protease inhibitor cocktail (ethylenediaminetetraacetic acid (EDTA)-free) added and frozen at −20 °C.

2.2.1.2 Purification

A pellet was thawed and lyzed by a French press with pressure set to 1.35 kbar. The cell lysate was cleared by centrifugation at 20 000 rpm for 40 min.

The cleared cell lysate was then loaded on a 1 mL HisTrap HP-column. Unbound protein was washed out by a 25 column volume (CV) wash, and the protein was eluted during a 25CV stepwise-elution from 0%-100% PBS+0.5 M Imidazole. Fractions containing HSP70 were pooled.

2.2.1.3 ATP-analog binding assay

5 mL of HSP70 from HisTrap was mixed with 1.25 mL 5x Binding-buffer (Jena Bioscience, AK-102B-S) and 50 µL 100 mM DTT for testing with ATP-analogs according to the protocol in subsection 2.1.2.

Then 1.2 mL of this mix was added to 50 µL equilibrated ATP-analog-resins. The mix was incubated on a nutating mixer for 2.5 h.

Samples were taken for SDS-PAGE at each step. Bands from elution fractions were also sent to MS/MS.

2.2.2 Aurora B kinase

2.2.2.1 ATP-analog binding assay

5.5 mL of AURKB from HisTrap was mixed with 1.25 mL 5x Binding-buffer (Jena Bioscience, AK-102B-S), 2.5 µL 200 mM sodium ortho-vanadate and 25 µL 100 mM DTT for testing with ATP-analogs according to the protocol in subsection 2.1.2.

Then 1.2 mL of this mix was added to 50 µL equilibrated ATP-analog-resins. The mix was incubated on a nutating mixer overnight.

SDS-PAGE was run to evaluate binding.

2.2.3 Dual specificity tyrosine-phosphorylation-regulated kinase 1B

2.2.3.1 Expression

1 µL of the catalytical domain of DYRK1B in a plasmid with a N-terminal His-tag was transformed by the protocol in subsection 2.1.3, but with 300 µL SOC-media on LB plates with ampicillin (AMP)/CHL. Precultures were also made following the same procedure, with AMP/CHL.

A 500 mL culture of ZYP-5052 with AMP/CHL was inoculated with the overnight preculture and was kept at 37 °C for 2.5 h before the temperature was lowered to 20 °C overnight.

The cells were spun down in 0.5 L-flasks at 5000 rpm for 40 min, and the pellet was frozen at −20 °C with one tablet of protease inhibitor cocktail added.

Table 2.6: Buffers for purification of DYRK1B

Name	Contents	pH
Lysis	50 mM Na_3PO_4, 500 mM NaCl,0.5% Tween-20	8
Wash	50 mM Na_3PO_4, 500 mM NaCl	8
Elution	50 mM Na_3PO_4, 300 mM NaCl, 500 mM Imidazole	8

2.2.3.2 Purification with HisTrap

A tube containing approximately 4.5 g of frozen cells was thawed and resuspended in 20 mL lysis-buffer (Table 2.6). The resuspended cells were sonicated for 13 min with 9 s pulses with 30% amplitude at 8 ℃. The cell lysate was cleared by centrifugation at 20 000 rpm for 30 min.

The cleared cell lysate was applied to a HisTrap FF Crude 1mL-column on the äkta Purifier-system (GE Healthcare) by the sample pump. The column was washed with 10 CV of wash-buffer (Table 2.6), then with a 10 CV 5% step of elution-buffer (Table 2.6), followed by a 25 CV gradient to 100% elution-buffer.

Samples were loaded on SDS-PAGE for analysis.

2.2.3.3 ATP-analog binding assay

The fractions containing the highest peak of DYRK1B from HisTrap was dialyzed against PBS+EDTA at 4 ℃ over night. The rest of the procedure was performed as described in subsection 2.1.2.

2.2.4 Dual specificity tyrosine-phosphorylation-regulated kinase 1A

2.2.4.1 ATP-analog binding assay

A purified sample of DYRK1A was diluted to 4 mL of approximately 0.5 mg mL^{-1}, and dialyzed against PBS+EDTA at 4 ℃ for 3 h. The rest of the procedure was performed as described in subsection 2.1.2.

2.3 Folding diagnostics

2.3.1 Abelson tyrosine-protein kinase 1

2.3.1.1 Verification of plasmid by restriction enzymes

To verify the incorporation of the ABL1 gene, both wild-type and gatekeeper-mutant, and the YOPH gene into plasmids a restriction digest was performed. For ABL1 a mix was made with 34 µL MQ-water,5 µL restriction-buffer, 5 µL plasmid, 1 µL bovine serum albumin (BSA), 5 µL NdeI and 5 µL XhoI. For YOPH a mix was made with

35 µL MQ-water,5 µL restriction-buffer, 5 µL plasmid, 5 µL AvrII and 5 µL NcoI. The restriction digest mixes was incubated at 37 °C for 90 min in a water-bath. 10 µL of 6x DNA loading buffer was added to each tube. A 1% Agarose-gel was prepared with 2.5 µL of 20000x RedSafe (CHEMBIO). Loaded the entire samples, and included 10 µL 1kb DNA-ladder (NEB). The gel was run for 1 h at 90 V.

2.3.1.2 Purification

Two tubes of wild-type ABL1 with protease inhibitor cocktail was thawed, and sonicated on icebath for 15 min with 9.9 s pulses with maximum temperature of 8 °C. The resulting cell-lysate was cleared by centrifugation in SS-34 tubes at 14 500 rpm for 40 min at 4 °C.

The buffer used was 50 mM 2-Amino-2-hydroxymethyl-propane-1,3-diol (TRIS) at pH 8, 500 mM NaCl and 5% Glycerol with 25 mM and 500 mM Imidazole for buffer A and B respectively.

80 mL of the cleared cell lysate was loaded on a 5 mL HisTrap HP column using a peristaltic pump. Unbound protein was washed out with buffer A until absorbance at 280 nm (UV280) approximated baseline. The protein was eluted by changing into 100% buffer B.

The fractions containing ABL1 were pooled and 7 mL was dialyzed overnight against 1 L PBS+DTT on a magnetic stirrer at 4 °C using Snakeskin 3350 dialyse-tubing.

2.3.1.3 ATP-analog binding assay

5 mL of ABL1 from HisTrap was mixed with 1.25 mL 5x Binding-buffer (Jena Bioscience, AK-102B-S) and 50 µL 100 mM DTT for testing with ATP-analogs according to the protocol in subsection 2.1.2..

Then 1.2 mL of this mix was added to 50 µL equilibrated ATP-analog-resins. The mix was incubated on a nutating mixer for 3 h.

Then 150 µL of cooled 1X elution-buffer (prepared from 5X elution buffer, Jena Bioscience, AK-102E-S) was added and the mix was incubated for 30 min before centrifugation and pipetting.

SDS-PAGE was run to evaluate binding. Bands from elution fractions were also sent to MS/MS.

2.3.2 Trigger factor-Abelson tyrosine-protein kinase 1

2.3.2.1 Expression

1 µL of ABL1 in pCold TF-vector (Takara) and 1 µL of YopH phosphatase in pCDF-Duet vector was tested with 50 µL of BL21-T1^R-cells (Sigma-Aldrich) and 100 µL BL21 (Takara). The cells were then tapped against the table to mix and left on ice for 30 min before heat shock. The heat shock was performed at 42 °C for BL21 and 37 °C for BL21-T1^R-cells for 45 s using two water-baths. Incubated on ice for 2 min before adding room-temperated SOC to the BL21-T1^R-cells and heated SOC to the BL21-cells.

Plates were set up for both cell lines with 50 µL and 150 µL transformation-mix plated, and grown overnight at 37 °C.

Prepared 50 mL preculture with LB media with AMP and KAN and inoculated with a single colony. Preculture was grown overnight in a 250 mL erlenmeyer flask at 37 °C with shaking in a incubator.

1 L of TB-media with AMP and KAN was inoculated with the preculture and poured into two 2.5 L shaking flasks. The culture was grown at 37 °C at 180 rpm.

After reaching high OD600 the cultures were put on ice-bath to cool down to approximately 15 °C. IPTG was then added to a final concentration of 0.2 mM. The cultures were then left at 15 °C overnight in the shaker.

Pellets were harvested by centrifugation at 5000 rpm for 30 min at 4 °C. The cells were transfered into 50 mL-falcon tubes and resuspended in the buffer from subsection 2.3.1.2 with 1 tablet Complete protease-inhibitor cocktail (Roche) added. The cells were then frozen at −20 °C.

2.3.2.2 Purification

Cells were partially thawed and sonicated for 16 min with 9.9 s pulses on/off with a 8 °C max. The resulting cell-lysate was cleared by centrifugation in SS-34 tubes at 14 500 rpm for 40 min at 4 °C.

45 mL of the cleared cell lysate was loaded on a 5 mL HisTrap HP column using a peristaltic pump. Unbound protein was washed out with buffer A until UV280 approximated baseline. The protein was eluted by changing into 100% buffer B.

2.3.2.3 ATP-analog binding assay

The assay was done as described in subsection 2.1.2, with clarified 1.2 mL cell-lysate for each resin. The sample binding incubation was done over 2 days.

2.4 Differentiation of phosphorylation states

2.4.1 Protein kinase A sixfold mutant model of Aurora B

2.4.1.1 Expression

Plasmid with PKA Aur6 in pT7-7-vector was thawed. 1 µL was added to 100 µL BL21 RIL-cells. The cells were incubated on ice for 30 min before being heat shocked for 45 s at 42 °C. The cells were then cooled down for 2 min in a ice-bath.

450 µL of room-temperated LB-media was added and the cells were grown for 1 h at 37 °C with shaking. Plated out 150 µL on a LB-plate with AMP and CHL. Then the rest of the transformation-mix was spun down using a table-top centrifuge. The supernantant was removed by careful pipetting, and the pellet was resuspended by pipetting the residual liquid. This concentrated transformation mix was also plated out on a separate plate.

Prepared precultures of 50 mL with 2xyeast extract and tryptone (YT)-media with AMP and CHL.

2 L of YT-media was prepared with AMP and CHL, and inoculated with 25 mL L^{-1} preculture. Cultures were grown to high OD600 and then cooled down in water-bath before inducing with IPTG to a final concentration of 1 mM. The cultures were left in the shaker at 20 °C overnight.

Pellets were collected by centrifugation, 5000 rpm for 30 min at 20 °C. Resuspended in 50 mM Tris at pH 7.5 with 500 mM NaCl to approximately 25 mL. A half tablet of protease-inhibitor cocktail was added to each. The resuspended cells were then frozen at −20 °C.

2.4.1.2 Purification with immobilized PKI

The frozen cells were thawed and sonicated for 15 min with 9 s pulses on/off with a temperature maximum of 10 °C. The cell lysate was cleared by centrifugation at 14 000 rpm for 30 min.

Affi-gel 10 affinity chromatography media was thawed and shaken for 5 min. To remove the storage-solution, isopropanol, 5 mL of the media was washed with 15 mL cold water. Water was added to the media, and then the suspension was centrifuged at 3000 rpm for 2 min. Then the supernantant was removed by pipetting, and the procedure was repeated until the smell of isopropanol disappeared. 5 mg of the 5-24 fragment of PKI was dissolved in 10 mL of preparation buffer (See Table 2.7) and mixed with the Affi-gel 10 media overnight in a nutating mixer at 4 °C.

The cleared cell lysate was prepared for purification by adding $MgCl_2$ and ATP to final concentrations of 5 mM and 2 mM respectively. The protein solution was then mixed with PKI which was immobilized on the Affi-gel media. The mix was incubated for 2 h at 4 °C in a nutating mixer.

The purification was done by decanting the mixture into a disposable PD-10 columns (GE Healthcare, 17-0435-01), and letting the lysate drain through. The column were washed with six CV of Wash I and then six CV Wash II (See Table 2.7). The purified PKA was eluted with six CV of Elution buffer (See Table 2.7).

2.4.1.3 Using ARCs to elute from immobilized PKI

The sample was prepared in the same manner as in subsection 2.4.1.2. The purification was done by decanting the mixture into four disposable PD-10 columns (GE Healthcare, 17-0435-01), and letting the lysate drain through. The columns were washed with six CV of Wash I and then six CV Wash II (See Table 2.7). The purified PKA was eluted with two CV of Elution buffers containing ARCb and ARCc with and without L-arginine (See Table 2.7).

2.4.1.4 Thermofluor

35 µM PKA Aur6 was tested with ARCs and H-89 on a MiniOpticon RT-PCR-machine (BioRad) configured for the dyes FAM/HEX using Sypro-Orange (Sigma Aldrich) in the

Table 2.7: Buffers used for purification of PKA through purification with immobilized PKI

Name	Contents	pH
Preparation buffer	50 mM HEPES	6.5
Wash I	50 mM TRIS, 50 mM NaCl, 2 mM $MgCl_2$, 400 µM ATP	7.5
Wash II	50 mM TRIS, 250 mM NaCl, 2 mM $MgCl_2$, 400 µM ATP	7.5
Elution	50 mM TRIS, 50 mM NaCl, 200 mM L-arginine	7.5
Elution-ARCb-	50 mM TRIS, 50 mM NaCl, 10 mM ARCb	7.5
Elution-ARCb+	50 mM TRIS, 50 mM NaCl, 10 mM ARCb, 200 mM L-arginine	7.5
Elution-ARCc-	50 mM TRIS, 50 mM NaCl, 10 mM ARCc	7.5
Elution-ARCc+	50 mM TRIS, 50 mM NaCl, 10 mM ARCc, 200 mM L-arginine	7.5

Table 2.8: Primers used for the site-directed mutagenesis of PKA Aur7

Primer	Sequence	Melting point
FWD	CCCGCCTTCGATGCAGACCAGCCCATCC	84.9 °C
RWD	CTGGATGGGCTGGTCTGCATCGAAGGGC	82.5 °C

temperature-range 20-90 °C using a temperature-gradient of 1 °C min^{-1} with 30 s-hold time.

2.5 Inhibitor design

2.5.1 Protein kinase A sevenfold mutant model of Aurora B

2.5.1.1 Site-directed mutagenesis

The mutant hPKA-Aur6 F240D was made by the use of the QuikChange II site-directed mutagenesis method with solutions provided by Stratagene (Cat#200523, La Jolla CA, USA) and with primers (Table 2.8) designed by the PrimerX-software[77] and synthesized by Sigma-Aldrich (St. Louis,MO). The forward and reverse primers Table 2.8 were diluted to 400 ng μL^{-1}. The initial polymerase chain reaction (PCR) was performed with both 10 and 50 mg of PKA Aur6-plasmid and with pWhitescript as a positive control using PfuUltra HF DNA polymerase, with denaturation at 95 °C for 30 s, annealing at 55 °C for 1 min and polymerisation at 68 °C for 3 min for a total of 16 cycles.

To remove the methylated unmodified PKA Aur6-plasmid 1 µL of 10 U/µL DPN1 was added, and the reaction was incubated for 60 min at 37 °C.

The mutated plasmid was transformed into XL1- Blue-cells by adding 1 µL of DPN1-

Table 2.9: 14X-Master-mix for Colony-PCR-analysis

Component	Volume
Ampliqon Master-mix	315 µL
pT7 FWD primer	14 µL
pT7 RWD primer	14 µL
ddH_2O	7 µL

treated plasmid to 50 µL of thawed XL1-Blue competent cells. The mixture was incubated on ice for 30 min before being heat-shocked at 42 ℃ for 45 s. The transformation-mixture was then cooled down in a icebath for 2 min. 500 µL of preheated NZY+-media (Table 2.4) was added, and the mixture was incubated at 37 ℃ for 1 h in a shaking-incubator.

250 µL was plated out on LB plates with AMP.

To confirm the mutation-efficiancy colony-PCR was performed in addition to dye-substitution sequencing. 10 single colonies from the transformation-plate were extracted with a pipette tip, and the pipette tip was used to inoculate a section of a second LB/AMP-plate as well as a PCR-tube with 25 µL of master-mix (Table 2.9). A positive control with unmodified plasmid and a negative control with water instead of plasmid was also included in the experiment.

The PCR was performed with denaturation at 95 ℃ for a initial 5 min followed by 30 s each cycle, annealing at 55 ℃ for 30 s and polymerization at 72 ℃ for 30 s each cycle followed by a 7 min polymerization-step to finish. 25 cycles was used.

A 1% agarose-gel was prepared with 5 µL RedSAFE added to 50 mL agarose. 5 µL of each sample was applied, and a 1 kb ladder was used. The gel was running for 1 h with 90 V.

5 mL precultures of LB/AMP were prepared for verified colonies overnight at 37 ℃.

DNA was extracted from the precultures by miniprep. 3 mL culture was spun down to pellet at 13 krpm for 25 s in two rounds in eppendorf-tubes. 200 µL of P1-buffer was added, and the tubes were vortexed to resuspend the pellet. 200 µL of P2-buffer was added, and mixed by invertion until purple-colour. 400 µL of P3-buffer was added, and the tube was shaken until the solution turned yellow. The solution was cleared by centrifugation at 13 krpm for 3 min. The supernantant was transferred to a Zymo-Spin 11N-column, and centrifuged at 13 krpm for 30 s. The column was then washed by 200 µL of endo-wash-buffer and centrifuged at 13 krpm for 15 s. The column was then washed by 400 µL of plasmid-wash-buffer and centrifuged at 13 krpm for 30 s. Finally, the column was transferred into a new 1.5 mL eppendorf-tube and the DNA eluted by the addition of 30 µL elution-buffer followed by centrifugation at 13 krpm for 15 s. DNA-concentration was measured by UV-absorbance.

The mutated plasmid was also sequenced by dye-substitution sequencing. 1 µL BigDye 3.1 was mixed with 4 µL 5X sequencing buffer, 2 µL plasmid (to a total of 200 ng), 1 µL 1 µM pT7-RWD primer and 12 µL nuclease-free dH_2O. The mixture was spun down in a table centrifuge before PCR. The PCR was performed with denaturation at 96 ℃ for a initial 5 min followed by 10 s each cycle, annealing at 50 ℃ for 5 s and polymerization

at 60 ℃ for 4 min. 25 cycles was used on a MJ research PTC-200 PCR-machine. The samples were then sent for sequencing.

2.5.1.2 Expression

1 µL of PKA Aur7-plasmid was used for transformation as described in subsection 2.1.3. Two 500 mL cultures of ZYP-5052 with AMP were inoculated with the overnight preculture and was kept at 37 ℃ for 2.5 h before the temperature was lowered to 20 ℃ overnight.

The cells were spun down in 0.5 L-flasks at 5000 rpm for 40 min, and the pellet was frozen at −20 ℃ with one tablet of protease inhibitor cocktail added.

2.5.1.3 Purification with immobilized PKI

Purification with immobilized PKI was done as described in subsection 2.4.1.2, with both unmodified PKI-peptide synthesized by GL Biochem (Shanghai, China) and modified PKI with a Phe-Asn-modification synthesized by NORUT (Tromsø, Norway).

2.5.1.4 ATP-analog binding assay

The assay was done as described in subsection 2.1.2, with clarified 1 mL cell-lysate for each resin. The sample binding incubation was done over 2 days.

2.5.1.5 Cook-assay

The assay was performed as described in subsection 2.1.4 with the inhibitor 34a.

2.5.2 Protein kinase A threefold mutant model of AKT

2.5.2.1 Expression

1 µL of PKA Aur7-plasmid was used for transformation as described in subsection 2.1.3. Eight 500 mL cultures of ZYP-5052 with AMP was inoculated with the overnight preculture and was kept at 37 ℃ for 6 h before the temperature was lowered to 20 ℃ overnight.

The cells were spun down in 1 L-flasks at 5000 rpm for 40 min, and the pellet was frozen at −20 ℃ with one tablet of protease inhibitor cocktail added per liter.

2.5.2.2 ATP-analog binding assay

The assay was done as described in subsection 2.1.2, with 1 mL clarified and dialyzed cell-lysate for each resin. The sample binding incubation was done over 2 days.

2.5.2.3 Cook-assay

The assay was performed as described in subsection 2.1.4 with the inhibitor 34a.

2.5.2.4 Thermofluor

45 µM PKAB3 was tested with ARCs at approximately 10 µM, 34a at 0.1 mM and 0.1 mg mL^{-1}N-[2-[[3-(4-Bromophenyl)-2-propenyl]amino]ethyl]-5-isoquinolinesulfonamide (H-89) with the buffer 50 mM MOPS pH 6.8, 50 mM KCl and 10 mM $MgCl_2$ on a MiniOpticon RT-PCR-machine (BioRad) configured for the dyes FAM/HEX using Sypro-Orange (Sigma Aldrich) in the temperature-range 10-90 °C using a temperature-gradient of 0.3 °C min^{-1} with 0.3 s-hold time.

2.5.2.5 Purification with immobilized PKI

The frozen cells were thawed and sonicated for 20 min with 9 s pulses on/off with a temperature maximum of 8 °C. The column and sample was prepared in the same manner as described earlier, see subsection 2.4.1.2, using Wash I, Wash II and Elution buffer from Table 2.7, with both unmodified PKI-peptide synthesized by GL Biochem (Shanghai, China) and modified PKI with a Phe-Asn-modification synthesized by NORUT (Tromsø, Norway). Protein concentration was estimated by Bradford-assay[21].

2.5.2.6 Cationic exchange

A MonoS-column was used with 20 mM KPO_4 at pH 6.5, and 20/500 mM KCl as running buffers. The sample was diluted five-fold with dH_2O to lower the ionic strength. The protein was eluted using a 0-50% gradient followed by a step to 100%.

2.5.2.7 Surface plasmon resonance

A fraction belonging to the second peak of the cationic exchanger (Figure 3.27) was dialyzed against 50 mM 3-(N-morpholino)propanesulfonic acid (MOPS) pH 6.8, 50 mM KCl and 10 mM $MgCl_2$ with a ratio of approximately 1:200 over a weekend. The dialyzed protein was diluted 1:20 into 10 mM Sodium Acetate-buffer at pH 4.5, 5.5 and 6.5 for pH-scouting. The pH-scouting was performed with 5 µL min^{-1} flow rate with 120 s contact time for the sample using PBS as the running-buffer. 1 M 2-Aminoethanol at pH 8.5 was used to regenerate the surface.

To immobilize the protein the dialyzed protein was diluted 1:20 into 10 mM Sodium Acetate-buffer at pH 4.5 containing 200 µM ATP and 2 mM $MgCl_2$. The CM5-surface was activated using a mixture of 62 µL 0.5 M 1-ethyl-3-(3-dimethylaminopropyl)carbodiimide (EDC) and 62 µL 0.2 M N-Hydroxysuccinimide (NHS) of which 70 µL was applied to the surface over 420 s using a flow of 10 µL min^{-1} with 50 mM MOPS pH 6.8, 50 mM KCl and 10 mM $MgCl_2$ as the running buffer. After a wash with running buffer, the protein-solution was applied to the surface 420 s using a flow of 10 µL min^{-1}. The chip's surface was finally blocked after another wash with buffer using 70 µL of 1 M 2-Aminoethanol at pH 8.5.

ATP was dissolved in running buffer to 10 mM and serial-dilutions were made 1:10 to 0.1 µM for kinetic/affinity-studies. All the concentrations were included in the experiment, with duplicates of 10 µM and the blank-sample (containing no protein). 120 s contact-

time was used with a flow of 30 µL min^{-1}, and the disassociation-time was 600 s. No regeneration-step used.

2.5.2.8 Microscale thermophoresis

Labelling of 20 µM PKAB3 was done by 30 min incubation with NHS and the dye NT-647. Unreacted dye was removed by gel-filtration using Sephadex G25-columns and the protein eluted in optimized MST-buffer.

The inhibitor 34a was diluted to 300 µM by addition of optimized MST-buffer. From this stock concentration, 15 serial dilutions were made 1:1 by adding 10 µL inhibitor-solution to 10 µL MST-buffer in PCR-tubes. To 10 µL of inhibitor-solution 10 µL of 1:50 diluted labelled PKAB3 was added. Samples were transferred into hydrophillic capillaries (NanoTemper) by capillary action, and loaded on the sample tray. The thermophoresis was then measured in a Monolith NT.115 machine (NanoTemper) with MST-power set to 20% and LED-power set to 60&.

PKAB3 was also used for a label-free experiment with the modified PKI-peptide, after checking the fluorescence of the protein sample. To 10 µL of inhibitor-solution 10 µL of 500 nM PKAB3 in 50 mM MOPS pH 6.8, 50 mM KCl, 10 mM $MgCl_2$ and 0.5 mM ATP. Modified PKI was used at a concentration of 100 µM and 15 serial dilutions were made as described for 34a. Samples were transferred into hydrophillic capillaries (NanoTemper) by capillary action, and loaded on the sample tray. The thermophoresis was then measured in a Monolith NT.LabelFree machine (NanoTemper) with MST-power set to 40% and LED-power set to 50&.

2.5.2.9 Crystallisation

Samples of approximately 10 mg mL^{-1} with 0.8 mM PKI and 1.5 mM Mega8 were crystallized using hanging drop method, with protein-drops of 1 µL equilibrated against 500 µL reservoirs of $12 - 18\%$ methanol at 4 °C.

For the crystal with the inhibitor 47a, the inhibitor was soaked in overnight[1], while the inhibitor 34a was cocrystallized[2]. Both inhibitors were used at a concentration of 1 mM.

Crystals were harvested and dipped in 30% 2-Methyl-2,4-pentanediol (MPD)-solution and flash-cooled in liquid N_2.

2.5.2.10 Data collection and processing

Diffraction-images were collected at the 14.1-beamline at BESSY (Berlin), using a wavelength of 0.9184 Å using a MARC MOSAIC3-detector with a distance of198.1 mm to the detector. The images were indexed, indexes were refined and spots were integrated using the XDSAPP- software package[75]. Choice of space group was verified using the

[1] by Kazi Asraful Alam and Richard A. Engh

[2] by Alexander Pflug

POINTLESS software-package through the Collaborative Computational Project No. 4 (CCP4) Program Suite 6.3[45, 44, 14].

Python-based Hierarchical ENvironment for Integrated Xtallography (PHENIX)[2] was used to perform molecular replacement using phaser[91, 126]. The structures were refined using phenix.refine[3]. The web-service PRODRG was used to generate coordinates and molecular topologies of the ligands[117] for use in the refinement. Densities,geometries and rotamers were evaluated in coot[41], and waters and ligands were also added using coot.

2.5.3 Protein kinase A mutant model of Rho

2.5.3.1 Expression

Plasmids containing the catalytical domain of PKAR4 and PKAR5 was transformed as described in subsection 2.1.3 into BL21 Star pRARE pLysS-cells. Precultures were made by transferring single colonies from the transformants-plate to 25 mL of LB-media with AMP-added.

1 L of autoinduction-media (Table 2.4) was inoculated with 2*25 mL preculture, and grown for approximately three hours at 37 ℃ before the temperature was lowered to 20 ℃ for overnight expression. Cells were harvested by centrifugation at 5000 rpm for 35 min in a JLA9.100-rotor.

The cells were resuspended to 50 mL with 50 mM Tris at pH 7.5 with 50 mM NaCl with one tablet of protease inhibitor cocktail added. After resuspension the cells were lysed by sonication, 15 min active with 9/9 s pulses with 8 ℃ max temperature and 40% amplitude. The cell lysate was then cleared by centrifugation at 20 000 rpm for 35 min using a JA25.50-rotor.

2.5.3.2 ATP-analog binding assay

The assay was done as described in subsection 2.1.2, with 1 mL clarified and dialyzed cell-lysate from both mutants for each resin. The sample binding incubation was done over 2 days for PKAR4 and 1 day for PKAR5.

Chapter 3

Results

3.1 Verification of binding

3.1.1 70kDa Heat shock protein

3.1.1.1 Expression

Transformation of the hexa-histidine tagged nucleotide-binding domain of HSP70 in pET28 vector into BL21 DE3 RIL-cells produced viable transformants giving colonies when plated on LB-plates with CHL/KAN.

Overnight precultures from single colonies gave highly turbid samples, which was successfully used to inoculate larger cultures. In three hours the OD600 went from 0 to 1.

3.1.1.2 Purification

Some clogging of the HisTrap column occurred during sample loading, and not all the sample was loaded. The elution however proceeded as planned, and is shown in Figure 3.1. The purification gave a single elution peak consisting primarily of HSP70 as indicated by SDS-PAGE(data not shown).

3.1.1.3 ATP-analog binding assay

SDS-PAGE results in Figure 3.2 show that HSP70 binds two of the four ATP analogs from Jena Bioscience. These ATP-analogs are linked to the matrix on the nucleotide-moiety of the ATP-analogs by C10-linkers.

3.1.2 Aurora B kinase

3.1.2.1 ATP-analog binding assay

Based on the results shown in Figure 3.3 there is no evidence that AURKB binds to the ATP-analogs. The major band of the SDS-PAGE is of the correct size for the catalytical domain of protein kinases.

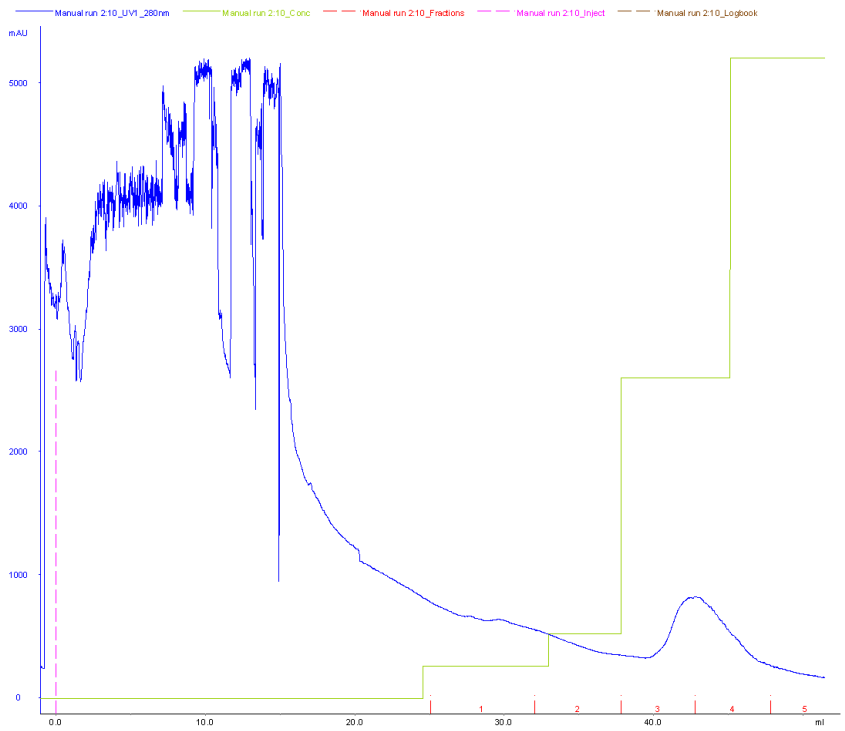

Figure 3.1: Chromatogram showing the washing and elution of HSP70 from a HisTrap column

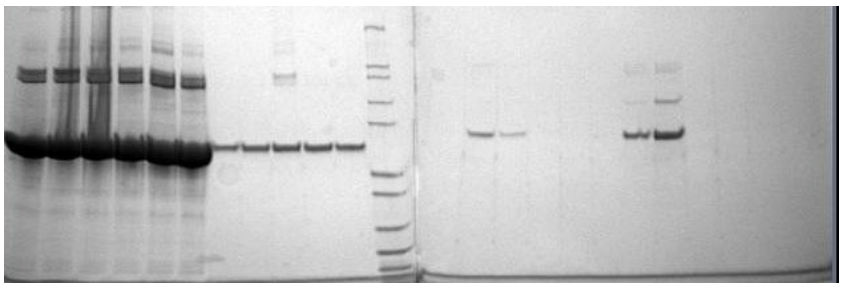

Figure 3.2: SDS-PAGE showing the fractions resulting from the ATP-analog kit, showing single band of HSP70 for fractions E2 and E3.

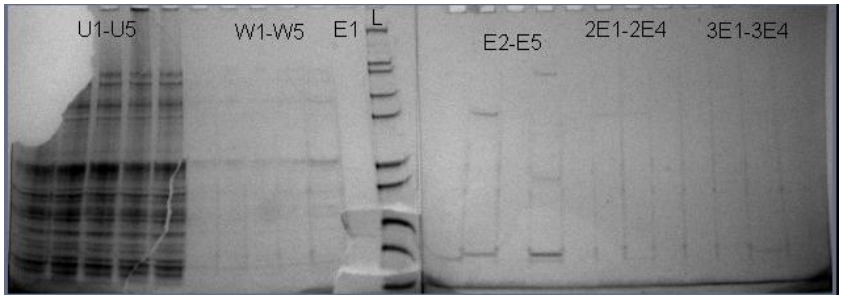

Figure 3.3: SDS-PAGE showing the fractions resulting from the ATP-analog kit, showing no bound AURKB

3.1.3 Dual specificity tyrosine-phosphorylation-regulated kinase 1B

3.1.3.1 Expression

The transformation of the hexahistidine-tagged catalytical domain of DYRK1B into BL21 yielded many colonies on LB-plates with AMP/CHL.

Overnight precultures were highly turbid, and gave the main culture a quick start reaching high OD600 in only a couple of hours. 0.5 L of culture gave approximately 4.5 g of cells.

3.1.3.2 Purification with HisTrap

Purification of DYRK1B with HisTrap did concentrate the protein sample, and removed lots of host-proteins, however it is clear from the SDS-PAGE-results (Figure 3.4) that more purification steps are necessary to obtain pure protein.

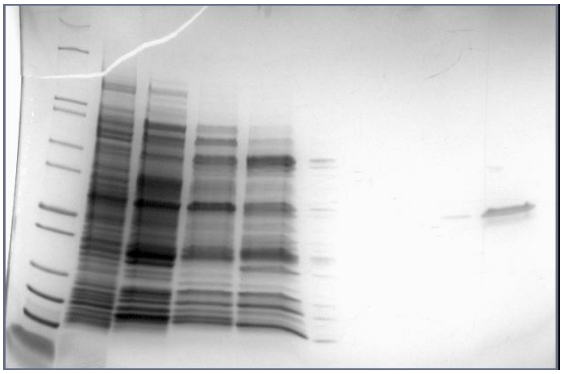

Figure 3.4: SDS-PAGE results showing the purification of DYRK1B by HisTrap. From the left; Mark12 molecular weight ladder, FT, fractions A2,A3,A4. To the right: Positive control catalytical domain of PKA.

3.1.3.3 ATP-analog binding assay

There were issues with precipitation after the addition of the binding buffer. Only a single band was observed in the SDS-PAGE-results (Figure 3.5) for the elution from 6AH-ATP-Agarose, and the molecular weight ladder indicates a size of approximately 60 kDa.

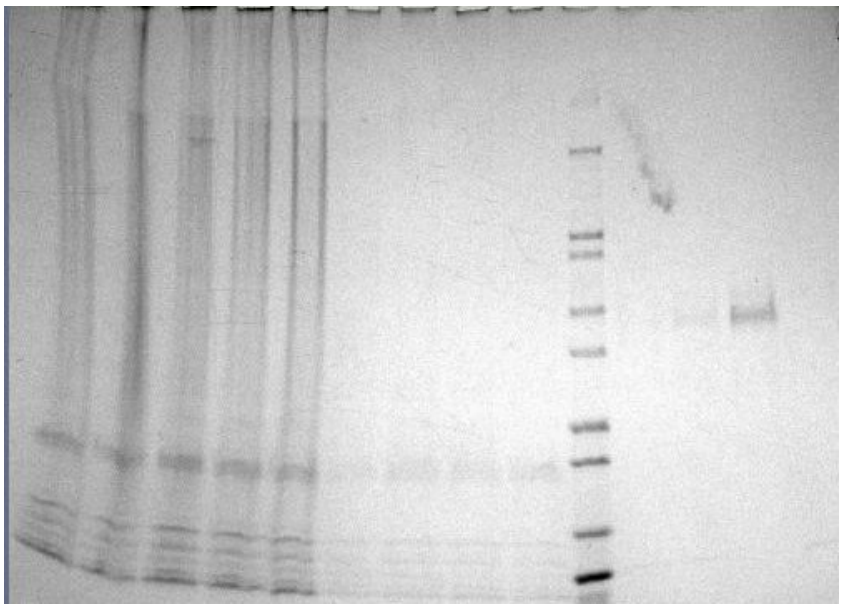

Figure 3.5: SDS-PAGE results showing the results from the ATP-analog binding assay. Only one band is visible for the elution fractions to the left.

3.1.4 Dual specificity tyrosine-phosphorylation-regulated kinase 1A

3.1.4.1 ATP-analog binding assay

A single band was observed in the SDS-PAGE-results (Figure 3.6) for the elution from EDA-ATP-Agarose, the molecular weight ladder indicates a size of approximately 43 kDa. MS/MS-results indicate that the eluted protein is DYRK1A.

3.2 Folding diagnostics

3.2.1 Abelson tyrosine-protein kinase 1

3.2.1.1 Verification of plasmid by restriction enzymes

The plasmid restriction digest shown in Figure 3.7 indicates that the plasmids in fact carry the genes of YOPH and ABL1 (both wild-type and gatekeeper-mutant) as the

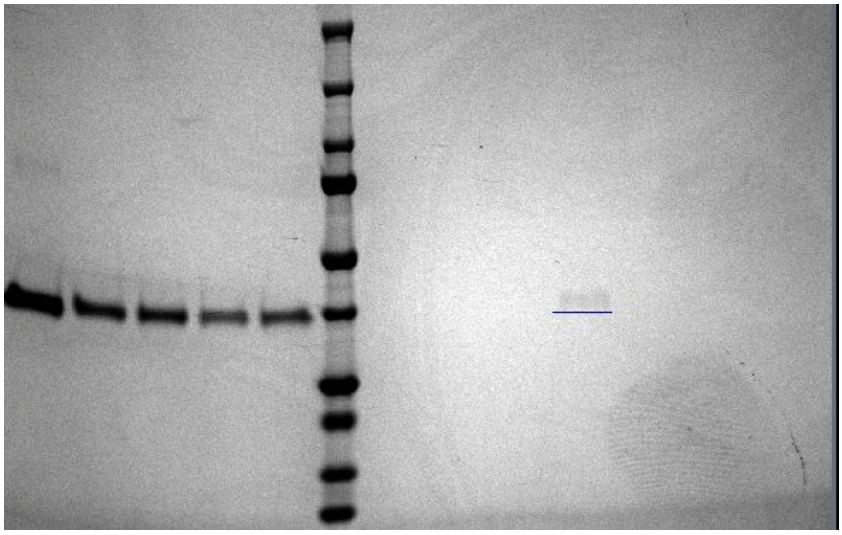

Figure 3.6: SDS-PAGE results showing the results from the ATP-analog binding assay for DYRK1A. Only one band is visible for the elution fractions to the left.

bands visible at the gel are single bands and of the correct size, approximately 4kb for YOPH and 6kb for ABL1.

3.2.1.2 Purification

Purification with HisTrap as shown in Figure 3.8 resulted in much a purer protein sample, while the cell lysate and FT had many bands from *E.coli*-proteins, only two bands are clearly visible for the eluted fraction as shown in the SDS-PAGE-results in Figure 3.9. The SDS-PAGE-results also show that the protein produced is of the correct size.

3.2.1.3 ATP-analog binding assay

SDS-PAGE results in Figure 3.10 show that ABL1 binds two of the four ATP analogs from Jena Bioscience. These ATP-analogs are linked to the matrix on the ribose-moiety and the γ-phosphate of the ATP-analogs. ABL1 appears where it is expected to appear on the SDS-PAGE based on its size, but there exists two other bands corresponding to binding to the nucleotide-moieties. MS/MS confirmed that the correctly sized bands were ABL1 and the larger bands were chaperones.

3.2.2 Trigger factor-Abelson tyrosine-protein kinase 1

3.2.2.1 Purification

TF-ABL1 is captured and eluted by IMAC as shown in Figure 3.11, however many other proteins co-elute.

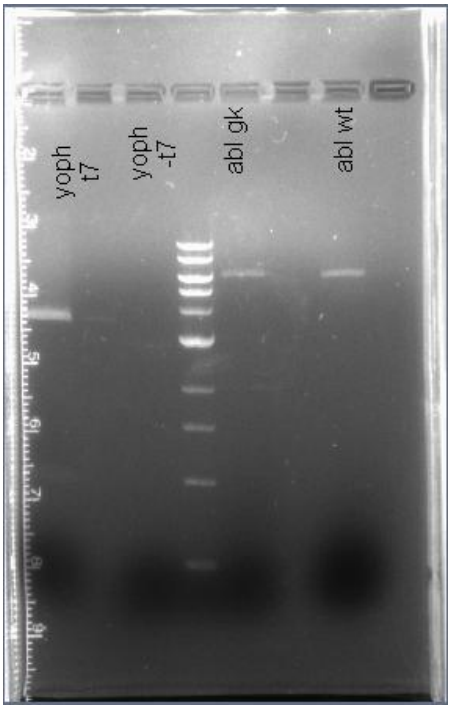

Figure 3.7: Restriction-digest of the plasmids of YOPH and ABL1 (for wild-type and gatekeeper-mutant) with a 1kb DNA-ladder (NEB).

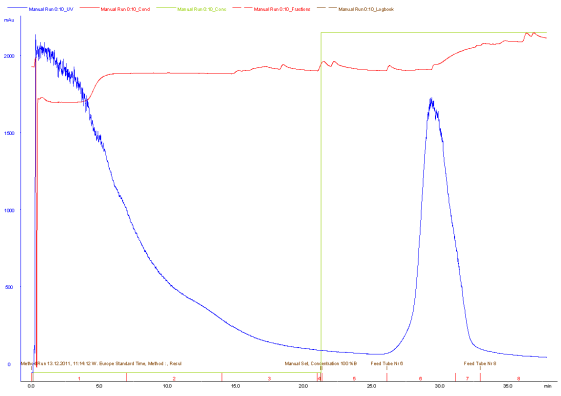

Figure 3.8: Chromatogram showing the washing and elution of ABL1 from a HisTrap column

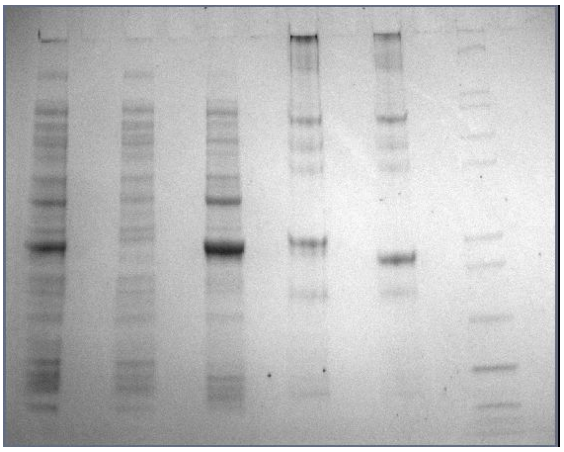

Figure 3.9: SDS-PAGE showing the results from washing and elution of ABL1 from a HisTrap column. From the left: Cell-lysate,FT from peristaltic pump,FT from the äkta-machine,fractions 15-20, fractions 15-20 cleaved overnight with TeV protease, Mark12 molecular weight ladder

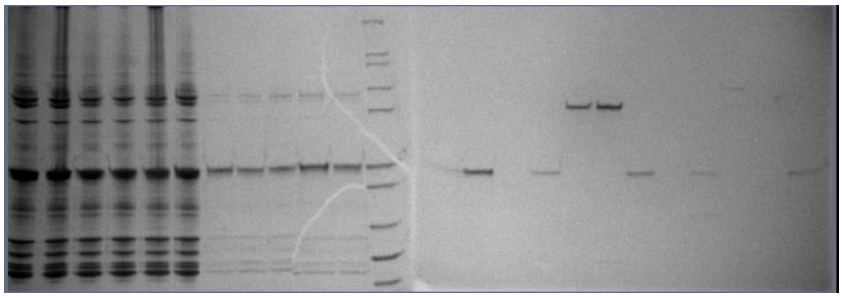

Figure 3.10: SDS-PAGE from testing with the ATP-analogs kit, showing binding of ABL1 to two of the ATP-analogs. From the left: 5 fractions of unbound protein, 5 fractions from washing, molecular weight ladder, 5 fractions from first elution, 5 fractions from second elution and 2 fractions from the last elution.

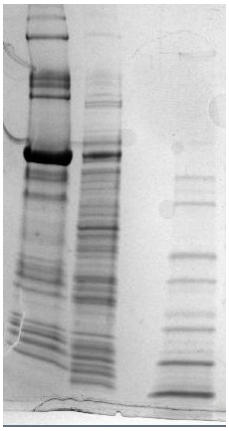

Figure 3.11: SDS-PAGE showing the FT and elution fraction of TF-ABL1 together with Mark12 molecular weight ladder

3.2.2.2 ATP-analog binding assay

Binding of TF-ABL1-sized protein is observed to AP-ATP-Agarose as shown in Figure 3.12. Many other proteins also bind to the different resins.

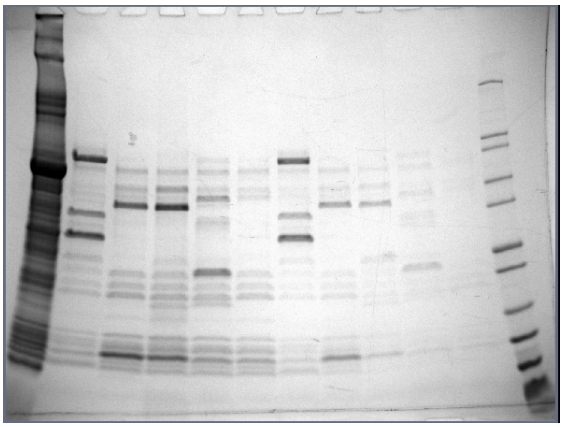

Figure 3.12: SDS-PAGE results for TF-ABL1 tested with ATP-analogs. From the left: Unbound fraction from all resins, first elution for all the resins and second elution for the non-blank resins, and Mark12 molecular weight ladder.

3.3 Differentiation of phosphorylation states

3.3.1 Protein kinase A sixfold mutant model of Aurora B

3.3.1.1 Expression and purification

PKA Aur6 was produced in high yields, clearly overexpressed compared to the endogenous proteins based on SDS-PAGE-results. Purification with PKI-column as previously described gave quite pure protein, however two bands on SDS-PAGE shown in Figure 3.13 were visible close in range of each other. Protein concentration was estimated by Bradford-assay to be in the range of 0.1-0.2 $\mathrm{mg\,mL^{-1}}$ after elution, and with elution-volumes of approximately 30 mL this gives a total yield of 3-6 mg. Elution with bisubstrate inhibitors

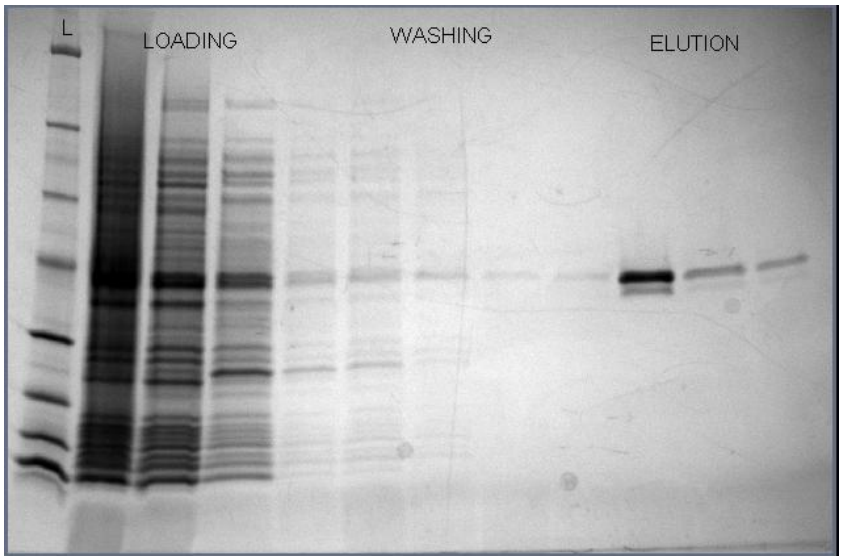

Figure 3.13: SDS-PAGE showing the purification of PKA Aur6 by affinity-chromatography with PKI.

ARC-b and ARC-c however gave a single band on SDS-PAGE shown in Figure 3.14. MSMS results confirmed that these bands from SDS-PAGE all consisted of PKA Sixfold Mutant Model Of Aurora B, however there were differences in phosphorylation as shown in Figure 3.16.

3.3.1.2 Purification with Cationic exchange

Further purification of PKA Aur6 purified with PKI and the bisubstrate inhibitor ARC-c with Arginine to elute, with a HiTrap SP HP 1mL cationic exchanger gives several peaks, as shown in Figure 3.15.

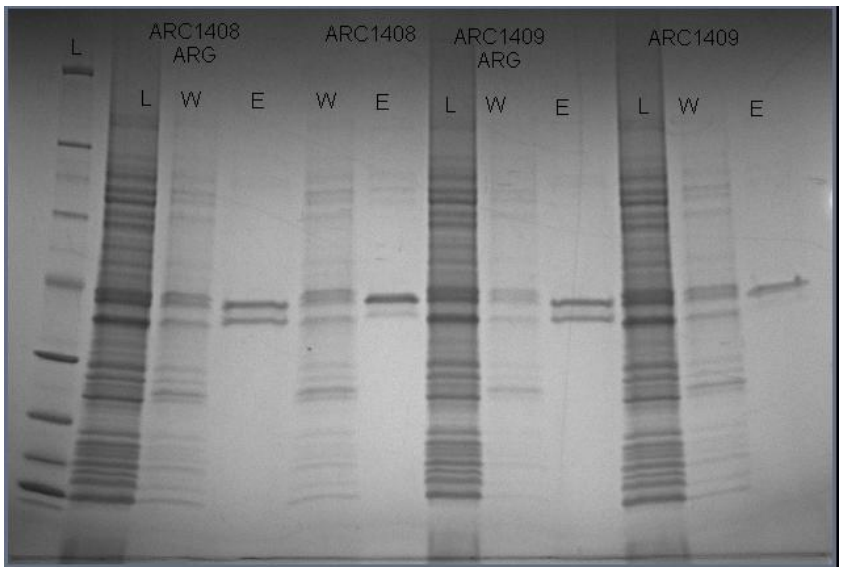

Figure 3.14: SDS-PAGE showing the purification of PKA Aur6 by affinity-chromatography with PKI using bisubstrate inhibitors (ARCs) with and without L-Arg to elute.

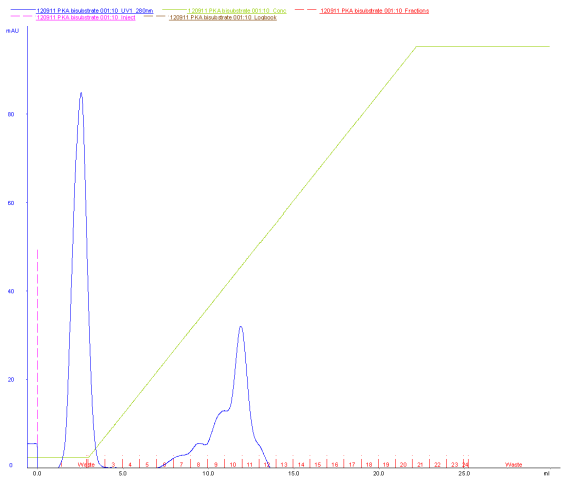

Figure 3.15: Chromatogram showing the washing and elution of PKA Aur6 from a HiTrap SP HP 1mL column.

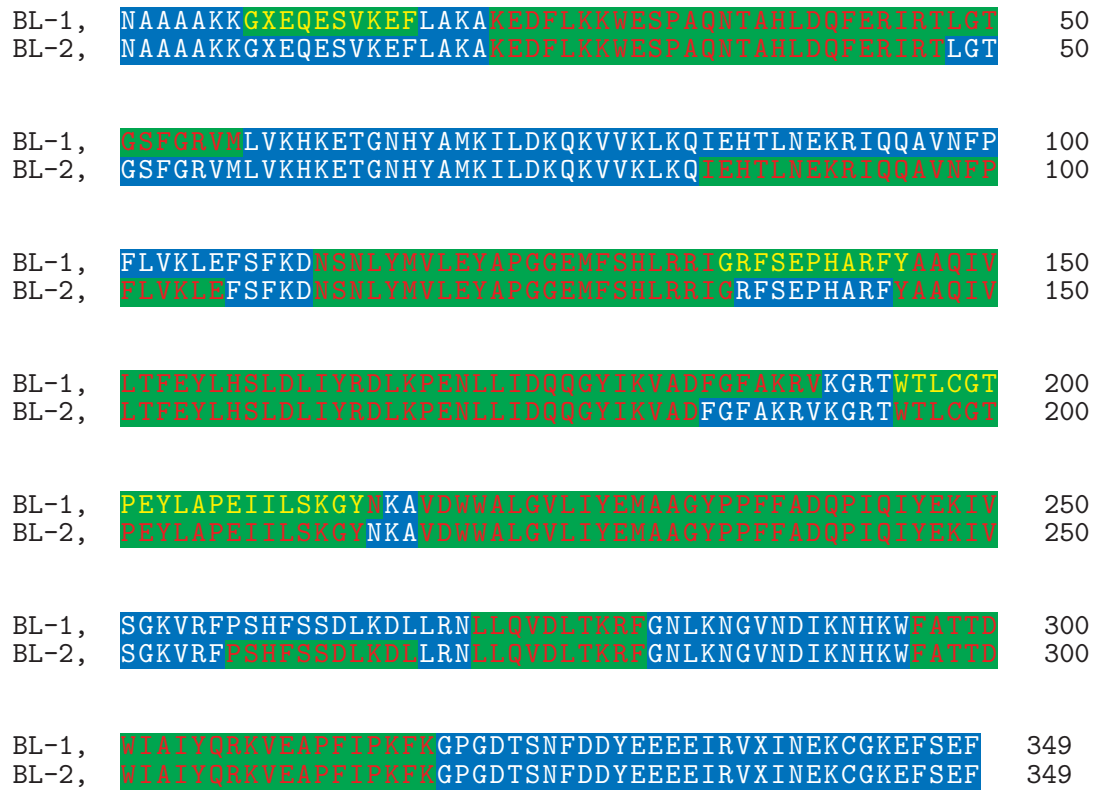

Figure 3.16: MSMS results for PKA Aur6. Green background coloring means matched sequence, yellow text shows phosphorylated matches (phosphorylation at Ser/Thr) while blue background with white text only shows the reference sequence

Table 3.1: Thermofluor-results for PKA Aur6 with selected inhibitors.

Compound	T_m (°C)	ΔT_m (°C)	K_d (nM)
PKA Aur6	41		
H-89	47	6	23[79]
ARC-a	46	5	22[62]
ARC-b	53	12	0.19[62]
ARC-c	51.5	10.5	0.61[62]
ARC-d	57.5	16.5	0.005[62]
ARC-e	55.8	14.8	0.013[62]

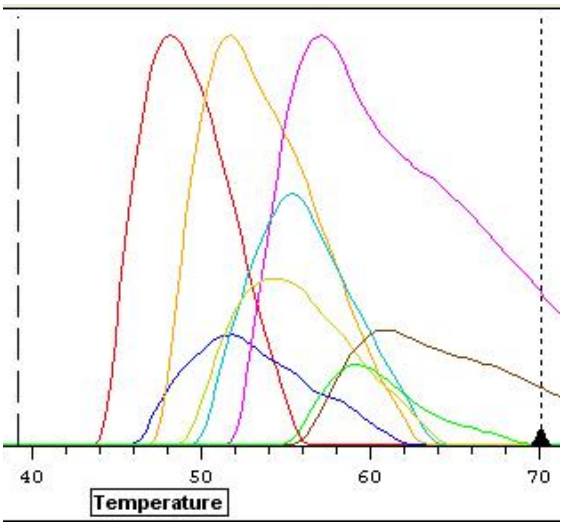

Figure 3.17: Thermofluor-results for PKA Aur6 showing the thermal shift induced by inhibitors

3.3.1.3 Thermofluor

Thermofluor-experiment clearly showed a stabilizing effect when PKA Aur6 was mixed with H-89 and different ARCs (Figure 3.17). All the inhibitors showed an increase in melting point for PKA Aur6 compared to the apo-form and the results are summarized in Table 3.1.

3.4 Inhibitor design

3.4.1 Protein kinase A sevenfold mutant model of Aurora B

3.4.1.1 Site-directed mutagenesis

The template plasmid concentration was measured to 100 ng μL^{-1}.

Transformation after treatment with DPN1 yielded colonies on all LB/AMP-plates except the control.

Restreaking to new plates coupled with the colony PCR (Figure 3.19) yielded colonies, which were used to inoculate pre-cultures. The pre-cultures grew turbid,and two of them was used for miniprep of DNA. DNA concentration from the two minipreps were estimated to 110 and 117 ng μL^{-1} with good purity according to the ratios and curves.

BigDye Dye-substitution sequencing (Figure 3.18) confirmed the successful site-directed mutagenesis.

```
3AMA   NFPFLVKLE.....F.......S.FKDNSNLYMVLEYAPGGEMFSHLRRI
PKA    .........TGGSTFRSLSNSSSPFKDNSNLYMVLEYAPGGEMFSHLRRI

3AMA   GRFSEPHARFYAAQIVLTFEYLHSLDLIYRDLKPE.NLLIDQQGYIKVAD
PKA    GRFSEPHARFYAAQIVLTFEYLHSLDLIYRDLKP.XNLLIDQQGYIKVAD

3AMA   FGFAKRVKGRTWTLCGTPEYLAPEIILSKGYNKAVDWWALGVLIYEMAAG
PKA    FGFAKRVKGRTWTLCGTPEYLAPEIILSKGYNKAVDWWALGVLIYEMAAG

3AMA   YPPFFADQPIQIYEKIVSGKVRFPSHFSSDLKDLLRNLLQVDLTKRFGNL
PKA    YPPFDADQPIQIYEKIVSGKVRFPSHFSSDLKDLLRNLLQVDLTKRFGNL

3AMA   KNGVNDIKNHKWFAT
PKA    KNGVNDIKNHKWFAT
```

Figure 3.18: Dye-substitution sequencing results for PKA Aur7

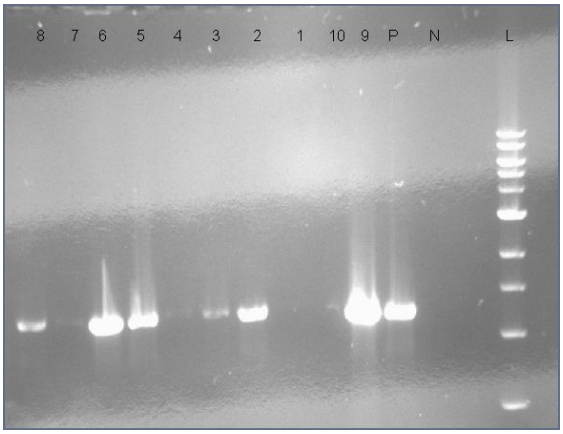

Figure 3.19: Colony-PCR results for PKA Aur7 showing the size of the mutated plasmids. Numbered colonies as well as positive control with unmutated PKA Aur6 and negative control without plasmid. Also included is a 1 kp-ladder.

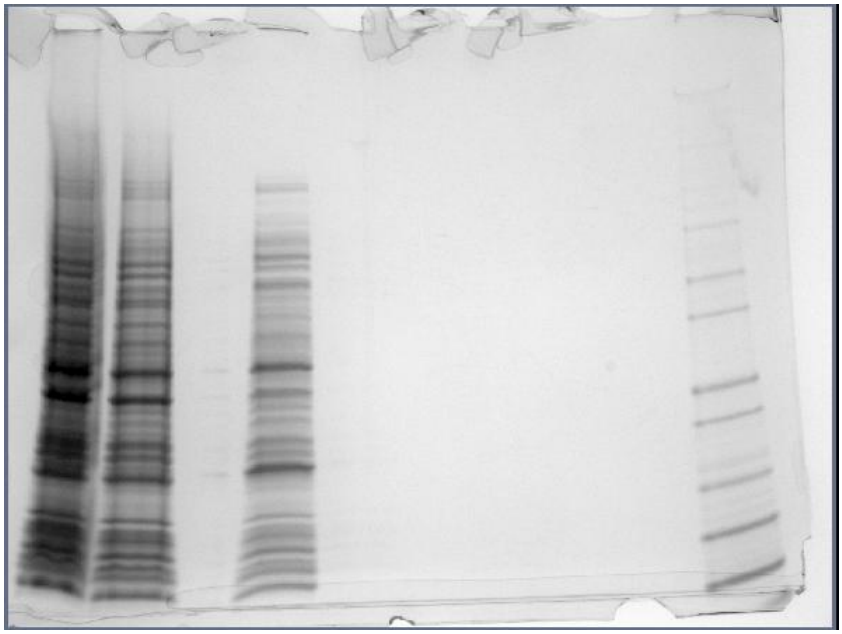

Figure 3.20: SDS-PAGE showing the purification of PKA Aur7 by affinity-chromatography with Phe-Asn-modified PKI .

3.4.1.2 Purification with immobilized PKI

No elution of PKA Aur7 was observed with either the regular or the modified PKI (Figure 3.20).

3.4.1.3 ATP-analog binding assay

PKA Aur7-sized protein was found in the elution fractions of AP-ATP-Agarose and 6AH-ATP-Agarose, but many other proteins are also eluted (including in the blank agarose-resin).

3.4.1.4 Cook-assay

It was not possible to establish activity of PKA Aur7 using the results from the cook-assay. The changes in absorbance at 340 nm were erratic and not generally declining.

3.4.2 Protein kinase A threefold mutant model of AKT

3.4.2.1 Expression

The catalytical domain of PKAB3 was successfully transformed into BL21-cells, and up to 30 g of cells were produced per liter in autoinduction-media.

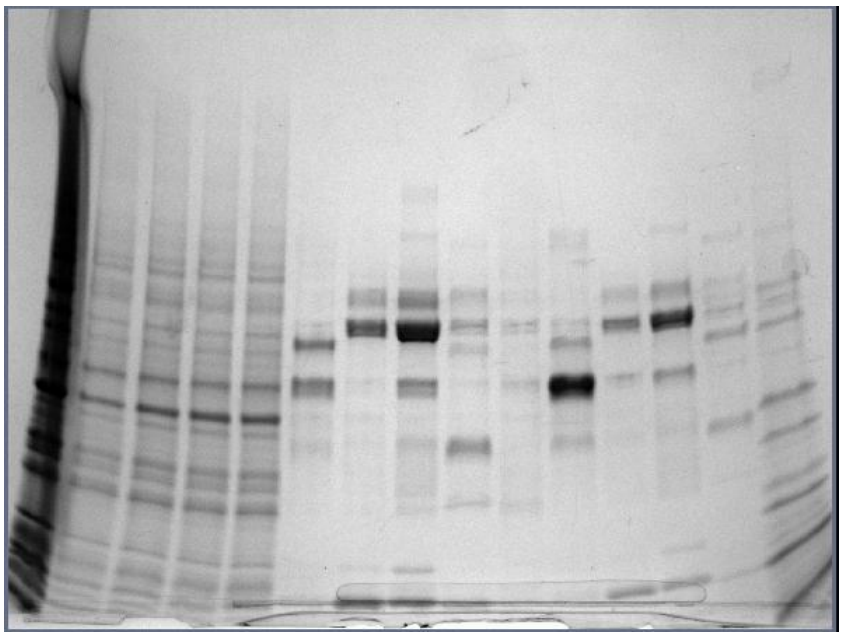

Figure 3.21: SDS-PAGE results for PKA Aur7 tested with ATP-analogs. From the left: Cell-lysate, 4 wash-fractions (excluding blank), 5 first-elution fractions, 4 second elution fractions (excluding blank) and Mark12 molecular weight ladder

3.4.2.2 ATP-analog binding assay

The results were consistent with what was observed for PKA Aur7. PKAB3-sized protein was found in the elution fractions of AP-ATP-Agarose and 6AH-ATP-Agarose, but many other proteins are also eluted (including in the blank agarose-resin).

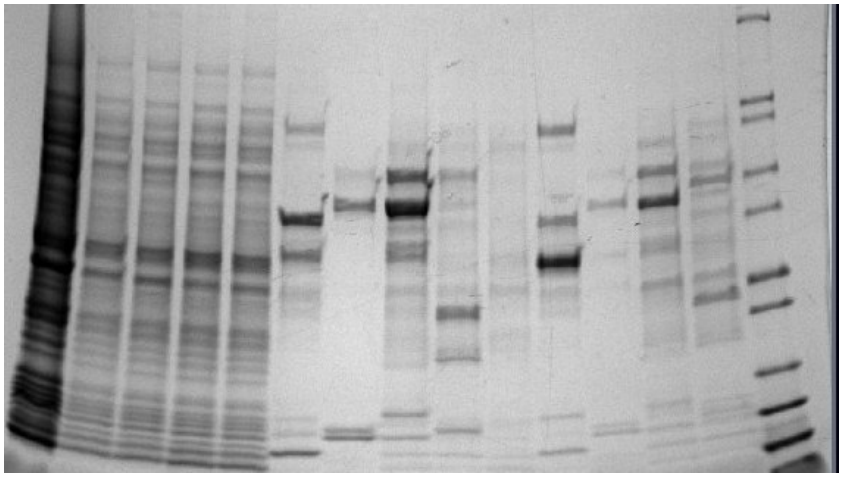

Figure 3.22: SDS-PAGE results for PKAB3 tested with ATP-analogs. From the left: Unbound-fraction from blank-resin, 4 wash-fractions (excluding blank), 5 first-elution fractions, 4 second elution fractions (excluding blank) and Mark12 molecular weight ladder

3.4.2.3 Cook-assay

By non-linear fitting using the least-squares routine of Levenberg-Marquardt in fityk[137] with the Michaelis-Menten equation the decrease of absorbance at 340 nm against the concentration of the substrate ATP (Figure 3.23) it was possible to determine K_m to be $21,221 \pm 7,155$µM and $V_{\max}$ to be $-9,04768 \pm 0,61$ with a 95% confidence-level. Fitting the rate of decrease of absorbance at 340 nm against the logarithm of the concentration of the inhibitor using a four-parameter logistic fit (Equation 1.6) in SoftMax Pro (Molecular Devices), as shown in Figure 3.24, gives the IC50-value as parameter C[118].

Fitting the rate of decrease of absorbance at 340 nm against the logarithm of the concentration of the inhibitor using a four-parameter logistic fit (Equation 1.6) in SoftMax Pro (Molecular Devices), as shown in Figure 3.24, gives the IC50-value as parameter C[118]. The plot (Figure 3.24) shows that the IC50-value for the inhibitor 34a is $\approx 3\,\mu$M. This was also done for the bisubstrate inhibitor ARC-e, however without taking the logarithm of the concentration. The plot (Figure 3.25) shows that the IC50-value for ARC-e is ≈6 nM.

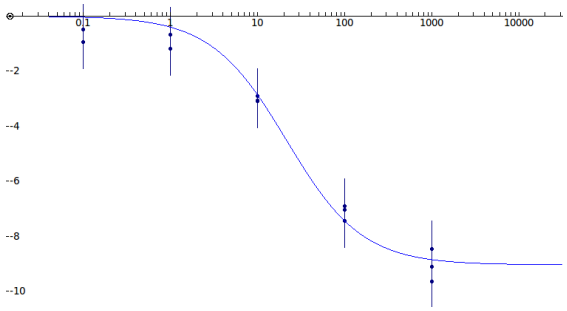

Figure 3.23: Velocities of absorbance-decrease in different concentrations of ATP fitted using the Michaelis-Menten equation in fityk

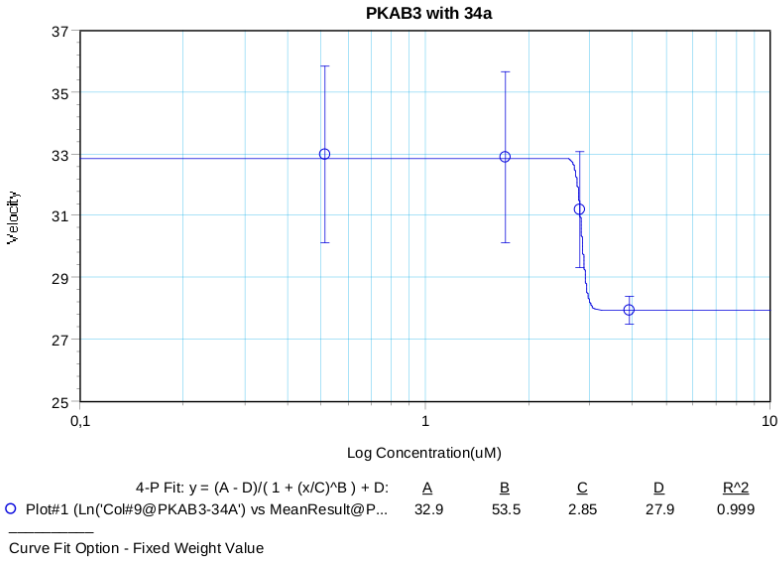

Figure 3.24: The avaraged measured velocity of decrease in absorbance at 340 nm plotted against the logarithm of the inhibitor concentration for the inhibitor 34a with PKAB3

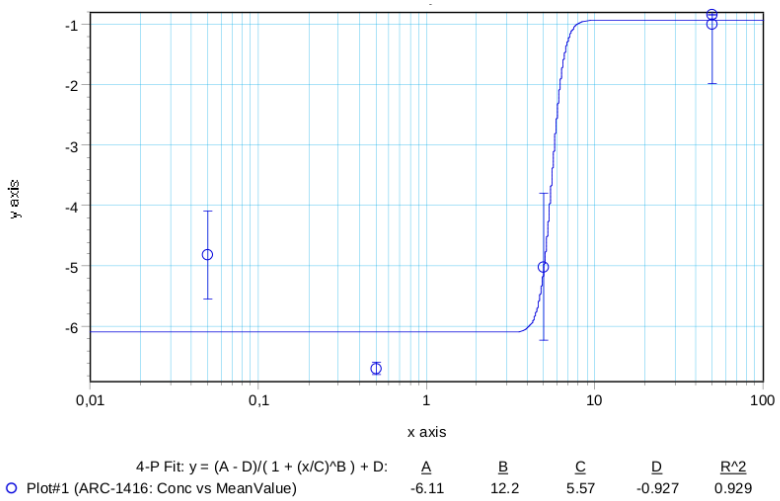

Figure 3.25: Cook-assay-result for PKAB3 with the bisubstrate inhibitor ARC-e. Concentration is shown on the X-axis in nanomolars, and on the y-axis the rate of decrease in absorbance is shown.

Table 3.2: Thermofluor-results for PKAB3 with selected inhibitors.

Compound	T_m (°C)	ΔT_m (°C)	K_d (nM)
PKAB3	42.9		
34a	43.5	0.6	2850
H-89	47.3	4.4	23[79]
ARC-c	57.3	14.4	0.61[62]
ARC-f	56.4	13.5	0.002[62]
ARC-d	60.6	17.7	0.005[62]
ARC-e	54.85	11.95	0.013[62]

3.4.2.4 Thermofluor

Binding of inhibitors increased the melting point of PKAB3 for all the inhibitors tested (Table 3.2). The results were similar, but not identical to the results for PKA Aur6.

3.4.2.5 Purification with immobilized PKI

PKAB3 was produced in high yields, clearly overexpressed compared to the endogenous proteins based on SDS-PAGE-results, from both unmodified and modified PKI. Purification with PKI-column as previously described gave very pure protein, however two bands on SDS-PAGE shown in Figure 3.26 were visible close in range of each other as was also observed with PKA Aur6. Protein concentration was estimated by Bradford-assay to be in the range of 0.1-0.2 $\mathrm{mg\,mL^{-1}}$ after elution, and with elution-volumes of approximately

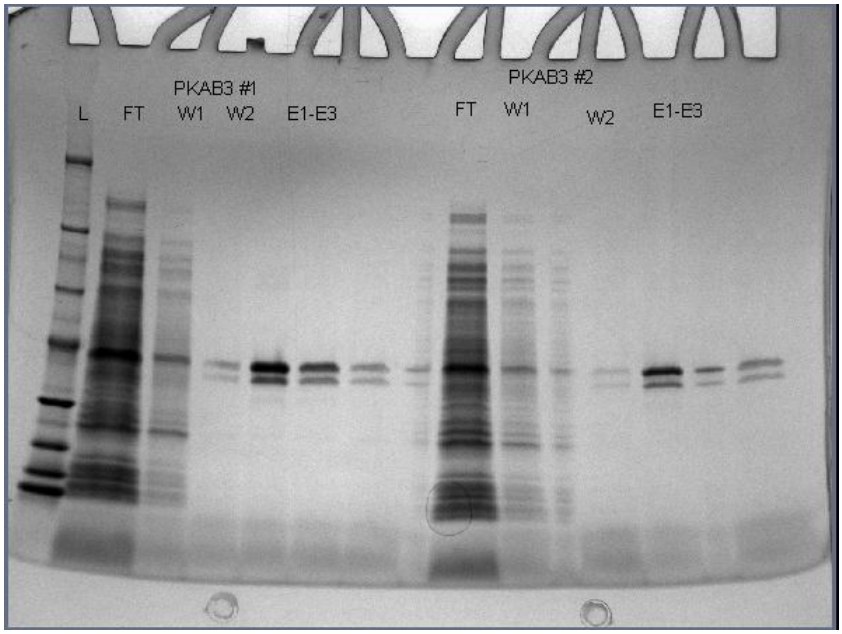

Figure 3.26: SDS-PAGE showing the purification of PKAB3 by affinity-chromatography with PKI.

30 mL this gives a total yield of 3-6 mg.

3.4.2.6 Purification with Cationic exchange

Further purification of PKAB3 purified with PKI with a MonoS 5/50GL cationic exchanger gives two peaks both containing PKAB3, as shown in Figure 3.27.

3.4.2.7 Surface plasmon resonance

pH-scouting showed highest immobilization-levels for PKAB3 in 10 mM Sodium Acetate-buffer at pH 4.5(Figure 3.28).

PKAB3 was immobilized to a level of 6000 RU, and showed stability after regeneration with 1 M 2-Aminoethanol at pH 8.5.

However, no significant binding of ATP to the surface was observed.

3.4.2.8 Microscale thermophoresis

Binding of 34a to PKAB3 was observed with a $K_d = 114 \pm 24,5 nM$ (Figure 3.29).

500 nM PKAB3 in was found to have high enough fluorescence to be used for label-free experiments in the Monolith NT.LabelFree (NanoTemper). No significant binding was shown to modified PKI (Figure 3.30)

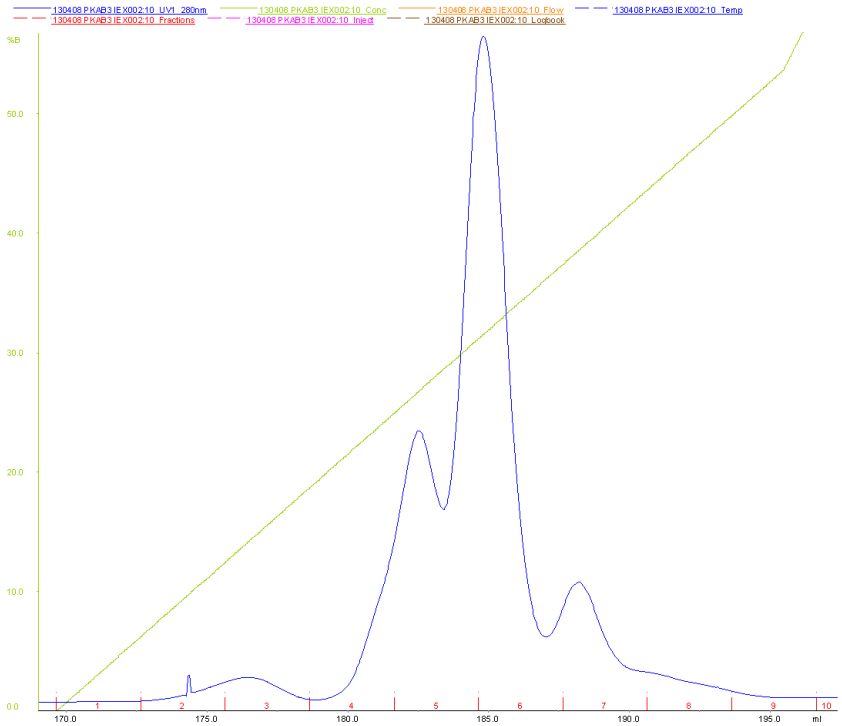

Figure 3.27: Chromatogram showing the washing and elution of PKAB3 from a HiTrap SP HP 1mL column.

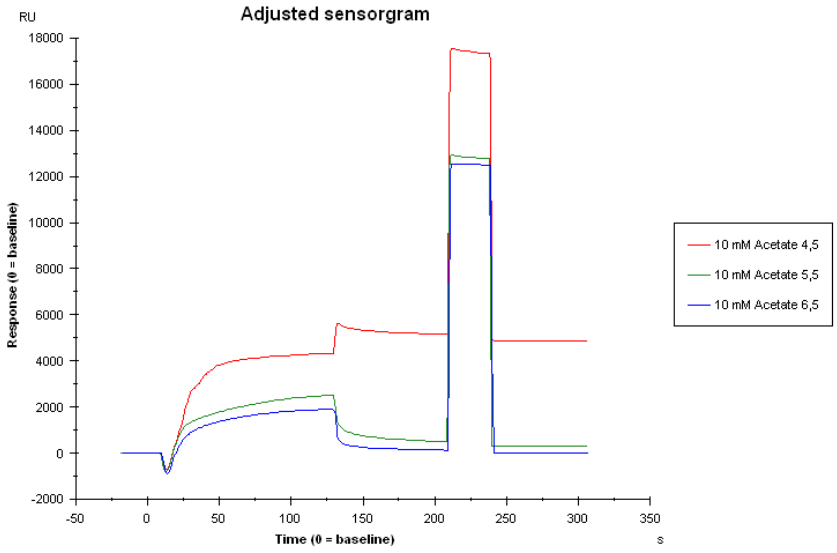

Figure 3.28: pH-scouting immobilization-results for PKAB3

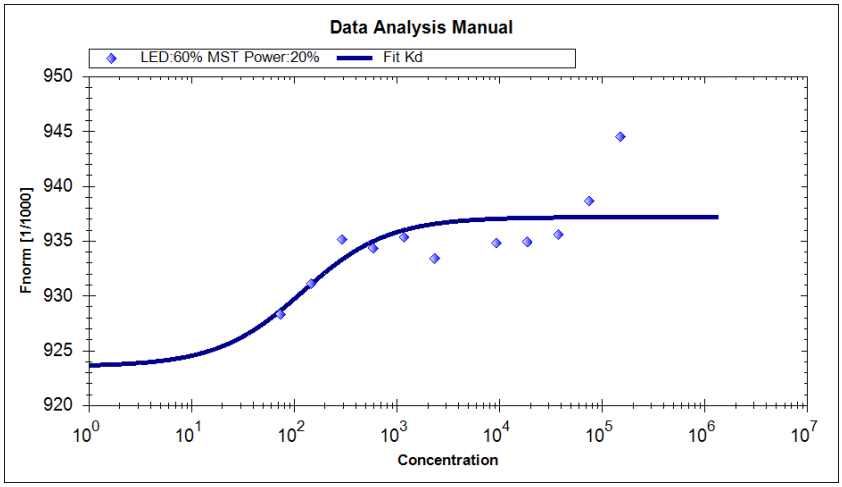

Figure 3.29: Binding analysis studies for PKAB3 and the inhibitor 34a with MST showing the relationship between the normalized fluorescent signal and the concentration of the inhibitor

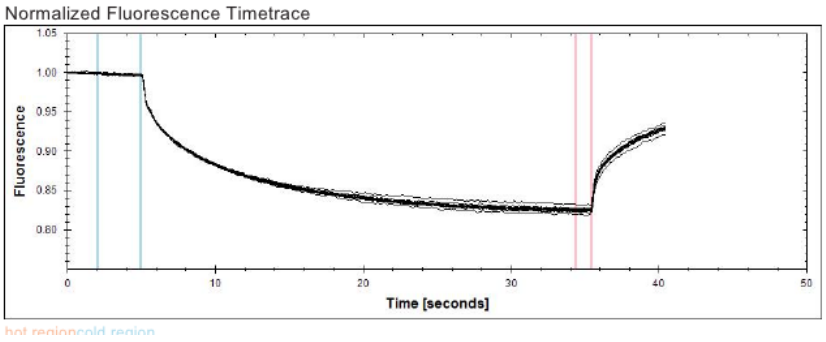

Figure 3.30: Fluorescence timetrace for PKAB3 versus modified PKI

Table 3.3: Data collection and processing statistics for PKAB3 in complex with inhibitors 34a and 47a. Numbers in parenthesis refer to the outer-most resolution-shell.

	PKAB3 in complex with 47A	PKAB3 in complex with 34A
Wavelength (Å)		
Resolution range (Å)	24.6 - 1.96 (2.03 - 1.96)	24.88 - 1.95 (1.86 - 1.796)
Space group	P 21 21 21	P 21 21 21
Unit cell	82.25 61.382 78.938 90 90 90	61.953 78.563 79.615 90 90 90
Total reflections	113388 (11219)	116519 (7576)
Unique reflections	29003 (2779)	35847 (3263)
Multiplicity	3.9 (4.0)	3.3 (2.3)
Mean I/sigma(I)	9.96 (2.24)	9.36 (1.53)
Wilson B-factor	22.74	16.68
R-merge	0.1011 (0.5298)	0.09327 (0.4741)
R-meas	0.117	0.1108
R-work	0.1860 (0.2360)	0.1937 (0.3346)
R-free	0.2206 (0.2652)	0.2386 (0.3372)
Number of atoms	6245	6349
macromolecules	2941	2963
ligands	49	47
water	317	351
Protein residues	357	357
RMS(bonds)	0.013	0.013
RMS(angles)	1.41	1.40
Clashscore	12.31	6.39
Average B-factor	34.00	25.90
macromolecules	33.30	25.30
ligands	38.60	34.30
solvent	39.70	29.80

3.4.2.9 Data collection and processing

It was possible to solve the structure of PKAB3 in complex with both inhibitors 47a and 34a. Molecular replacement and refinement produced clear electron density maps showing side-chain conformations and ligands to 1.95 Å-resolution. Both were in the P212121-space group, the 47a structure had R-work/R-free values of 18%/22% and a Wilson B-factor of 22.74 $Å^2$ while the 34a structure had had R-work/R-free values of 19%/24% and a Wilson B-factor of 16.69 $Å^2$ Important statistics from the processing is summarized in Table 3.3. An example diffraction image is shown in Figure 3.31.

3.4.3 Protein kinase A mutant model of Rho

3.4.3.1 Expression

Transformation yielded many single colonies on the plates, and cultures grew cloudy in reasonable time. From one liter of culture, approximately 20 g of cells were collected for PKAR4 and PKAR5.

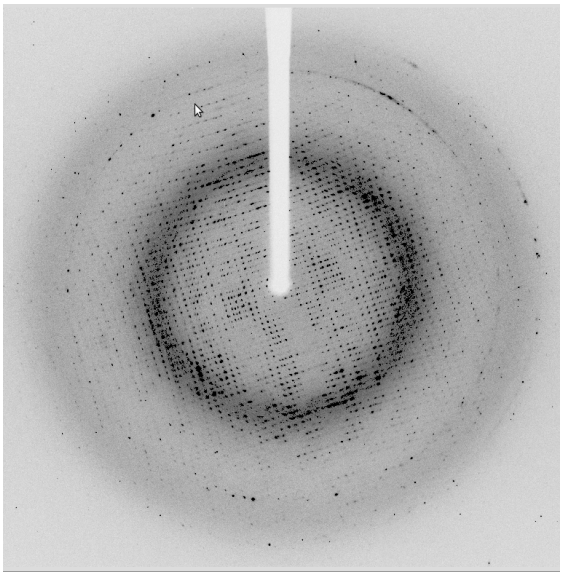

Figure 3.31: Diffraction image of PKAB3 in complex with the inhibitor LH726. 0.5° oscillation.

3.4.3.2 ATP-analog binding assay

The result for PKAR4 and PKAR5 were consistent with what was observed for PKA Aur7 and PKAB3. In Figure 3.32 binding of PKAR4-sized protein to AP-ATP-Agarose is shown.

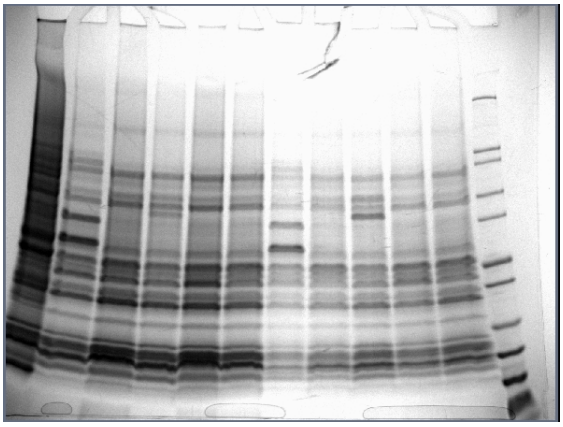

Figure 3.32: SDS-PAGE results for PKAR4 tested with ATP-analogs. From the left: Unbound fraction from all resins, first elution for all the resins and second elution for the non-blank resins, and Mark12 molecular weight ladder.

Chapter 4

Discussion

4.1 Verification of binding

4.1.1 70 kDa heat shock proteins

4.1.1.1 Expression and purification

HSP70 was expressed in the same manner as suggested in the literature, and the yield was high. The purification with HisTrap was successful, even though the column clogged during sample-loading. Because of the high expression of HSP70, enough protein was purified for analysis of binding mode.

4.1.1.2 Verification of binding mode of HSP70

It is not surprising to see HSP70 bind to the ATP-analogs as HSP70 has a K_d in the range of 100 nM. When looking at the structure of HSP70 with an ADP bound[88] (shown in Figure 4.1) it is also clear that the nucleotide-moiety of ATP is surface-accessible and well suited as a linkage-group for chaperones and other proteins that share the ATPase fold. HSP70 bound to the resins 8AH-ATP-Agarose and 6AH-ATP-Agarose, both of which have their linker attached to the nucleotide-moiety.

4.1.2 Aurora B kinase

4.1.2.1 ATP-analog binding assay

Only one experiment was carried out with AURKB as there was only enough sample for one attempt. Na-orthovanadate was added to the sample by mistake before binding to the ATP-analog resins, the instructions only specify that it should be added to the wash-buffer and the elution-buffer. It is debatable whether this could explain the lack of binding to the ATP-analog resins, as orthovanadate could potentially lock the enzyme in a transition state unable to bind ATP. However, there were problems with this construct of AURKB with poor folding[96], this might also affect the binding of ATP analogs. There is also the possibility that the linkers are simply not able to enter the ATP-binding

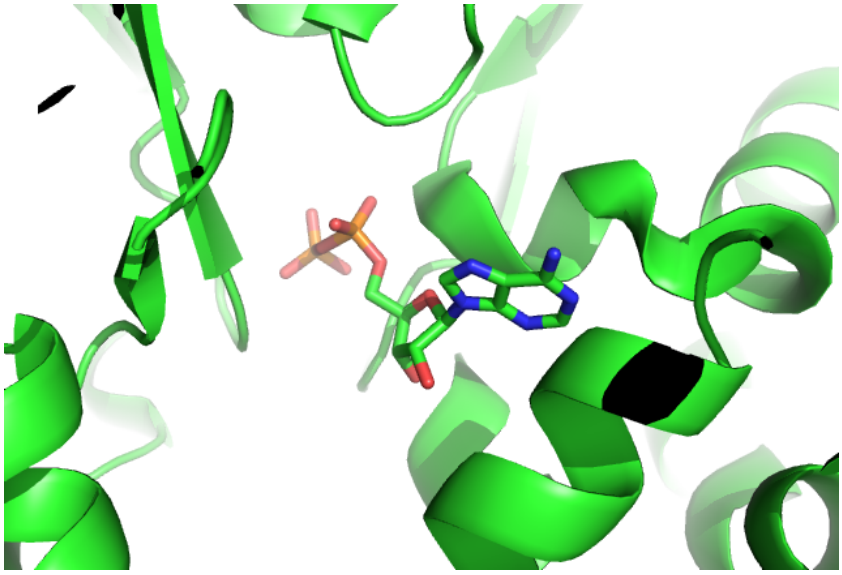

Figure 4.1: Structure of HSP70 showing binding of ADP[88]

site of AURKB or that the amount of sample was not sufficient because of low affinity for the modified substrates.

4.1.3 Dual specificity tyrosine-phosphorylation-regulated kinase 1B

4.1.3.1 ATP-analog binding assay

The results from testing with ATP-analogs were not encouraging. The catalytical domain of DYRK1B should be sized around 43 kDa, and should probably elute from the AP-ATP-Agarose-resin, in contrast the only band came from the elution of 6AH-ATP-Agarose and it was sized at approximately 60 kDa. Most probably the eluted protein is a contaminating chaperone with ATP-binding.

As mentioned in the Result-section, there were precipitation issues with the protein sample after mixing with the binding buffer, it could be that DYRK1B precipitates because of the addition of the detergent NP-40 which is included in the binding buffer. There is also the possibility that the concentration of the protein eluted from the HisTrap was not high enough to achieve measurable binding.

4.1.4 Dual specificity tyrosine-phosphorylation-regulated kinase 1A

4.1.4.1 ATP-analog binding assay

A weak band can be observed from binding to EDA-ATP-Agarose, and this is very interesting. ABL1 was also observed to bind to EDA-ATP-Agarose, and the sequence-alignment shows that what in PKA is a Glutamic acid is an Asparagine in both ABL1

and DYRK1A. However, no binding was observed to AP-ATP-Agarose. It is not clear from the structure why DYRK1A does not bind to AP-ATP-Agarose.

4.2 Folding diagnostics

4.2.1 Abelson tyrosine-protein kinase 1

4.2.1.1 Purification

The purification procedure with IMAC could be optimized with the use of a gradient to elute the protein, this was not done because it was not necessary with a higher level of purity for the ATP-binding assay. Based on the SDS-PAGE-results it appears that the cleavage with TEV protease was successful.

4.2.1.2 ATP-analogs used to verify folded state of ABL1

When looking at the structure of ABL1 with an ATP-analog bound[85] as visualized in Figure 4.2 it is also clear that the sugar-moiety of ATP is surface-accessible and applicable to linkage. The phosphates are also surface-accessible and possible to use for linkage. This explains the success of the two resins AP-ATP-Agarose which is linked by the γ-phosphate and EDA-ATP-Agarose which is linked by the ribose-ring. The linker of AP-ATP-Agarose includes a phenyl-ring which is the sidechain of tyrosine[130], this is optimal for the tyrosine protein kinase ABL1. The result is supporting evidence that ABL1 is folded, as the binding of ATP is dependent on correct folding[32].

It is interesting to notice that chaperonins, which are also ATP-binding, fail to bind to the same resins as ABL1. This is presumably because the chaperonins share the binding motif of HSP70 with the only the Adenine-ring surface-accessible.

4.2.2 Trigger factor-Abelson tyrosine-protein kinase 1

4.2.2.1 Purification

If a gradient had been used instead of the simple step to 0.5 M Imidazole, the eluted protein sample would most likely be much purer. However, the main concern for the purification step was to capture and concentrate the protein from the cell lysate.

4.2.2.2 ATP-analog binding assay

TF-constructs are often made for proteins with poor folding to increase their solubility during expression. After expression the tag may be cleaved off. However, for TF-ABL1 cleavage with Factor Xaa-protease did not break the complex (results not shown), and it was speculated that this might be due to poor folding of the ABL1-protein. The successful binding of the TF-ABL1-fusion-protein to the AP-ATP-Agarose resin shows that the protein is folded, as the ATP-binding is dependent on proper folding[32].

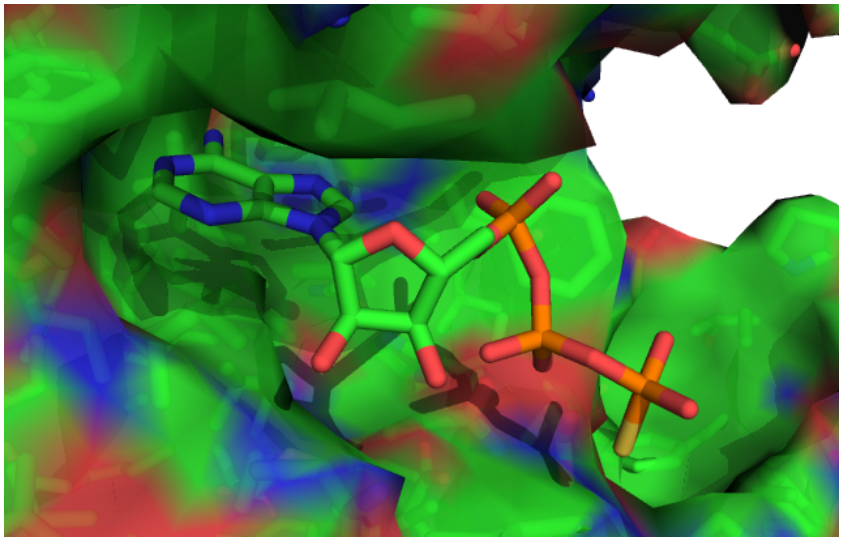

Figure 4.2: Structure of the ABL1 in with the ATP-analog AGS[85]

It is interesting to notice the failure of the fusion-protein to bind to EDA-ATP-Agarose. There is a possibility that the TF-protein covers part of the ABL1-surface, preventing the binding of the ribose-linked EDA-ATP-Agarose. One hypothetical model of how this might occur is shown in Figure 4.3, a model generated by the GRAMM-X web-service[128, 127] which uses Fast Fourier Transformation (FFT) and a Lennard-Jones potential to dock protein-protein complexes. This model (one of several) shows TF blocking the entrance of a ribose-linked ATP, however there is no evidence to support this model outside of the observation that the ribose-linked ATP did not bind the complex in this experiment.

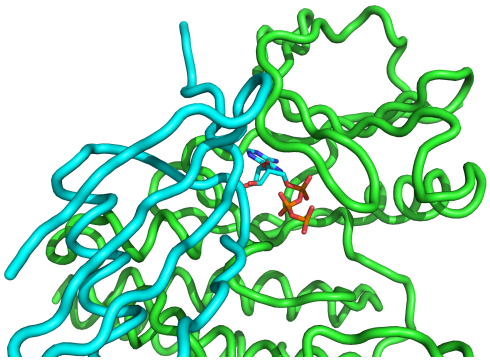

Figure 4.3: Protein-protein docking-model of the TF-ABL1 complex from the public web-server GRAMM-X[128, 127]. ABL1 is shown in green, TF in cyan and ATP in cyan/orange.

4.3 Differentiation of phosphorylation states

4.3.1 Protein kinase A sixfold mutant model of Aurora B

4.3.1.1 Thermofluor

The software had to be configured for the dyes HEX/FAM to get the correct absorption/emission wavelengths for Sypro Orange, as this dye is not included in the vendor-supplied software. From the results it is clear that tight binders stabilize PKA Aur6 more than weaker binders. Regression analysis in Libreoffice Calc with a logarithmic function (Figure 4.4) gives a very well fitting function with $R^2 = 0.99$. It is known from the literature that the shift in melting point is proportional to the affinity of the ligand[90, and references therein]. In fact, the relationship is so well described that it is possible to use the thermal shift data to determine the protein-ligand binding constants.

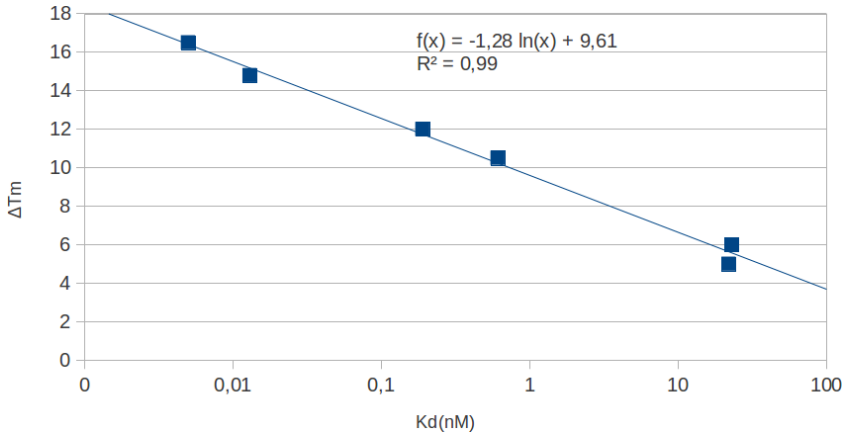

Figure 4.4: The shift in melting point plotted against the affinity shows a logarithmic relationship

4.3.1.2 Cationic exchange

The difference in retention on the cationic exchanger can be attributed to differences in phosphorylation. The charge-difference depends on pH, but each phosphorylation adds at least one negative charge to the protein, and negative charges weaken the binding to the negatively-charged matrix of the cationic exchanger. The shallow gradient used in the purification allows the recognition of several phosphorylation-states, yet the resolution is not good enough to give a homogeneous sample in terms of phosphorylation. Tuning of the pH and/or salt could potentially give better separation.

4.3.1.3 Purification with immobilized PKI

Purification with PKI is the standard method of purification of PKA. Double bands of approximately the correct size was observed, as shown in Figure 3.13, MS/MS confirmed that both bands were in fact PKA Aur6. However, the MS/MS results as presented in Figure 3.16 indicated that the difference in migration might be due to differences in phosphorylation. This was supported by the elution of single bands with the bisubstrate-inhibitors ARC-b and ARC-c (shown in Figure 3.14) which is known to bind preferably to the active phosphorylation-state of PKA, and in experiments with a serine/threonine-active phosphatase (data not shown) which changed the mobility on SDS-PAGE. This has also been studied previously and shown to be an effect of phosphorylation of the Thr-197[123, 138].

The elution of PKA Aur6 with ARC-b is an interesting observation on its own, the traditional elution with 200 mM L-Arg gives samples with ionic strength to high for IEX and the L-Arg may also interfere with protein characterization methods, notably protein concentration measurements using UV280.

4.4 Inhibitor design

4.4.1 Protein kinase A sevenfold mutant model of Aurora B

4.4.1.1 Site-directed mutagenesis

The primers were synthesized shorter (28bp rather than 35bp) than what the PrimerX-software suggested to avoid issues with secondary-structure formation. For some reason the pWhitescript-control-plasmid failed to yield colonies from the transformation-mix. This could be due to the shorter time for polymerization, as the PT7-7 vector of PKA Aur7 is only 3 kb with the gene inserted compared to pWhitescript at 4.5 kb.

All results indicate that the mutagenesis was successful, and the while the yield has not been quantitatively measured, the mutant appears to be well-expressed.

4.4.1.2 Purification with immobilized PKI

The lack of binding to the immobilized unmodified PKI-peptide indicates that the F240D-mutation in PKA Aur7 interrupts the interaction with Phe-10 in PKI severely lowering the binding affinity. Without further experiments it is not possible to quantify this reduction.

Introducing an Asparagine in the PKI was supposed to create a hydrogen-bond between the electron-rich Asp-240 in PKA Aur7 and the electron-poor Asn-10 in the modified PKI, however with the results obtained it is not clear whether this bond is formed, or if the orientations and distances are incompatible with hydrogen bonding.

4.4.1.3 ATP-analog binding assay

The incubation time was prolonged extensively for the experiments, as no binding was observed in experiments with the recommended shorter incubation times. However, the incubation time was not optimized, and a somewhat shorter time might be sufficient. The extended incubation time could be due to required conformational changes in the protein, as these processes could be quite slow.

The results indicate that a complex mixture of proteins is eluted from the resins. *E.coli*, as other organisms, have many endogenous ATP-binding proteins including chaperonins (as demonstrated in subsection 3.2.1.3) which would be expected to bind to 6AH-ATP-Agarose and 8AH-ATP-Agarose and several kinases[132, 31] which could potentially bind to AP-ATP-Agarose and EDA-ATP-Agarose. Since cell-lysate was used for this experiment, it is not surprising that many proteins endogenous to *E.coli* would be present, which the MS/MS-results also confirmed.

A surprising observation was the presence of a PKA Aur7-sized band in the fractions of 6AH-ATP-Agarose; this could indicate either some alternative binding site for ATP as the crystal structures of PKA indicates too much steric hindrance for any linker to the Adenine-ring or that the resin acts as a weak cationic exchanger[60], the latter being the most likely explanation.

It is interesting to notice that PKA Aur7 does not share the binding to EDA-ATP-Agarose which ABL1 exhibited. This could be due to steric hindrance in the ribose-binding part of PKA. In Figure 4.7 the binding site of ATP is shown for both ABL1 and PKA where ABL1 is superimposed on the PKA-structure with an RMSD of 1.8 using the pymol-software package[116], and the sequence alignment (Figure 1.1) shows that where ABL1 has an Asparagine, PKA has a Glutamic acid oriented towards the ribose-ring. This could be a major cause of steric hindrance. The Glu-127 has earlier been studied, as it is an Aspartic acid in the other AGC-kinases[18],and the substitution has been shown to have several effects including binding to the 3'-OH of the ribose and it has been speculated that the natural rotamer will cause clashes with inhibitors with groups going out from the ribose-binding pocket[18]. Figure 4.5 shows the distribution of different residues for the 127-position for the kinome, and there is major differences. It would be interesting to test representatives of more protein kinase families to investigate the effect on selectivity versus the ribose-linked ATP-resin EDA-ATP-Agarose.

4.4.1.4 Cook-assay

PKA Aur7 does not appear to be active based on the results from the Cook-assay. It is interesting to see this in connection with the failure to bind to the immobilized PKI-column. Perhaps the F240D-mutation caused a change in the substrate-binding of PKA Aur7, preventing both PKI, Kemptide-binding and/or autophosphorylation. It is not clear what the mechanism of this change would be, yet it should be investigated further.

It could also be that remaining vanadate from the elution buffer causes inhibition of the protein kinase activity[36, and references therein].

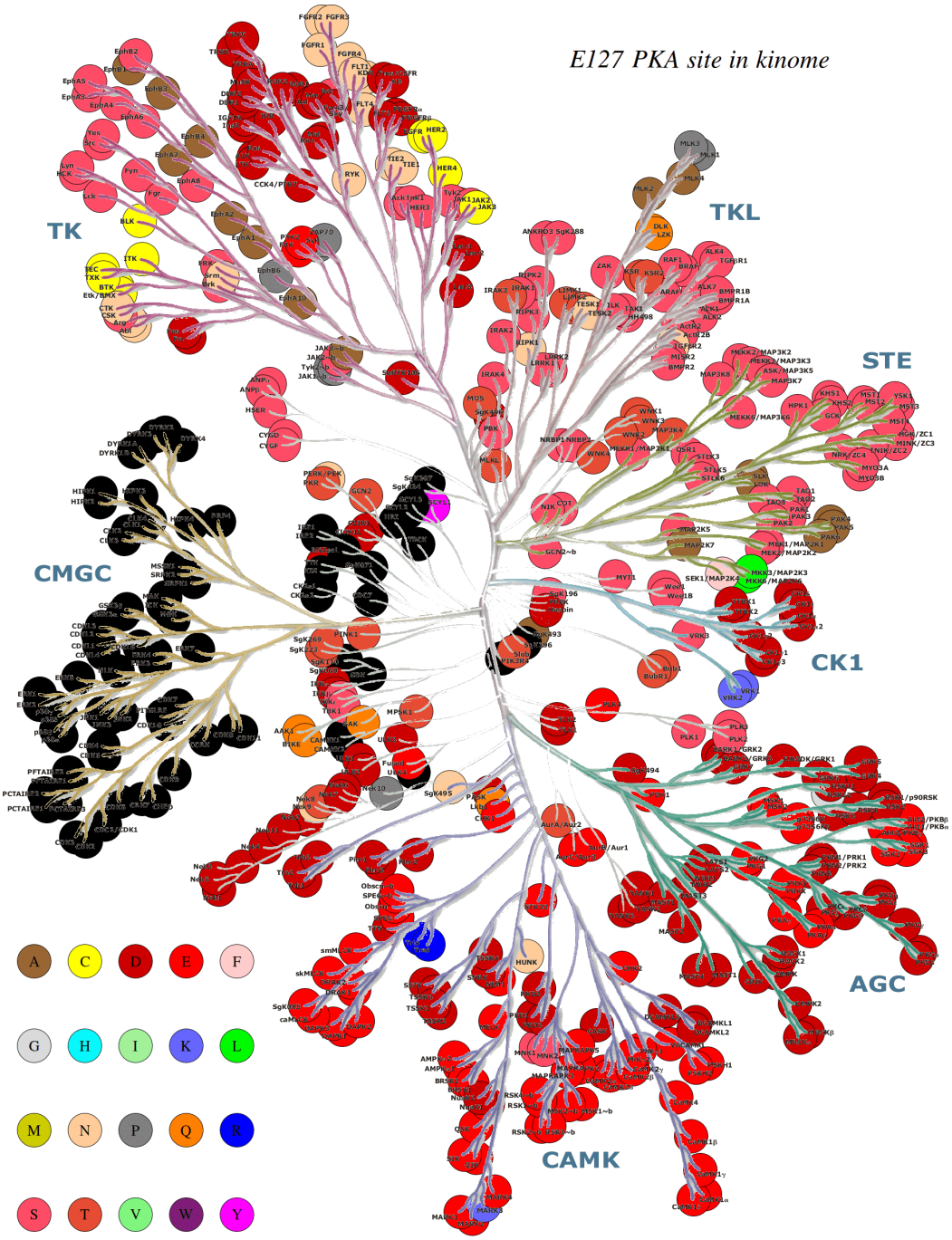

Figure 4.5: Manning-style plot of the kinome with the different residues for PKA-position 127. CMGC-kinases including DYRKs did not match the alignment, and is plotted in black (DYRK1A has an asparagine). The figure was prepared by Richard A. Engh

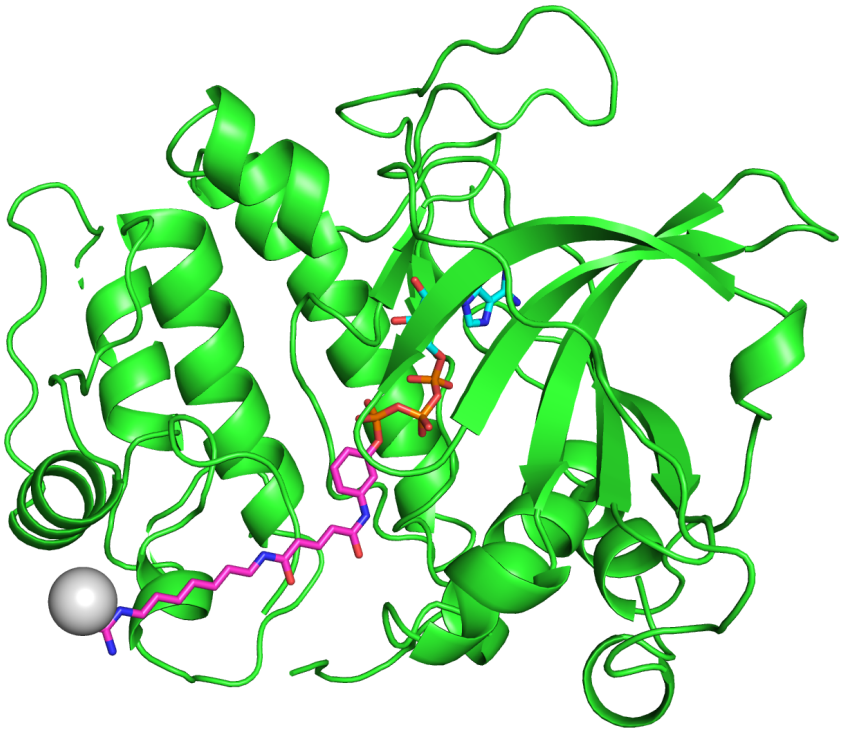

Figure 4.6: Hypothetical model of how binding of AP-ATP-Agarose to PKA might occur. Grey sphere illustrates the agarose-beads, the purple part of the stick-figure is the linker-moiety and the orange/blue is the linked ATP

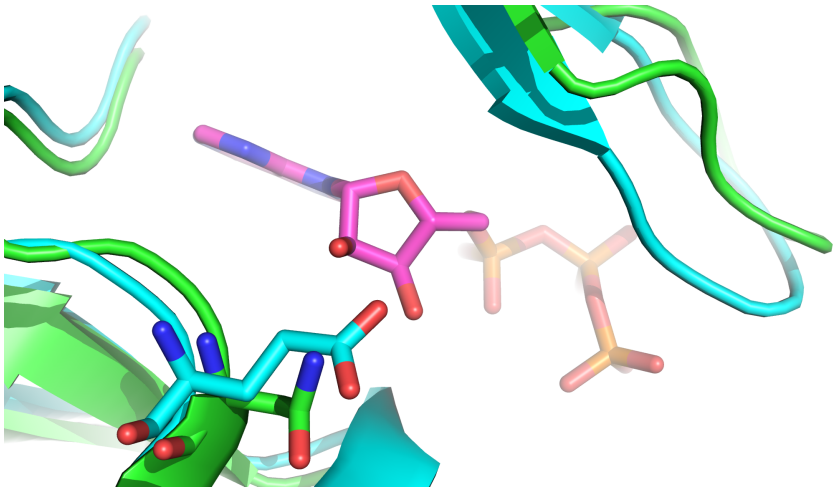

Figure 4.7: ABL1 (green) and PKA (cyan) superimposed with ATP (purple/orange) with Glu 127 (PKA) and Asn 322 (ABL1) shown with stick-figures.

4.4.2 Protein kinase A threefold mutant model of AKT

4.4.2.1 ATP-analog binding assay

The results observed are very similar to the results of PKA Aur7 which is not surprising given the high sequence identity of the two samples.

4.4.2.2 Purification with immobilized PKI

It was surprising to see binding to the modified PKI-peptide, and while the purification was not done "analytically", the binding appeared to be of similiar strength compared to the unmodified peptide (SDS-PAGE-bands were as strong for the elution-fraction). The Phe-10 is known to be very important for the affinity of PKI to PKA[56], so that this substitution of an hydrophobic residue to a polar residue still gives binding might just be because of high concentrations of PKAB3 in the sample.

4.4.2.3 Cationic exchange

The difference in retention on the cationic exchanger can be attributed to differences in phosphorylation. The charge-difference depends on pH, but each phosphorylation adds at least one negative charge to the protein, and negative charges weaken the binding to the negatively-charged matrix of the cationic exchanger. A shallower gradient might give better resolution, and perhaps indicate a higher number of phosphorylation states.

4.4.2.4 Surface plasmon resonance

The pH of the coupling is important because of the electrostatics of the interactions between the carboxymethylated dextran-surface and the protein. At 1 pH-unit below the pI of the protein, the protein has a overall positive charge and will be attracted to the surface. PKA has a pKa-value above 8, and does not need a very low pH to be attracted to the surface. However, highest immobilization was observed at pH 4.5. Amino-coupling involves converting the carboxyl-groups of the dextran to reactive succinimide esters which react with amine-groups on the protein.

Several attempts were made to demonstrate activity of the surface by using ATP as an analyte. ATP has previously been tested on Biacore with PKA[53, 131] and has a known affinity[131]. The lack of surface-activity may be due to the low pH used for immobilization, a higher pH may increase the stability of PKAB3, or it might be due to amino-coupling to amine-groups in the active site[119] although the inclusion of ATP and $MgCl_2$ was done in order to protect the active-site lysine[131, and references therein].

4.4.2.5 Cook-assay

The affinity of PKA to ATP is known to be approximately 10 µM, however different mutants have been shown to have different affinities for ATP[53, 101]. Non-linear fitting using computers gives better results than linearised methods such as Lineweaver-Burk, Hanes-Woolf and Eadie-Hofstee[58]. A weighted sum of square residuals-value or χ^2 of

3.78892 was obtained for the fit, the tables of p-values give 4.075 for $p < 0.995$ with 14 degrees of freedom (16 measurements were used - 2 parameters fitted).

The standard-deviation in the velocity-measurement for the inhibitor was significant, as illustrated by the error-bars on Figure 3.24. Three samples were used for each inhibitor-concentration. A higher number of parallels would most likely reduce the standard deviation, at a cost of sample and time. More dilutions should have been included, to have at least two samples at each side of the "bend"[118]. The four-parameter logistic fit gave good results with the data with $R^2 = 0.999$.

The determined IC50 for 34a was in range with previously determined values[4]. Using the Cheng-Prusoff equation (Equation 4.1) it is possible to transform the IC50-value into a K_i, which is an absolute value not dependent on the substrate-concentration. In Equation 4.1 the substrate considered is ATP, which has a known K_m-value[53].

$$K_i = \frac{IC_{50}}{1 + \frac{[S]}{K_m}} = \frac{2,85\mu\text{M}}{1 + \frac{0,5\mu\text{M}}{21\mu\text{M}}} = 2,78\mu\text{M} \tag{4.1}$$

The IC50-value for ARC-1416 is closer to the value reported for PKB, $K_d = 3,5n\text{M}$[62], than the value reported for PKA, $K_d = 0,013n\text{M}$[62], even though K_d can not be compared directly to IC50 (which is the concentration where half of the enzymes activity is inhibited and also depends on the experimental setup) or K_m (which includes a term for K_{cat}). This shows that the three mutations introduced to PKA makes the enzyme more PKB-like.

4.4.2.6 Thermofluor

It was not possible to fit the thermal shifts induced by the inhibitors against the affinities given for PKA-wildtype in the same manner as done for PKA Aur6. All the inhibitors are known to bind with lower affinity to PKB, so it is as expected that the affinity is lowered for PKAB3 (as shown for ARC-1416).

It is however clear that the inhibitor 34a has a affinity much lower than the other inhibitors, as it only stabilises PKAB3 slightly. The thermal shift is also so small that it would fall far outside of the standard curve. It has been suggested that a thermal shift of 4 ℃ corresponds to a IC50-value below 1 µM[47], but the thermal shift induced by 34a was even smaller. This indicates that the IC50-value obtained from the Cook-assay in the correct range.

4.4.2.7 Microscale thermophoresis

The affinity of PKAB3 to 34a was shown to be in the nM range, which shows that $K_d < K_m$. This is likely if $k_{-1} >> k_{\text{cat}}$, which is true for efficient enzymes[9, p.525]. This validates the usage of the amine-labelling with NHS as it shows that the labelling does not interfere with the binding of the inhibitor, and makes the failure of SPR more surprising as the coupling-chemistry is equivalent. It was necessary to use the MST-buffer and hydrophillic capillaries to prevent aggregation and binding to the surface of the capillaries which could be observed as bumps in the spectrum for the trials with standard buffer and standard capillaries.

The fluorescence timetrace shows the lack of binding to the modified PKI sample, as there is no change in fluorescence signal proportional to the change in concentration. The lack of binding to modified PKI may be due to inproper storage of the modified peptide which contains asparagine, dissolved in water stored at 4 ℃. The peptide should preferably have been stored at −20 ℃ or lower.

4.4.2.8 Data collection and processing

Both structures were solved by molecular replacement, as there already existed several crystal structures of PKA and even PKAB3. This allowed the determination of phases without the use of experimental phasing methods such as single-wavelength anomalous dispersion (SAD) or multiple-wavelength anomalous dispersion (MAD). Nonetheless, attempts were made to determine the phases by the use of the anomalous-signal of the Bromine in the inhibitor 47a, as the wavelength (0.918 41 Å) is just beyond the absorption-peak of Bromine, in a SAD-experiment, however the anomalous signal was too weak for the software to fully determine the phases. A higher multiplicity or collection at multiple wavelengths (MAD) could have made it possible to determine the phases experimentally by using the Bromine in the inhibitor.

The overall geometry of the two structures are good: 47a has a Molprobity-score of 1.98 (ideally the number should be lower than the resolution of the structure which is 1.95[26]) with no Ramachandran-outliers and one rotamer-outlier. 34a has a Molprobity-score of 1.57 (which is lower than the 1.95) with no Ramachandran outliers and no rotamer-outliers as shown in Figure 4.8.

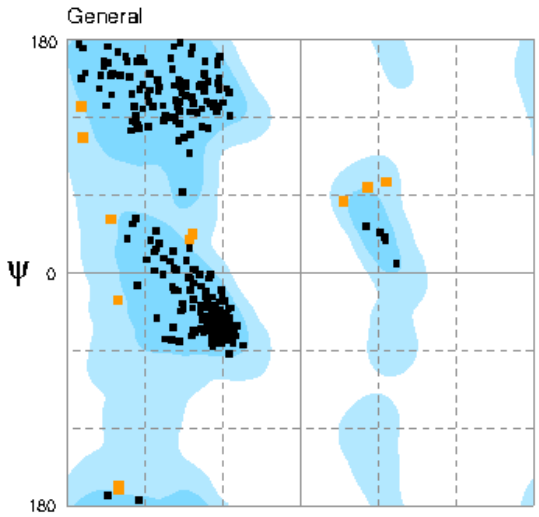

Figure 4.8: Ramachandran-plot for PKAB3 in complex with 34a visualized by RAMPAGE[82].Darker blue shows the generally favored conformations, while the light blue shows the generally allowed conformations.

The R-factors are close to the R-free-factors[71], which indicate that the model is not overfitted. A R-free above 40% indicates that the model is incorrect[70], but these models have R-free values beneath 24%. The number of water molecules (317 and 351) built into the model is close to the number of protein residues (357), which is reasonable for a model of approximately 2 Å-resolution[70].

The bound inhibitors 47a and 34a have weaker electron density for the halogens bromine and chlorine. 34a also has weaker density for a sulfur-atom in the five-ring. Radiation damage is a probable cause for this discrepancy, as this is known for at least halogenated aromatics and methionine/cysteine[42, 109, 108] as these are electron-rich atoms.

For the soaked inhibitor 47a the observed Wilson B-factor is larger than for the cocrystallized 34a-structure, with an exception for the ligand-B-factor which is only somewhat larger for 47a. Soaking is a hard process for the crystal, and many crystals do crack or show damages when a new compound is soaked in. It has been claimed that the proteins in soaked crystals do not go through the full range of conformational changes which the cocrystallized proteins are allowed to[59], and perhaps this causes the crystal to be in a less ordered state (with higher B-factors). Another explanation might be the radiation damage, which is known to increase B-factors[109] and would be more apparent for 47a with its electron-rich Bromine than the 34a with the smaller chlorine.

The inhibitors bind in the ATP-binding pocket, as they were expected to based on their competitive inhibition and their structural similarity to ATP. Electron density maps and modelled coordinates for 34a in complex with PKAB3 is shown in Figure 4.9.

No major structural changes can be observed compared to one of the previous structures of PKAB3, 1Q61[53], and alignment using CEalign[120] in PyMOL[116] gives a root mean square deviation (RMSD) of 0.411379 over 352 residues for the 47a-structure and 0.620324 over 352 residues for the 34a-structure. One of differences observed is the shift of the glycine-rich loop of approximately 2.5 Å. This flexibility of the glycine-rich loop has previously been described[53] and the structures presented here appears to belong to group B-glycine-rich loops since they point away from the cleft and have ψ-angles for Phe-54 moderately positive at around 25°. This could be explained by the introduction of larger and more aliphatic groups in the inhibitors compared to the phosphates of ATP.

4.4.3 Protein kinase A mutant model of Rho

4.4.3.1 ATP-analog binding assay

The results were comparable to the results for PKA Aur6 and PKAB3. This is as expected given the high sequence-identity of the mutants. PKAR5 has an E127D substitution, and was expressed to check whether this substitution with a shorter acidic side-chain would allow the entrance of the ribose-linked ATP by reducing the steric hindrance. This does not appear to happen, even though ABL1 with its asparagine does have binding with the ribose-linked ATP. It might be that there is other variations in the ATP-binding site preventing the binding, or that the negative charge of the aspartic and glutamic acid prevents the binding.

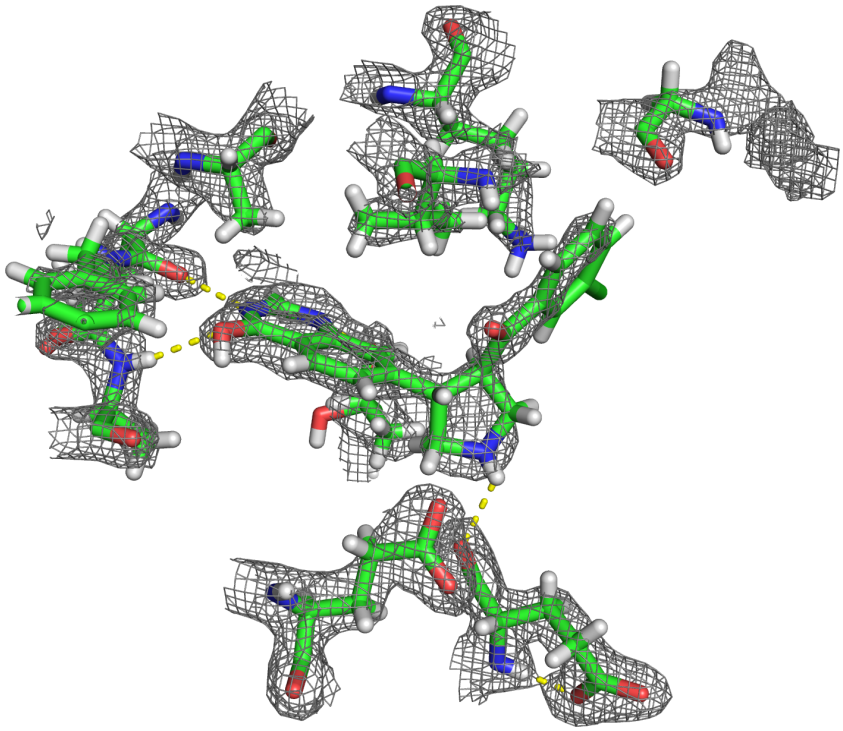

Figure 4.9: Coordinates and electron density maps for the inhibitor 34a in complex with PKAB3. The carbons are shown in green, oxygens in red and nitrogens in blue.

The shorter incubation time for PKAR5 gave weaker bands in SDS-PAGE, but also less binding of endogenous proteins.

Chapter 5

Conclusions and future work

5.1 Protein production

In this project four different ATP-analogs have been evaluated as resins for affinity chromatography. Each of the targeted proteins have responded differently to the set of ATP-analogs. ABL1 showed binding to both AP-ATP-Agarose and EDA-ATP-Agarose, while DYRK1A only shows binding to EDA-ATP-Agarose. The mutants of PKA binds to AP-ATP-Agarose, yet PKA Aur7 also binds to 6AH-ATP-Agarose. The chaperone HSP70 binds to both 6AH-ATP-Agarose and 8AH-ATP-Agarose. The difference in binding opens opportunities for further research into the structural origins of this diversity. One particular discrepancy was in the binding of the ribose-linked ATP, which ABL1 and DYRK1A bound to and PKA did not bind to; this observation could be due to differences in the properties of the residues around the ribose as suggested in this paper, however this speculation should be investigated with point-mutations and further experiments. A E127N-mutant of PKA to make PKA more ABL1- and DYRK1A-like would be a first step. It is possible to conclude that the *E.coli*-expressed ABL1 is folded, as it binds ATP, which solved an previously open question about the TF-ABL1-construct.

Unfortunately, no work was done to scale the use of ATP-analogs up to a preparative scale, further work would be required to compare the preparative application of ATP-affinity chromatography to other purification methods.

The usage of bisubstrate inhibitors as eluants from immobilized PKI appears to be novel, and the major advantage is the more selective eluation of the active form of PKA. It would be interesting to test with different classes of inhibitors, to investigate whether different forms may be eluted.

5.2 Drug discovery

For cAMP-dependent protein kinase/protein kinase A purification with PKI has been studied. Investigations with site-directed mutagenesis have resulted in a mutant, PKA Aur7 which has lowered affinity for PKI. An interesting application of this could be in the study of catalytically inactive mutants of PKA, which is not able to autophosphorylate

in *E.coli*. The unphosphorylated PKA has lower stability, and for this reason it could be beneficial to coexpress with a catalytically active mutant[138]. If the mutation of PKA Aur7 does not interfere with its activity, PKA Aur7 might be a valuable tool, as it would allow easy purification of the coexpressed protein by immobilized-PKI where PKA Aur7 would not bind.

Two new PKB-inhibitors, 34a and 47a, were characterized by Cook-assay, Thermofluor, MST and X-ray crystallography with PKAB3, a surrogate-model of PKB. In combination these methods validate and quantify the binding of the inhibitors.

Bibliography

[1] Espen Åberg, Bjarte Aarmo Lund, Alexander Pflug, Osman a.B.S.M. Gani, Ulli Rothweiler, Taianà M. de Oliveira, and Richard A. Engh. "Structural origins of AGC protein kinase inhibitor selectivities: PKA as a drug discovery tool". In: *Biological Chemistry* 393.10 (Oct. 2012), pp. 1121–1129. DOI: 10.1515/hsz-2012-0248 (cit. on pp. 2, 24).

[2] Paul D Adams, Pavel V Afonine, Gábor Bunkoczi, Vincent B Chen, Ian W Davis, Nathaniel Echols, Jeffrey J Headd, L-W Hung, Gary J Kapral, Ralf W Grosse-Kunstleve, et al. "PHENIX: a comprehensive Python-based system for macromolecular structure solution". In: *Acta Crystallographica Section D: Biological Crystallography* 66.2 (2010), pp. 213–221 (cit. on p. 43).

[3] Pavel V Afonine, Ralf W Grosse-Kunstleve, Nathaniel Echols, Jeffrey J Headd, Nigel W Moriarty, Marat Mustyakimov, Thomas C Terwilliger, Alexandre Urzhumtsev, Peter H Zwart, and Paul D Adams. "Towards automated crystallographic structure refinement with phenix. refine". In: *Acta Crystallographica Section D: Biological Crystallography* 68.4 (2012), pp. 352–367 (cit. on p. 43).

[4] Kazi Asraful Alam. "Doctoral work at University of Tromsø" (cit. on p. 79).

[5] B. Alberts, A. Johnson, J. Lewis, M. Raff, K. Roberts, P. Walter, et al. "Fractionation of Cells". In: (2002) (cit. on pp. 14, 15).

[6] Amy C. Anderson. "The Process of Structure-Based Drug Design". In: *Chemistry & Biology* 10.9 (Sept. 2003), pp. 787–797. DOI: 10.1016/j.chembiol.2003.09.002 (cit. on p. 10).

[7] Paul D Andrews, Elena Knatko, William J Moore, and Jason R Swedlow. "Mitotic mechanics: the auroras come into view". In: *Current opinion in cell biology* 15.6 (2003), pp. 672–683 (cit. on p. 26).

[8] Richard M Angell, Tony D Angell, Paul Bamborough, Mark J Bamford, Chun wa Chung, Stuart G Cockerill, Stephen S Flack, Katherine L Jones, Dramane I Laine, Timothy Longstaff, Steve Ludbrook, Rosannah Pearson, Kathryn J Smith, Penny A Smee, Don O Somers, and Ann L Walker. "Biphenyl amide p38 kinase inhibitors 4: DFG-in and DFG-out binding modes." In: *Bioorganic & medicinal chemistry letters* 18.15 (Aug. 2008), pp. 4433–7. DOI: 10.1016/j.bmcl.2008.06.028 (cit. on p. 5).

[9] E.V. Anslyn and D.A. Dougherty. *Modern physical organic chemistry*. University Science Books, 2006 (cit. on p. 79).

[10] Sergi Aranda, Ariadna Laguna, and Susana de la Luna. "DYRK family of protein kinases: evolutionary relationships, biochemical properties, and functional roles". In: *The FASEB Journal* 25.2 (2011), pp. 449–462. DOI: 10.1096/fj.10-165837. eprint: http://www.fasebj.org/content/25/2/449.full.pdf+html (cit. on p. 26).

[11] C ARTEAGA. "Targeting HER1/EGFR: A molecular approach to cancer therapy". In: *Seminars in Oncology* 30.3 (June 2003), pp. 3–14. DOI: 10.1016/S0093-7754(03)70010-4 (cit. on p. 10).

[12] *ATP Affinity Test Kit Screening Kit for the purification of ATP binding proteins*. Jena Bioscience. 2013 (cit. on p. 16).

[13] Clive R. Bagshaw. "ATP analogues at a glance". In: *Journal of Cell Science* 114.3 (2001), pp. 459–460. eprint: http://jcs.biologists.org/content/114/3/459.full.pdf+html (cit. on p. 16).

[14] S Bailey. "The CCP4 suite: programs for protein crystallography". In: *Acta Crystallogr. D* 50 (1994), pp. 760–763 (cit. on p. 43).

[15] S. Barker, Daniel B. Kassel, D. Weigl, X. Huang, M. Luther, and Wilson B. Knight. "Characterization of pp60c-src Tyrosine Kinase Activities Using a Continuous Assay: Autoactivation of the Enzyme Is an Intermolecular Autophosphorylation Process". In: *Biochemistry* 34.45 (Nov. 1995), pp. 14843–14851. DOI: 10.1021/bi00045a027 (cit. on p. 1).

[16] RobertJ. Beynon and Simon Oliver. "Avoidance of Proteolysis in Extracts". English. In: *Protein Purification Protocols*. Ed. by Paul Cutler. Vol. 244. Methods in Molecular Biology. Humana Press, 2004, pp. 75–84. DOI: 10.1385/1-59259-655-X:75 (cit. on p. 14).

[17] Julie Blouin, Philippe Roby, Mathieu Arcand, Lucille Beaudet, and Francesco Lipari. "Catalytic specificity of human protein tyrosine kinases revealed by Peptide substrate profiling." In: *Current chemical genomics* 5 (Jan. 2011), pp. 115–21. DOI: 10.2174/1875397301105010115 (cit. on p. 7).

[18] Stefan Bonn, Saturnino Herrero, Christine B. Breitenlechner, Andrea Erlbruch, Wolf Lehmann, Richard A. Engh, Michael Gassel, and Dirk Bossemeyer. "Structural Analysis of Protein Kinase A Mutants with Rho-kinase Inhibitor Specificity". In: *Journal of Biological Chemistry* 281.34 (2006), pp. 24818–24830. DOI: 10.1074/jbc.M512374200. eprint: http://www.jbc.org/content/281/34/24818.full.pdf+html (cit. on pp. 2, 24, 75).

[19] D Bossemeyer, R A Engh, V Kinzel, H Ponstingl, and R Huber. "Phosphotransferase and substrate binding mechanism of the cAMP-dependent protein kinase catalytic subunit from porcine heart as deduced from the 2.0 A structure of the complex with Mn2+ adenylyl imidodiphosphate and inhibitor peptide PKI(5-24)." In: *The EMBO journal* 12.3 (Mar. 1993), pp. 849–59 (cit. on pp. 5, 7, 10, 24).

[20] Dirk Bossemeyer. "Protein kinases — structure and function". In: *FEBS Letters* 369.1 (1995), pp. 57–61. DOI: 10.1016/0014-5793(95)00580-3 (cit. on pp. 2, 5).

[21] M M Bradford. "A rapid and sensitive method for the quantitation of microgram quantities of protein utilizing the principle of protein-dye binding." In: *Analytical biochemistry* 72 (May 1976), pp. 248–54 (cit. on p. 41).

[22] C I Branden and J Tooze. *Introduction to protein structure*. 2nd ed. Introduction to Protein Structure Series. Garland Pub., 1999 (cit. on pp. 22, 23).

[23] Christine B Breitenlechner, Dirk Bossemeyer, and Richard a Engh. "Crystallography for protein kinase drug design: PKA and SRC case studies." In: *Biochimica et biophysica acta* 1754.1-2 (Dec. 2005), pp. 38–49. DOI: 10.1016/j.bbapap.2005.09.014 (cit. on pp. 10, 24).

[24] Linda C., Morton John F., Treuting Piper R., Emond Mary J., Wolf Norman S., McKnight G. S., Rabinovitch Peter S., and Ladiges Warren C. Enns. "Disruption of Protein Kinase A in Mice Enhances Healthy Aging". In: *PLoS ONE* 4.6 (June 2009), e5963. DOI: 10.1371/journal.pone.0005963 (cit. on p. 1).

[25] Renaud Capdeville, Elisabeth Buchdunger, Juerg Zimmermann, and Alex Matter. "Glivec (STI571, imatinib), a rationally developed, targeted anticancer drug." In: *Nature reviews. Drug discovery* 1.7 (July 2002), pp. 493–502. DOI: 10.1038/nrd839 (cit. on p. 10).

[26] Vincent B Chen, W Bryan Arendall III, Jeffrey J Headd, Daniel A Keedy, Robert M Immormino, Gary J Kapral, Laura W Murray, Jane S Richardson, and David C Richardson. "MolProbity: all-atom structure validation for macromolecular crystallography". In: *Acta Crystallographica Section D* 66.1 (Jan. 2010), pp. 12–21. DOI: 10.1107/S0907444909042073 (cit. on p. 80).

[27] Natalia Cheshenko, Janie B. Trepanier, Martha Stefanidou, Niall Buckley, Pablo Gonzalez, William Jacobs, and Betsy C. Herold. "HSV activates Akt to trigger calcium release and promote viral entry: novel candidate target for treatment and suppression". In: *The FASEB Journal* (2013). DOI: 10.1096/fj.12-220285. eprint: http://www.fasebj.org/content/early/2013/03/29/fj.12-220285.full.pdf+html (cit. on p. 1).

[28] P. Cohen. "The development and therapeutic potential of protein kinase inhibitors". In: *Current opinion in chemical biology* 3.4 (1999), pp. 459–465 (cit. on p. 10).

[29] John Colicelli. "ABL tyrosine kinases: evolution of function, regulation, and specificity." In: *Science signaling* 3.139 (Jan. 2010), re6. DOI: 10.1126/scisignal.3139re6 (cit. on p. 9).

[30] Paul F. Cook, Maynard E. Neville, Kent E. Vrana, F. Thomas Hartl, and Robert Roskoski. "Adenosine cyclic 3',5'-monophosphate dependent protein kinase: kinetic mechanism for the bovine skeletal muscle catalytic subunit". In: *Biochemistry* 21.23 (1982), pp. 5794–5799. DOI: 10.1021/bi00266a011. eprint: http://pubs.acs.org/doi/pdf/10.1021/bi00266a011 (cit. on p. 20).

[31] Frederick F. Correia, Anthony D'Onofrio, Tomas Rejtar, Lingyun Li, Barry L. Karger, Kira Makarova, Eugene V. Koonin, and Kim Lewis. "Kinase Activity of Overexpressed HipA Is Required for Growth Arrest and Multidrug Tolerance in Escherichia coli". In: *Journal of Bacteriology* 188.24 (December 15, 2006), pp. 8360–8367. DOI: 10.1128/JB.01237-06. eprint: http://jb.asm.org/content/188/24/8360.full.pdf+html (cit. on p. 75).

[32] Richard H. Cowan. "Refolding of protein kinases". PhD thesis. University of Warwick, 2009 (cit. on p. 71).

[33] J Crowe and K Henco. "The QIAexpressionist". In: *Qiagen Inc, Chatsworth, CA, USA* (1992) (cit. on p. 16).

[34] Eric D and Bourne Philip E Scheeff. "Structural Evolution of the Protein Kinase–Like Superfamily". In: *PLoS Comput Biol* 1.5 (Oct. 2005), e49. DOI: 10.1371/journal.pcbi.0010049 (cit. on p. 2).

[35] George D Dalton and William L Dewey. "Protein kinase inhibitor peptide (PKI): a family of endogenous neuropeptides that modulate neuronal cAMP-dependent protein kinase function." In: *Neuropeptides* 40.1 (Mar. 2006), pp. 23–34. DOI: 10.1016/j.npep.2005.10.002 (cit. on pp. 1, 10).

[36] Douglas R Davies and Wim G J Hol. "The power of vanadate in crystallographic investigations of phosphoryl transfer enzymes." In: *FEBS letters* 577.3 (2004), pp. 315–321 (cit. on pp. 7, 75).

[37] Stephen P. DAVIES, Simon A. HAWLEY, Angela WOODS, David CARLING, Timothy A. J. HAYSTEAD, and D. Grahame HARDIE. "Purification of the AMP-activated protein kinase on ATP-γ-Sepharose and analysis of its subunit structure". In: *European Journal of Biochemistry* 223.2 (1994), pp. 351–357. DOI: 10.1111/j.1432-1033.1994.tb19001.x (cit. on p. 16).

[38] J.S. Duncan, TA Haystead, and D.W. Litchfield. "Chemoproteomic characterization of protein kinase inhibitors using immobilized ATP." In: *Methods in molecular biology (Clifton, NJ)* 795 (2012), p. 119 (cit. on p. 10).

[39] R.M. Eglen and Terry Reisine. "The current status of drug discovery against the human kinome". In: *Assay and drug development technologies* 7.1 (Feb. 2009), pp. 22–43. DOI: 10.1089/adt.2008.164 (cit. on p. 1).

[40] D. Eisenberg. "Amino acid scale: Normalized consensus hydrophobicty scale". In: *J. Mol. Biol.* 179 (1984), pp. 125–142 (cit. on p. 8).

[41] Bernhard Lohkamp William Scott Paul Emsley and Kevin Cowtan. "Features and Development of Coot". In: *Acta Crystallographica Section D - Biological Crystallography* 66 (2010), pp. 486–501 (cit. on p. 43).

[42] E Ennifar, P Carpentier, J-L Ferrer, P Walter, and P Dumas. "X-ray-induced debromination of nucleic acids at the Br K absorption edge and implications for MAD phasing". In: *Acta Crystallographica Section D: Biological Crystallography* 58.8 (2002), pp. 1262–1268 (cit. on p. 81).

[43] Ulrika B Ericsson, B Martin Hallberg, George T Detitta, Niek Dekker, and Pär Nordlund. "Thermofluor-based high-throughput stability optimization of proteins for structural studies." In: *Analytical biochemistry* 357.2 (Oct. 2006), pp. 289–98. DOI: 10.1016/j.ab.2006.07.027 (cit. on p. 21).

[44] Philip Evans. "Scaling and assessment of data quality". In: *Acta Crystallographica Section D: Biological Crystallography* 62.1 (2005), pp. 72–82 (cit. on p. 43).

[45] Philip R Evans. "An introduction to data reduction: space-group determination, scaling and intensity statistics". In: *Acta Crystallographica Section D: Biological Crystallography* 67.4 (2011), pp. 282–292 (cit. on p. 43).

[46] Doriano Fabbro, SandraW. Cowan-Jacob, Henrik Möbitz, and Georg Martiny-Baron. "Targeting Cancer with Small-Molecular-Weight Kinase Inhibitors". English. In: *Kinase Inhibitors*. Ed. by Bernhard Kuster. Vol. 795. Methods in Molecular Biology. Humana Press, 2012, pp. 1–34. DOI: 10.1007/978-1-61779-337-0_1 (cit. on pp. 7, 10).

[47] Oleg Fedorov, Brian Marsden, Vanda Pogacic, Peter Rellos, Susanne Müller, Alex N Bullock, Juerg Schwaller, Michael Sundström, and Stefan Knapp. "A systematic interaction map of validated kinase inhibitors with Ser/Thr kinases". In: *Proceedings of the National Academy of Sciences* 104.51 (2007), pp. 20523–20528 (cit. on p. 79).

[48] Stefano Ferrari, Oriano Marin, Mario A Pagano, Flavio Meggio, Daniel Hess, Mahmoud El-Shemerly, Agnieszka Krystyniak, and Lorenzo A Pinna. "Aurora-A site specificity: a study with synthetic peptide substrates." In: *The Biochemical journal* 390.Pt 1 (Aug. 2005), pp. 293–302. DOI: 10.1042/BJ20050343 (cit. on p. 9).

[49] Eileen Friedman. "Mirk/Dyrk1B in cancer". In: *Journal of Cellular Biochemistry* 102.2 (2007), pp. 274–279. DOI: 10.1002/jcb.21451 (cit. on p. 26).

[50] Dmitrij Frishman and Patrick Argos. "Knowledge-based protein secondary structure assignment". In: *Proteins: Structure, Function, and Bioinformatics* 23.4 (1995), pp. 566–579. DOI: 10.1002/prot.340230412 (cit. on p. 3).

[51] Osman A B S M Gani and Richard A Engh. "Protein kinase inhibition of clinically important staurosporine analogues." en. In: *Natural product reports* 27.4 (Apr. 2010), pp. 489–98. DOI: 10.1039/b923848b (cit. on p. 10).

[52] M Gaßel, C Breitenlechner, R Engh, S Herrero, and D Bossemeyer. "Inhibitors of PKA and Related Protein Kinases". In: *Inhibitors of Protein Kinases and Protein Phosphates*. Ed. by Lorenzo A Pinna and Patricia T W Cohen. Vol. 167. Handbook of Experimental Pharmacology. Springer Berlin Heidelberg, 2005, pp. 85–124 (cit. on pp. 10, 24).

[53] M. Gaßel, C.B. Breitenlechner, P. Rüger, U. Jucknischke, T. Schneider, R. Huber, D. Bossemeyer, R.A. Engh, et al. "Mutants of protein kinase A that mimic the ATP-binding site of protein kinase B (AKT)." In: *Journal of molecular biology* 329.5 (2003), p. 1021 (cit. on pp. 2, 24, 78, 79, 81).

[54] Michael Gaßel, Christine B. Breitenlechner, Petra Rüger, Ute Jucknischke, Thorsten Schneider, Robert Huber, Dirk Bossemeyer, and Richard A. Engh. "Mutants of Protein Kinase A that Mimic the ATP-binding Site of Protein Kinase B (AKT)". In: *Journal of Molecular Biology* 329.5 (June 2003), pp. 1021–1034. DOI: 10.1016/S0022-2836(03)00518-7 (cit. on pp. 24, 25).

[55] Fiona Girdler, Karen E. Gascoigne, Patrick A. Eyers, Sonya Hartmuth, Claire Crafter, Kevin M. Foote, Nicholas J. Keen, and Stephen S. Taylor. "Validating Aurora B as an anti-cancer drug target". In: *Journal of Cell Science* 119.17 (2006), pp. 3664–3675. DOI: 10.1242/jcs.03145. eprint: http://jcs.biologists.org/content/119/17/3664.full.pdf+html (cit. on p. 26).

[56] DB Glass, LJ Lundquist, BM Katz, and DA Walsh. "Protein kinase inhibitor-(6-22)-amide peptide analogs with standard and nonstandard amino acid substitutions for phenylalanine 10. Inhibition of cAMP-dependent protein kinase." In: *Journal of Biological Chemistry* 264.24 (1989), pp. 14579–14584 (cit. on p. 78).

[57] S. Gräslund, P. Nordlund, J. Weigelt, J. Bray, O. Gileadi, S. Knapp, U. Oppermann, C. Arrowsmith, R. Hui, J. Ming, et al. "Protein production and purification". In: *Nature Methods* 5.2 (2008), pp. 135–146 (cit. on pp. 13, 14).

[58] William R Greco and Maire T Hakala. "Evaluation of methods for estimating the dissociation constant of tight binding enzyme inhibitors." In: *Journal of Biological Chemistry* 254.23 (1979), pp. 12104–12109 (cit. on p. 78).

[59] Anne M. Hassell, Gang An, Randy K. Bledsoe, Jane M. Bynum, III H. Luke Carter, Su-Jun J. Deng, Robert T. Gampe, Tamara E. Grisard, Kevin P. Madauss, Robert T. Nolte, Warren J. Rocque, Liping Wang, Kurt L. Weaver, Shawn P. Williams, G. Bruce Wisely, Robert Xu, and Lisa M. Shewchuk. "Crystallization of protein–ligand complexes". In: *Acta Crystallographica Section D* 63.1 (2007), pp. 72–79. DOI: 10.1107/S0907444906047020 (cit. on p. 81).

[60] Clare M. M. HAYSTEAD, Peter GREGORY, Thomas W. STURGILL, and Timothy A. J. HAYSTEAD. "γ-Phosphate-linked ATP-Sepharose for the affinity purification of protein kinases". In: *European Journal of Biochemistry* 214.2 (1993), pp. 459–467. DOI: 10.1111/j.1432-1033.1993.tb17942.x (cit. on pp. 16, 75).

[61] J.N. Israelachvili. *Intermolecular and Surface Forces: Revised Third Edition*. Intermolecular and Surface Forces. Elsevier Science, 2011 (cit. on pp. 12, 13).

[62] Taavi Ivan. "Written communication 2012". University of Tartu (cit. on pp. 55, 62, 79).

[63] J.C. Janson. *Protein Purification: Principles, High Resolution Methods, and Applications*. Methods of Biochemical Analysis. Wiley, 2012 (cit. on pp. 14–16, 18).

[64] Duane P Jeansonne, Tammy J Bordes, Cecily A Bennett, Geetha Kothandaraman, John G Bush, and Joseph A Vaccaro. "A rapid ATP affinity-based purification for the human non-receptor tyrosine kinase c-Src". In: *Protein expression and purification* 46.2 (2006), pp. 240–247 (cit. on p. 16).

[65] P Jenö, N Jäggi, H Luther, M Siegmann, and G Thomas. "Purification and characterization of a 40 S ribosomal protein S6 kinase from vanadate-stimulated Swiss 3T3 cells." In: *Journal of Biological Chemistry* 264.2 (1989), pp. 1293–1297. eprint: `http://www.jbc.org/content/264/2/1293.full.pdf+html` (cit. on p. 16).

[66] Moran Jerabek-Willemsen, Chistoph J Wienken, Dieter Braun, Philipp Baaske, and Stefan Duhr. "Molecular interaction studies using microscale thermophoresis". In: *Assay and drug development technologies* 9.4 (2011), pp. 342–353 (cit. on p. 21).

[67] Juliette, Anamika Krishanpal, and Srinivasan Narayanaswamy Martin. "Classification of Protein Kinases on the Basis of Both Kinase and Non-Kinase Regions". In: *PLoS ONE* 5.9 (Sept. 2010), e12460. DOI: `10.1371/journal.pone.0012460` (cit. on p. 2).

[68] B.E. Kemp and R.B. Pearson. "Protein kinase recognition sequence motifs". In: *Trends in biochemical sciences* 15.9 (1990), pp. 342–346 (cit. on p. 9).

[69] B Klebl, G Müller, M Hamacher, R Mannhold, H Kubinyi, and G Folkers. *Protein Kinases as Drug Targets*. Methods and Principles in Medicinal Chemistry. John Wiley & Sons, 2011 (cit. on pp. 1, 10).

[70] Gerard J Kleywegt. "Validation of protein crystal structures". In: *Acta Crystallographica Section D: Biological Crystallography* 56.3 (2000), pp. 249–265 (cit. on p. 81).

[71] Gerard J Kleywegt, Axel T Brünger, et al. "Checking your imagination: applications of the free R value". In: *Structure* 4.8 (1996), pp. 897–904 (cit. on p. 81).

[72] Anthony J. Koleske. *Abl Family Kinases in Development and Disease*. Molecular Biology Intelligence Unit. New York, NY: Springer New York, 2006. DOI: `10.1007/978-0-387-68744-5` (cit. on p. 25).

[73] Krisztián A. Kovács, Myriam Steinmann, Pierre J. Magistretti, Olivier Halfon, and Jean-René Cardinaux. "CCAAT/Enhancer-binding Protein Family Members Recruit the Coactivator CREB-binding Protein and Trigger Its Phosphorylation". In: *Journal of Biological Chemistry* 278.38 (2003), pp. 36959–36965. DOI: `10.1074/jbc.M303147200`. eprint: `http://www.jbc.org/content/278/38/36959.full.pdf+html` (cit. on p. 18).

[74] Andrey Y. Kovalevsky, Hanna Johnson, B. Leif Hanson, Mary Jo Waltman, S. Zoe Fisher, Susan Taylor, and Paul Langan. "Low- and room-temperature X-ray structures of protein kinase A ternary complexes shed new light on its activity". In: *Acta Crystallographica Section D* 68.7 (2012), pp. 854–860. DOI: 10.1107/S0907444912014886 (cit. on pp. 6, 8).

[75] Michael Krug, Manfred S. Weiss, Udo Heinemann, and Uwe Mueller. "*XDSAPP*: a graphical user interface for the convenient processing of diffraction data using *XDS*". In: *Journal of Applied Crystallography* 45.3 (2012), pp. 568–572. DOI: 10.1107/S0021889812011715 (cit. on p. 42).

[76] Peter Kyomuhendo. "Post-doctoral work at University of Tromsø" (cit. on p. 26).

[77] C Lapid and Y Gao. *PrimerX-Automated design of mutagenic primers for site-directed mutagenesis*. 2003 (cit. on p. 38).

[78] Darja Lavogina, Erki Enkvist, and Asko Uri. "Bisubstrate inhibitors of protein kinases: from principle to practical applications." In: *Chemmedchem* 5.1 (2010), pp. 23–34 (cit. on p. 11).

[79] Darja Lavogina, Marje Lust, Indrek Viil, Norbert Konig, Gerda Raidaru, Jevgenia Rogozina, Erki Enkvist, Asko Uri, and Dirk Bossemeyer. "Structural Analysis of ARC-Type Inhibitor (ARC-1034) Binding to Protein Kinase A Catalytic Subunit and Rational Design of Bisubstrate Analogue Inhibitors of Basophilic Protein Kinases". In: *Journal of Medicinal Chemistry* 52.2 (2009). PMID: 19143565, pp. 308–321. DOI: 10.1021/jm800797n. eprint: http://pubs.acs.org/doi/pdf/10.1021/jm800797n (cit. on pp. 55, 62).

[80] Nurit LIVNAH Mazkeret Batya (IL), Tamar YECHEZKEL Ramat-Gan (IL), Yosef SALITRA Rehovot (IL), Boris PERLMUTTER Gane Aviv (IL), Onsat OHNE Kfar Saba (IL), Ilana COHEN Nes Ziona (IL), Pninit LITMAN Nes Ziona (IL), and Hanoch SENDEROWITZ Tel Aviv (IL). *Protein kinase inhibitors comprising ATP mimetics conjugated to peptides or pertidomimetics*. US, Feb. 2005 (cit. on p. 11).

[81] Mart Loog, Asko Uri, Jaak Järv, and Pia Ek. "Bi-substrate analogue ligands for affinity chromatography of protein kinases". In: *FEBS letters* 480.2 (2000), pp. 244–248 (cit. on p. 11).

[82] Simon C Lovell, Ian W Davis, W Bryan Arendall, Paul IW de Bakker, J Michael Word, Michael G Prisant, Jane S Richardson, and David C Richardson. "Structure validation by Cα geometry: ϕ, ψ and Cβ deviation". In: *Proteins: Structure, Function, and Bioinformatics* 50.3 (2003), pp. 437–450 (cit. on p. 80).

[83] B. A. Lund. *Modelling affinity-interactions of cAMP-dependent protein kinase*. KJE-3810, University of Tromsø. 2012 (cit. on pp. 10, 11).

[84] Carol J Lusty. "A gentle vapor-diffusion technique for cross-linking of protein crystals for cryocrystallography". In: *Journal of applied crystallography* 32.1 (1999), pp. 106–112 (cit. on p. 24).

[85] Nicholas M, Kuchment Olga, Shen Kui, Young Matthew A, Koldobskiy Michael, Karplus Martin, Cole Philip A, and Kuriyan John Levinson. "A Src-Like Inactive Conformation in the Abl Tyrosine Kinase Domain". In: *PLoS Biol* 4.5 (May 2006), e144. DOI: 10.1371/journal.pbio.0040144 (cit. on pp. 71, 72).

[86] Haiching Ma, Sean Deacon, and Kurumi Horiuchi. "The challenge of selecting protein kinase assays for lead discovery optimization". In: *Expert Opinion on Drug Discovery* 3.6 (2008), pp. 607–621. DOI: 10.1517/17460441.3.6.607. eprint: http://informahealthcare.com/doi/pdf/10.1517/17460441.3.6.607 (cit. on pp. 19, 20).

[87] Madhusudan, Akamine Pearl, Xuong Nguyen-Huu, and Taylor Susan S. "Crystal structure of a transition state mimic of the catalytic subunit of cAMP-dependent protein kinase". In: *Nat Struct Mol Biol* 9.4 (2002). 10.1038/nsb780, pp. 273–277. DOI: 10.1038/nsb780 (cit. on p. 5).

[88] Magdalena, Karlberg Tobias, Lehtiö Lari, Johansson Ida, Kotenyova Tetyana, Moche Martin, and Schüler Herwig Wisniewska. "Crystal Structures of the ATPase Domains of Four Human Hsp70 Isoforms: HSPA1L/Hsp70-hom, HSPA2/Hsp70-2, HSPA6/Hsp70B', and HSPA5/BiP/GRP78". In: *PLoS ONE* 5.1 (Jan. 2010), e8625. DOI: 10.1371/journal.pone.0008625 (cit. on pp. 69, 70).

[89] G Manning, D B Whyte, R Martinez, T Hunter, and S Sudarsanam. "The protein kinase complement of the human genome." In: *Science (New York, N.Y.)* 298.5600 (Dec. 2002), pp. 1912–34. DOI: 10.1126/science.1075762 (cit. on pp. 1, 2).

[90] Daumantas Matulis, James K Kranz, F Raymond Salemme, and Matthew J Todd. "Thermodynamic stability of carbonic anhydrase: measurements of binding affinity and stoichiometry using ThermoFluor". In: *Biochemistry* 44.13 (2005), pp. 5258–5266 (cit. on pp. 21, 73).

[91] Airlie J McCoy, Ralf W Grosse-Kunstleve, Paul D Adams, Martyn D Winn, Laurent C Storoni, and Randy J Read. "Phaser crystallographic software". In: *Journal of applied crystallography* 40.4 (2007), pp. 658–674 (cit. on p. 43).

[92] Georgia B. McGaughey, Marc Gagné, and Anthony K. Rappé. "π-Stacking Interactions: ALIVE AND WELL IN PROTEINS". In: *Journal of Biological Chemistry* 273.25 (1998), pp. 15458–15463. DOI: 10.1074/jbc.273.25.15458. eprint: http://www.jbc.org/content/273/25/15458.full.pdf+html (cit. on p. 13).

[93] AnneF. McGettrick and D.Margaret Worrall. "Extraction of Recombinant Protein From Bacteria". English. In: *Protein Purification Protocols*. Ed. by Paul Cutler. Vol. 244. Methods in Molecular Biology. Humana Press, 2004, pp. 29–35. DOI: 10.1385/1-59259-655-X:29 (cit. on pp. 13, 14).

[94] Evgeny V. Mymrikov, Alim S. Seit-Nebi, and Nikolai B. Gusev. "Large Potentials of Small Heat Shock Proteins". In: *Physiological Reviews* 91.4 (2011), pp. 1123–1159. DOI: 10.1152/physrev.00023.2010. eprint: http://physrev.physiology.org/content/91/4/1123.full.pdf+html (cit. on p. 12).

[95] Martin E M Noble, Jane a Endicott, and Louise N Johnson. "Protein kinase inhibitors: insights into drug design from structure." In: *Science (New York, N.Y.)* 303.5665 (Mar. 2004), pp. 1800–5. DOI: 10.1126/science.1095920 (cit. on p. 1).

[96] Taiana Maia de Oliveira. "Inhibitor selectivity determinants for the Aurora protein kinases". PhD thesis. Universitetet i Tromsø, 2011 (cit. on pp. 26, 69).

[97] Avondale PA Michael W. Pantoliano, Libertyville IL Alexander W. Rhind, and Yardley PA Francis R. Salemme. *Microplate thermal shift assay for ligand development and multi-variable protein chemistry optimization.* Patent. US, Feb. 2000 (cit. on p. 21).

[98] Keykavous Parang and Philip A Cole. "Designing bisubstrate analog inhibitors for protein kinases". In: *Pharmacology & Therapeutics* 93 (2002), pp. 145–157 (cit. on p. 11).

[99] Keykavous [US] PARANG Saunders Town RI (US), Gongqin [US] SUN Wakefield RI (US), Anil [IN] KUMAR Pilani (IN), Nguyen H [VN] NAM Hanoi (VN), Yue-Hao [US] WANG Houston TX (US), and Guofeng [US] YE Quincy MA (US). *Bisubstrate inhibitors of protein tyrosine kinases as therapeutic agents.* US, Sept. 2010 (cit. on p. 11).

[100] Patricia Pellicena, David S King, Arnold M Falick, John Kuriyan, Markus A Seeliger, Matthew Young, and M Nidanie Henderson. "High yield bacterial expression of active c-Abl and c-Src tyrosine kinases". In: *Protein Science* 14.12 (2005), pp. 3135–3139. DOI: 10.1110/ps.051750905.kemia (cit. on pp. 14, 26).

[101] A. Pflug, T.M. de Oliveira, D. Bossemeyer, and R.A. Engh. "Mutants of protein kinase A that mimic the ATP-binding site of Aurora kinase". In: *Biochemical Journal* 440.1 (2011), pp. 85–93 (cit. on pp. 2, 24, 78).

[102] Alexander Pflug. "Expression, purification & crystallization of the catalytic subunit alpha of protein kinase A (PKA)". 2012 (cit. on p. 32).

[103] Alexander Pflug, Jevgenia Rogozina, Darja Lavogina, Erki Enkvist, Asko Uri, Richard Alan Engh, and Dirk Bossemeyer. "Diversity of bisubstrate binding modes of adenosine analogue-oligoarginine conjugates in protein kinase a and implications for protein substrate interactions." In: *Journal of molecular biology* 403.1 (Oct. 2010), pp. 66–77. DOI: 10.1016/j.jmb.2010.08.028 (cit. on pp. 10, 11).

[104] Alexander Pflug, Taianá Maia de Oliveira, Dirk Bossemeyer, and Richard A Engh. "Mutants of protein kinase A that mimic the ATP-binding site of Aurora kinase." In: *The Biochemical journal* 440.1 (Nov. 2011), pp. 85–93. DOI: 10.1042/BJ20110592 (cit. on p. 25).

[105] Lorenzo A Pinna and Maria Ruzzene. "How do protein kinases recognize their substrates?" In: *Biochimica et Biophysica Acta (BBA) - Molecular Cell Research* 1314.3 (1996), pp. 191–225 (cit. on p. 9).

[106] *Protein Structure*. http://www.nature.com/scitable/topicpage/protein-structure-14122136. Nature (cit. on p. 12).

[107] Madhavi J. Rane, Yong Pan, Saurabh Singh, David W. Powell, Rui Wu, Timothy Cummins, Qingdan Chen, Kenneth R. McLeish, and Jon B. Klein. "Heat Shock Protein 27 Controls Apoptosis by Regulating Akt Activation". In: *Journal of Biological Chemistry* 278.30 (2003), pp. 27828–27835. DOI: 10.1074/jbc.M303417200. eprint: http://www.jbc.org/content/278/30/27828.full.pdf+html (cit. on p. 12).

[108] Raimond BG Ravelli and Elspeth F Garman. "Radiation damage in macromolecular cryocrystallography". In: *Current opinion in structural biology* 16.5 (2006), pp. 624–629 (cit. on pp. 23, 81).

[109] Raimond BG Ravelli, Hanna-Kirsti Schrøder Leiros, Baocheng Pan, Martin Caffrey, and Sean McSweeney. "Specific radiation damage can be used to solve macromolecular crystal structures". In: *Structure* 11.2 (2003), pp. 217–224 (cit. on pp. 23, 81).

[110] Erwin M Reimann, Donal A Walsh, and Edwin G Krebs. "Purification and properties of rabbit skeletal muscle adenosine 3', 5'-monophosphate-dependent protein kinases". In: *Journal of Biological Chemistry* 246.7 (1971), pp. 1986–1995 (cit. on p. 20).

[111] G Rhodes. *Crystallography Made Crystal Clear: A Guide for Users of Macromolecular Models*. Complementary Science Series. Elsevier/Academic Press, 2006 (cit. on p. 22).

[112] Rebecca L Rich and David G Myszka. "Higher-throughput, label-free, real-time molecular interaction analysis". In: *Analytical biochemistry* 361.1 (2007), pp. 1–6 (cit. on p. 20).

[113] Maurice Rigby, E Brian Smith, William A Wakeham, and Geoffrey C Maitland. *The forces between molecules*. Clarendon Press Oxford, 1986 (cit. on p. 13).

[114] Phillip Saylor, Chengqian Wang, T. John Hirai, and Joseph A. Adams. "A Second Magnesium Ion Is Critical for ATP Binding in the Kinase Domain of the Oncoprotein v-Fps†". In: *Biochemistry* 37.36 (1998), pp. 12624–12630. DOI: 10.1021/bi9812672. eprint: http://pubs.acs.org/doi/pdf/10.1021/bi9812672 (cit. on p. 5).

[115] DIETMAR SCHOMBURG, IDA SCHOMBURG, and ANTJE CHANG. *Springer handbook of enzymes Volume 36*. Ed. by Antje Chang. 2nd ed. Vol. 36. Springer New York, 2003 (cit. on p. 1).

[116] LLC Schrödinger. "The PyMOL Molecular Graphics System". Aug. 2010 (cit. on pp. 75, 81).

[117] Alexander W Schuttelkopf and Daan MF van Aalten. "PRODRG: a tool for high-throughput crystallography of protein-ligand complexes". In: *Acta Crystallographica Section D: Biological Crystallography* 60.8 (2004), pp. 1355–1363 (cit. on p. 43).

[118] J. L. Sebaugh. "Guidelines for accurate EC50/IC50 estimation". In: *Pharmaceutical Statistics* 10.2 (2011), pp. 128–134. DOI: 10.1002/pst.426 (cit. on pp. 20, 60, 79).

[119] *Sensor Surface Handbook*. AB. Biacore Sensor Surface Handbook BR-1005-71 Edition AB. GE Healthcare. 2008 (cit. on p. 78).

[120] I N Shindyalov and P E Bourne. "Protein structure alignment by incremental combinatorial extension (CE) of the optimal path." In: *Protein Engineering* 11.9 (1998), pp. 739–747. DOI: 10.1093/protein/11.9.739. eprint: http://peds.oxfordjournals.org/content/11/9/739.full.pdf+html (cit. on p. 81).

[121] S E Shoelson, S Chatterjee, M Chaudhuri, and M F White. "YMXM motifs of IRS-1 define substrate specificity of the insulin receptor kinase". In: *Proceedings of the National Academy of Sciences* 89.6 (1992), pp. 2027–2031. eprint: http://www.pnas.org/content/89/6/2027.full.pdf+html (cit. on p. 9).

[122] O. Smidsrød and S.T. Moe. *Biopolymerkjemi*. Tapir, 1995 (cit. on p. 12).

[123] R A Steinberg, R D Cauthron, M M Symcox, and H Shuntoh. "Autoactivation of catalytic (C alpha) subunit of cyclic AMP-dependent protein kinase by phosphorylation of threonine 197." In: *Molecular and Cellular Biology* 13.4 (1993), pp. 2332–2341. DOI: 10.1128/MCB.13.4.2332. eprint: http://mcb.asm.org/content/13/4/2332.full.pdf+html (cit. on pp. 18, 74).

[124] F William Studier. "Protein production by auto-induction in high-density shaking cultures". In: *Protein expression and purification* 41.1 (2005), pp. 207–234 (cit. on pp. 29, 30).

[125] Susan S Taylor, Elzbieta Radzio-Andzelm, Madhusudan, Xiaodong Cheng, Lynn Ten Eyck, and Narendra Narayana. "Catalytic Subunit of Cyclic AMP-Dependent Protein Kinase: Structure and Dynamics of the Active Site Cleft". In: *Pharmacology & Therapeutics* 82.2–3 (1999), pp. 133–141. DOI: 10.1016/S0163-7258(99)00007-8 (cit. on p. 5).

[126] Thomas C Terwilliger. "Using prime-and-switch phasing to reduce model bias in molecular replacement". In: *Acta Crystallographica Section D: Biological Crystallography* 60.12 (2004), pp. 2144–2149 (cit. on p. 43).

[127] Andrei Tovchigrechko and Ilya A Vakser. "Development and testing of an automated approach to protein docking". In: *Proteins: Structure, Function, and Bioinformatics* 60.2 (2005), pp. 296–301 (cit. on p. 72).

[128] Andrey Tovchigrechko and Ilya A Vakser. "GRAMM-X public web server for protein–protein docking". In: *Nucleic acids research* 34.suppl 2 (2006), W310–W314 (cit. on p. 72).

[129] Jeffrey A Ubersax and James E Ferrell Jr. "Mechanisms of specificity in protein phosphorylation". In: *Nature Reviews Molecular Cell Biology* 8.7 (2007), pp. 530–541 (cit. on pp. 7, 9).

[130] *Usage tips for Affinity Material carrying immobilized ATP*. Jena Bioscience. 2009 (cit. on pp. 16, 71).

[131] Kaido Viht, Sonja Schweinsberg, Marje Lust, Angela Vaasa, Gerda Raidaru, Darja Lavogina, Asko Uri, and Friedrich W Herberg. "Surface-plasmon-resonance-based biosensor with immobilized bisubstrate analog inhibitor for the determination of affinities of ATP- and protein-competitive ligands of cAMP-dependent protein kinase." In: *Analytical biochemistry* 362.2 (Mar. 2007), pp. 268–77. DOI: 10.1016/j.ab.2006.12.041 (cit. on pp. 11, 20, 78).

[132] Carole Vincent, Patricia Doublet, Christophe Grangeasse, Elisabeth Vaganay, Alain J Cozzone, and Bertrand Duclos. "Cells of Escherichia coli contain a protein-tyrosine kinase, Wzc, and a phosphotyrosine-protein phosphatase, Wzb". In: *Journal of bacteriology* 181.11 (1999), pp. 3472–3477 (cit. on p. 75).

[133] R. Westermeier and T. Naven. *Proteomics in practice: a laboratory manual of proteome analysis*. Wiley-VCH, 2002 (cit. on pp. 18, 19).

[134] Christoph J Wienken, Philipp Baaske, Ulrich Rothbauer, Dieter Braun, and Stefan Duhr. "Protein-binding assays in biological liquids using microscale thermophoresis". In: *Nature communications* 1 (2010), p. 100 (cit. on p. 21).

[135] Douglas S Williamson, Jenifer Borgognoni, Alexandra Clay, Zoe Daniels, Pawel Dokurno, Martin J Drysdale, Nicolas Foloppe, Geraint L Francis, Christopher J Graham, Rob Howes, Alba T Macias, James B Murray, Rachel Parsons, Terry Shaw, Allan E Surgenor, Lindsey Terry, Yikang Wang, Mike Wood, and Andrew J Massey. "Novel adenosine-derived inhibitors of 70 kDa heat shock protein, discovered through structure-based design." In: *Journal of medicinal chemistry* 52.6 (Mar. 2009), pp. 1510–3. DOI: 10.1021/jm801627a (cit. on p. 27).

[136] Magdalena Wisniewska, Tobias Karlberg, Lari Lehtiö, Ida Johansson, Tetyana Kotenyova, Martin Moche, and Herwig Schüler. "Crystal structures of the ATPase domains of four human Hsp70 isoforms: HSPA1L/Hsp70-hom, HSPA2/Hsp70-2, HSPA6/Hsp70B', and HSPA5/BiP/GRP78." In: *PloS one* 5.1 (Jan. 2010). Ed. by Nick Gay, e8625. DOI: 10.1371/journal.pone.0008625 (cit. on p. 27).

[137] Marcin Wojdyr. "Fityk: a general-purpose peak fitting program". In: *Journal of Applied Crystallography* 43.5 (2010), pp. 1126–1128 (cit. on p. 60).

[138] W Yonemoto, M L McGlone, B Grant, and S S Taylor. "Autophosphorylation of the catalytic subunit of cAMP-dependent protein kinase in Escherichia coli." In: *Protein Engineering* 10.8 (1997), pp. 915–925. DOI: 10.1093/protein. eprint: http://peds.oxfordjournals.org/content/10/8/915.full.pdf+html (cit. on pp. 18, 74, 86).

[139] Jianhua Zheng, Daniel R. Knighton, Lynn F. Ten Eyck, Rolf Karlsson, N. Xuong, Susan S. Taylor, and Janusz M. Sowadski. "Crystal structure of the catalytic subunit of cAMP-dependent protein kinase complexed with magnesium-ATP and peptide inhibitor". In: *Biochemistry* 32.9 (1993), pp. 2154–2161. DOI: 10.1021/bi00060a005. eprint: http://pubs.acs.org/doi/pdf/10.1021/bi00060a005 (cit. on pp. 5, 7).


UNIVERSITY OF TROMSØ